Virginia Journal of Science
Volume 68, Issue 3 & 4
Fall & Winter 2017
doi: 10.25778/XJT5-TR11

Note: This manuscript has been accepted for publication and is online ahead of print. It will undergo copyediting, typesetting, and review of the resulting proof before it is published in its final form.

Microstructure of Attachment Mechanisms of Newly Hatched Larvae of Four Cyprinid Species with Comments on Terminology

George E. Maurakis, College of Science, Virginia Tech, Blacksburg, VA 24061
Eugene G. Maurakis, University of Richmond, 28 Westhampton Way, Richmond VA 23173 and Science Museum of Virginia, 2500 W. Broad St., Richmond, VA 23220

ABSTRACT

An adhesive organ is a prominent, protruding mucus secreting gland that is used by newly hatched tadpoles and larvae of some fishes to attach to aquatic vegetation. The objective of this research is to test the hypothesis that newly hatched cyprinid larvae of *Hybognathus hankinsoni*, *Notemigonus crysoleucas*, *Cyprinus carpio* and *Gila atraria* contain cephalic adhesive organs. Newly hatched larvae of *Semotilus atromaculatus,* which do not attach to submerged aquatic vegetation, were used as the control. SEM examination of newly hatched larvae indicate there were no adhesive organs on the control species (*S. atromaculatus*) or test species (*H. hankinsoni, N. crysoleucas, C. carpio* and *G. atraria*). Rather, newly hatched larvae of test species contain a localized highly modified epidermis (i.e., primarily on the ventral cephalic and anterioventral yolk sac surfaces of *H. hankinsoni*, *N. crysoleucas*, *C. carpio*, and *G. atraria*, and sometimes on dorsal cephalic epidermal cells of *H. hankinsoni*, *C. carpio*, and *G. atraria*). This modified epidermis is composed of epidermal cells with unculi-like projections, elevated microridges at peripheries of epidermal cells, and mucus from apical pores of goblet cells that probably are responsible for attachment of test species to substrates. We hypothesize that the unculi-like projections at centers of epidermal cells in newly hatched larval test cyprinids are true unculi. There is a need to define and clarify the meanings of words and phrases (i.e., cement gland, cement gland apparatus, cement gland-like structure, casquette, temporary adhesive glands, adhesive apparatus, adhesive gland, adhesive organ, attachment organ, and glue secretion and adhesion) for structures used by newly hatched larvae to attach to substrates. Definitions should be based on homologies, crucial in phylogenetic reconstructions of species relationships and in identifying developmental homologues of cells, tissues, glands, and organs that have been described as mechanisms for attachment by newly hatched larvae of various species to substrates. We proposed the phrase "attachment mechanism" as a broad definition for the ways in which newly hatched larvae attach and adhere to substrates during early development. This broad definition, however, should be modified to define specific methods of attachment (e.g. attachment mechanism of unculi, elevated epidermal microridges, and mucus) to assist in defining homologies.

Keywords: newly hatched cyprinid larvae, attachment mechanism, SEM

INTRODUCTION

Various terms (e.g. cement gland, adhesive organ) have been used to describe the attachment mechanism of newly hatched larvae of some frogs and fishes to substrates. Snyder et al. (2016), following Auer et al. (1982) and Wallus et al. (2008), presented a broad definition of cement gland: "discrete or diffuse structures which permit a larva to adhere to a substrate." Other researchers, however, have proffered a strict definition of cement gland/adhesive organ in which an adhesive organ is a single prominent, protruding gland composed of an aggregation of elongated, tubular secretory cells surrounding a pyriform acinus (Rétaux and Pottin, 2011; Bennemann and Pietzsch-Rohrschneider, 1978), which contain adhesive secretions. Adhesive organs (described as cement glands by Schäperclaus, 1962 and Blaxter, 1969) are used by newly hatched tadpoles and larvae of some fishes to attach to aquatic vegetation and other substrates during early development (Rétaux and Pottin, 2011). Adhesive organs have been reported in frogs (e.g. *Xenopus laevis* (Boothby and Roberts, 1992) and a variety of fishes [*Lepisosteus osseus* (Lepisosteidae), *Amia calva* (Amiidae), *Astyanax mexicanus* (Characidae), *Cichlasoma dimerus* (Cichlidae), *Oreochromis niloticus* (Cichlidae), *Pterophyllum scalare* (Cichildae), and *Tilapia mariae* (Cichlidae)](Eycleshymer and Wilson, 1908; Peters, 1965; Morrison et al., 1978; Boothby and Roberts, 1992; Britz et al., 2000; Meijide and Guerrero, 2000; Morrison et al., 2001; Groppelli et al., 2003; Pottin et al., 2010). In presenting a chordate phylogenetic tree highlighting the presence of adhesive organs in one sarcopterygian (Dipnoi) and seven species of actinopterygians (Polypteriformes, Acipenseriformes, Lepisosteiformes, Amiiformes, Osteoglossiformes, Characiformes, and Perciformes), Rétaux and Pottin (2011) hypothesized that the adhesive organ in *A. mexicanus* was homologous to that in *X. laevis* based on characteristics common to both: adhesive gland secretory cell morphology, mucus production, innervation by the trigeminal nerve, and the development of the adhesive organ by the same gene regulatory network, including *Bmp4* and *Pitx1/2*.

Blaxter (1969) and Balon (1975) hypothesized that the newly hatched larvae of some phytophilous species of Cyprinidae (Ostariophysi: Cypriniformes) attach themselves to aquatic vegetation with adhesive organs/cement glands. Likewise, Loos and Fuiman (1978) and Loos et al. (1979) hypothesized that newly hatched larvae of *Notemigonus crysoleucas* and *Cyprinus carpio* contained cephalic cement glands that allowed them to attach to aquatic vegetation during early development. To date, there have been no studies to test the adhesive organ/cement gland hypothesis in these cyprinids. The objective of this research was to test the hypothesis that cyprinid newly hatched larvae contain cephalic adhesive organs/cement glands described by Pottin et al. (2011). Independent variables are the New World newly hatched larval cyprinids, *Hybognathus hankinsoni*, *N. crysoleucas*, and *Gila atraria* and the Old World cyprinid, *C. carpio* (test group). *Hybognathus hankonsoni* and *G. atraria* were included as they are reported to be phytophilous spawners by Snyder et al. (2016). Newly hatched larvae of *Semotilus atromaculatus*, which do not adhere to substrates, were used as the control group. Dependent variables were the presence of an adhesive organ/cement gland and variations in epidermal characteristics (e.g. apical pores of goblet cells, epidermal unculi-like projections, mucus, and the peripheral microridge) of newly hatched larvae in control and test groups.

MATERIALS AND METHODS

Newly hatched (1 day old) larval specimens of control and test species, preserved in 10 % buffered formaldehyde, were acquired from Colorado State University, University of Richmond, and Academy of Natural Sciences of Drexel University. Collection data are available upon request.

Scanning electron microscopy (SEM): Three specimens of each species were dehydrated by the following procedure: one quick distilled water wash, two 10-minute distilled water washes; incremental 30, 50, 70, 90, and 100% ETOH (ethanol) 10-minute soaks, followed by two additional 100% ETOH 10-minute soaks. After dehydration, specimens were vacuum dried in a Samdri-795 critical point dryer. Critical point dried specimens were mounted on SEM stubs, and coated with two 6-micron palladium coatings in a Denton-4 sputter coater. The dorsal, anterior, ventral, and lateral areas of the head, the anteriorventral surface of the yolk sac, and the lateral body trunk of each early hatched larval specimen were examined with SEM to identify the presence/absence of adhesive organs, apical ends of goblet cells, mucus, and epidermal projections. Three newly hatched larvae of *S. atromaculatus* were used as controls.

RESULTS

SEM indicated there are no adhesive organs/cement glands as described by Rétaux and Pottin (2011) and Bennemann and Pietzsch-Rohrschneider (1978) on any cephalic areas of newly hatched larvae of cyprinid control species (*S. atromaculatus*) and all cyprinid test species (*H. hankinsoni*, *N. crysoleucas*, *C. carpio*, and *G. atraria*) (Table 1; Fig. 1). In all control and test species, surfaces of hexagonal (rarely pentagonal) epidermal cells contain micro-ridges (MR) *albeit* with varying lengths and patterns, and have well demarcated cell borders formed by peripheral micro-ridges of adjoining cells. Descriptions of the epidermis of all species is presented by region.

Dorsal Cephalic Region – In *S. atromaculatus*, the most striking feature of the dorsal epidermis is the abundance of goblet cell pores (Figs. 1A and 2A). Each epidermal cell is bordered by one to two surface pores of goblet cells (Figs. 1A and 2A). Micro-ridges at cell peripheries are elevated at adjoining cells and where they contact the elevated pores of goblet cells (Fig. 2A). No unculi-like projections were present.

In *H. hankonsoni*, the dorsal epidermis has few pores but a preponderance of unculi-like projections that emanate primarily from the central regions of epidermal cells (Figs. 2B). Ventral and lateral margins of the eyes contain numerous unculi-like projections (Fig. 2B). The dorsal surface of one specimen of *H. hankinsoni* had a thick mucus embedded with debris (Fig. 2F).

As in *H. hankinsoni*, the dorsal epidermis of *N. crysoleucas* has few pores. However, dorsal epidermal cells of *N. crysoleucas* do not have unculi-like projections (Fig. 2C).

The micro-ridge pattern of dorsal epidermal cells in *C. carpio* is not as pronounced as those in other species (Fig.2D). The dorsal epidermis of *C. carpio* has numerous pores, and the

centers of epidermal cells have nubby unculi-like projections. Lateral cephalic epidermal cells have longer unculi-like projections (Figs. 2C).

In *G. atraria* the dorsal epidermis contains numerous pores. Its epidermal cells have unculi-like projections and short MR (Fig. 2E). Location of the unculi-like projections is variable. Some are present in the center of cells whereas others are located at or near the periphery of the cells (Fig. 2E). Some epidermal cells have more than one unculi-like projections (Fig. 2E). The dorsal cephalic surface of one *G. atraria* specimen has a thick mucus embedded with debris (Fig 2G).

Ventral Cephalic Region – In *S. atromaculatus*, the ventral cephalic epidermis is much like that on the dorsum (Fig. 3A). There is clear definition of the micro-ridges in the hexagonal cells which do not have unculi-like projections (Fig. 3A). Numerous pores punctuate the epidermis where mucus spheres are present in some pores (Fig. 3A).

In *H. hankinsoni*, the ventral epidermis has an abundance of both apical pores of goblet cells and small to large unculi-like projections (Fig. 3B). The unculi-like projections are distributed in the centers of some cells, and at or near the periphery of other cells (Fig. 3B).

In *N. crysoleucas*, small to large unculi-like projections were present in ventral and anterioventral cephalic epidermal cells (Fig. 3C). Few apical pores of goblet cells were apparent in the ventral epidermis (Fig. 3C). Anteriolateral cephalic epidermal cells have long unculi-like projections (Fig. 3F).

The ventral epidermis of *C. carpio* has unculi-like projections and pores (Figs. 3D and 3G). Epidermal cells containing unculi-like projections appeared to be segregated from apical pores of goblet cells (Figs. 3D). Mucus and debris often obscure the epidermal unculi-like projections and pores like that imaged on the anterioventral cephalic region in one specimen (Fig. 3G).

In *G. atraria*, pores are prevalent (Figs 1E and 3E), and the unculi-like processes are relatively short (Figs. 3E and 3H). Some unculi-like projections appear to arise from the periphery of cells adjacent to apical pores of goblet cells (Fig. 3H).

Anterioventral Yolk Sac Region – The epidermis on the anterioventral regions of the yolk sac of *S. atromaculatus* has numerous apical pores of goblet cells which rise above the level of the hexagonal epidermal cells (Fig. 4A). No epidermal cells have unculi-like projections.

In *H. hankinsoni*, anterioventral and lateral epidermal cells of the yolk sac contain small to large unculi-like projections (Fig. 4B). Few pores are apparent. The anterioventral epidermal cells on the yolk sac of *N. crysoleucas* contain central, small to large unculi-like projections (Figs. 4C and 4F). Few pores are apparent. In *C. carpio*, epidermal cells of the anterioventral and ventrolateral areas of the yolk sac contain unculi-like projections and pores (Figs. 4D and 4G). Anterioventral yolk sac epidermal cells of *G. atraria* contain both unculi-like projections and pores (Fig. 4E).

Lateral-Ventral Trunk Region – In *S. atromaculatus*, the epidermal cells of the lateral trunk have well defined micro-ridge patterns (Fig. 5A) which and rise towards the cell periphery where they meet those of other cells (Fig. 5A). Numerous apical pores of goblet cells rise above the surface of the centers of the other epidermal cells (Fig. 5A). No unculi-like projections are present.

Lateral, lateroventral, and ventral trunk areas of *H. hankinsoni* contain primarily hexagonal epidermal cells with unculi-like projections that increase in numbers toward the ventral finfold (Fig. 5B). Apical pores of goblet cells are common but not prevalent.

In *N. crysoleucas*, epidermal cells on the lateral trunk do not have unculi-like projections but have short, pectinate MR (Fig 5C and 5F). Few apical pores of goblet cells were present on the lateral trunk (Fig. 5C).

The lateral trunk epidermis of *C. carpio* has apical pores of goblet cells (Fig. 5D). The frequency and size of unculi-like projections increases towards the ventral finfold (Fig. 5D).

In *G. atraria*, lateroventral and ventral epidermal cells have goblet cell pores and well-defined unculi-like projections (Figs. 5E).

DISCUSSION

The newly hatched larvae of test species (*H. hankinsoni*, *N. crysoleucas*, *C. carpio*, and *G. atraria*) in the present study do not possess cement glands/adhesive organs (i.e., a single prominent, protruding gland composed of an aggregation of elongated, tubular cells surrounding a pyriform acinus) as described for *X. laevis* (Amphibia) and *A. mexicanus* (Characidae) by Rétaux and Pottin (2011), *P. scalare* (Cichlidae) by Bennemann and Pietzsch-Rohrschneider (1978) and Groppelini et al. (2003), *Oreochromis niloticus* (Cichlidae) by Morrison et al. (2001), *Hypsophrys nicaraguensis* (Cichlidae) by Arias (2011), and *Amphilophus xiloaensis* (Cichlidae) by Kratochwil et al. (2015), *A. calva* (Amiidae) by Eycleshymer and Wilson (1908), *L. osseus* (Lepisosteidae) by Eycleshymer (1903) and Long and Ballard (2001), *Cichlasoma dimerus* (Cichlidae) by Meijide and Guerrero (2000), and *Octolasmis angulate* (Crustacean: Poecilasmatidae) by Yap et al. (2017). In contrast to these prominent protruding glands, a localized highly modified epidermis (i.e., primarily on the ventral cephalic and anterioventral yolk sac surfaces) occurs in newly hatched larval *H. hankinsoni*, *N. crysoleucas*, *C. carpio*, and *G. atraria*, and sometimes on dorsal cephalic epidermal cells of *H. hankinsoni*, *C. carpio*, and *G. atraria*. This modified epidermis is composed of epidermal cells with unculi-like projections, elevated microridges at peripheries of epidermal cells, and mucus from apical pores of goblet cells that in combination probably are responsible for attachment of test species to substrates. Unculi-like projections have been reported previously in newly hatched larval ostariophysans, *C. carpio* (Brizt et al., 2000; Appelbaum and Riehl, 1997), and *Rhodeus uyekii*, described as minute tubercles by Suzuki et al. (1985). Britz et al. (2000) reported the presence of projections in epidermal cells in specific cephalic regions in the gymnotiforms, *Apteronotus albifrons* and *Apteronotus leptorhynchus* (Britz et al., 2000), and proposed they aid in the adhesion of the newly hatched larvae to substrates during early development. Appelbaum and Riehl (1997) reported that centers of surface epidermal cells of the yolk sac of newly hatched larval *C. carpio*

contained protrusions, and that epidermal cells of the mouth region were comprised of keratinizing cells, but did not relate either to attachment. The reported presence of projections (Britz et al., 2000), protrusions (Appelbaum and Riehl, 1997), and minute tubercles (Suzuki, et al., 1985) is consistent with the presence and locations of the unculi-like projections on anterioventral yolk sac and ventral cephalic epidermal areas of newly hatched larval *H. hankinsoni*, *N. crysoleucas*, *C. carpio*, and *G. atraria* in our study.

We hypothesize that the unculi-like projections at centers of epidermal cells in newly hatched larval test cyprinids in our study, those reported for newly hatched larval gymnotiforms by Britz et al. (2000), and the minute tubercles primarily on the head and yolk sac of newly hatched larval *R. uyekii* by Suzuki et al. (1985) are true unculi (horny keratinized projections arising from single epidermal cells) as described by Roberts (1982). We plan to test this hypothesis with special keratin stains (i.e., Dane Herman method, ayoub-shklar method, Alcian blue-periodic acid Schiff's stain or hemotoxylin and eosin stains) described in Rao et al. (2014). Our hypothesis is based on the report by Li et al. (2011) who demonstrated the production of keratinized projections in epidermal cells of larval *Danio rerio* after treatment with morpholino-mediated knockdown of the anca12 and snap29 genes, and the fact that the unculi-like projections on epidermal cells of newly hatched larvae in this study, as well as those of the gymnotiforms, *A. albifrons* and *A. leptorhynchus* (Britz et al., 2000), *R. uyekii* (Suzuki et al., 1985), and *C. carpio* (Appelbaum and Riehl, 1997) are strikingly similar in appearance to unculi in SEM micrographs of adult epidermis reported in Roberts (1982). We do not find the presence of unculi in newly hatched larvae to be unexpected. Unculi are unique to ostariophysan fishes and have been found on adults of numerous species (Roberts, 1982). They also are part of the attachment mechanism in adult cyprinid hill stream fishes *Garra gotyla*, *Garra lissorhynchus*, *Garra pectinopterus*, and *Garra sulcatus* (Gaur et al., 2013; Massar, 2015) and adult mountain-stream catfish, *Pseudocheneis sulcatus* (Joshi et al., 2012), which use a combination of unculi and mucus to adhere to substrates in swift water currents.

Loos and Fuiman (1978) and Loos et al. (1979) stated that newly hatched larval *N. crysoleucas* and *C. carpio* contain cephalic adhesive organs/cement glands. With SEM, we did not find adhesive organs (cement glands) on any cephalic areas or anteriorventral epidermal yolk sacs of Old World and New World cyprinid newly hatched larvae examined in the present investigation. Loos and Fuiman (1978) and Loos et al. (1979) provided no evidence for the presence of cephalic adhesive organs/cement glands in newly hatched larval *N. crysoleucas* and *C. carpio*. Rather, their hypotheses were based on observations of these newly hatched larvae attaching themselves to aquatic vegetation as well as to the sides of aquaria, a plausible assumption at the time considering published descriptions of adhesive organs as means of attachment to submerged aquatic vegetation by newly hatched larvae of other species (e.g. adhesive glands described on larval *Amia calva* by Eycleshymer and Wilson, 1908, and those on larval *L. osseus* by Eycleshymer, 1903).

We could not corroborate the presence of an adhesive organ on the anterior end of the head of newly hatched larvae of *C. carpio* reported by Appelbaum and Riehl (1997). Appelbaum and Riehl (1997) simply labeled a sunken area on their specimen as an adhesive organ, not a protruding one as described by Rétaux and Pottin (2011). Our observations of the absence of an adhesive organ on newly hatched larval *C. carpio* are corroborated by the studies of Maitland

and Campbell (1992), Steffens (1980), and Sola et al. (1983) who state that newly hatched larval *C. carpio* do not possess cephalic adhesive organs but attach themselves to substrates with their mouths. Similarly, we did not find evidence of the presence of bilateral cement glands and pores anterior to the developing mouths of our test species that Fletcher and Wilkins (1999) reported for newly hatched larval *Pteronotropis hypselopterus*. Fletcher and Wilkins (1999) indicate that newly hatched larval *P. hypselopterus* do not have fibrils or specialized attachment appendages that were prevalent on ventral epidermal cells and those on the anterioventral surface of yolk sacs of test species in the current study.

The bilateral cement glands and pores anterior to the developing mouths in *P. hypselopterus* and the attachment mechanism described for our test species indicate there are at least two significantly different attachment mechanisms for newly hatched larval cyprinids (i.e., a combination of unculi-like projections, MR pattern, and mucus present in newly hatched larvae in the current study; and the bilateral cement glands without fibrils or specialized attachment appendages of *P. hypselopterus* reported by Fletcher and Wilkins (1999).

Mode of spawning and larval development relationship – We propose that the unculi-like projections at the centers of epidermal cells on the ventral cephalic regions and anterior ventral regions of all test species, mucus from the apical pores of goblet cells, and the elevated peripheral ridge of epidermal cells account for the attachment of the newly hatched larvae of test species to substrates (i.e., aquatic vegetation, roots, and rocks) during early development. Most likely, the micro-ridge pattern of epidermal cells helps to distribute mucus. Mucus from goblet cells contain mucopolysaccharides and serves as an adhesive (Long et al., 2013), and also facilitates gas exchange (Horng et al., 2009). Physical attachments of newly hatched larval *N. crysoleucas* and *C. carpio* to substrates during their early development have previously been confirmed by Loos et al. (1979). Developmental attachment dispositions of newly hatched larval *H. hankinsoni* and *G. atraria*, however, are unknown. Based on our results and life history aspects of these two species, we hypothesize that their newly hatched larvae attach and adhere to substrates during their early life history using a combination of the unculi-like projections, mucus, and the MR pattern of their epidermal cells that are present on their cephalic and anteriovental region of their yolk sacs. *Hybognathus hankinsoni* is an open-substrate phytophilous (non-obligatory plant spawner) that broadcast small, demersal, adhesive eggs over vegetation when available (Snyder et al., 2016). *Gila atraria* is an open-substrate phytophilous breeder, spawning adhesive eggs in shallow littoral shoals, usually over vegetation from April through August (Snyder et al., 2016). Graham (1955) reported that newly hatched fry were scattered through emergent vegetation and present in bank depressions in well protected pockets created by driftwood. In contrast, fertilized non-adhesive eggs are spawned by adult *S. atromaculatus* (control) in gravel nests where they hatch and develop progressively through protolarval, mesolarval, and metalarval stages before exiting the nest through its interstices (Maurakis et al., 1990, Maurakis et al., 1993). The cephalic epidermis of newly hatched larvae of the control (*S. atromaculatus*) do not contain unculi-like projections and is similar to the newly hatched larval epidermis of *D. rerio*, which has no unculi-like projections (Li et al., 2011). These results are comparable to those of Rétaux and Pottin (2011) who stated that the genome model cyprinid, *Danio rerio* (Zebrafish), does not possess a cement gland-like adhesive organ. *Danio rerio*, considered a group spawner and egg scatterer, spawns non-adhesive eggs (Spence et al., 2008), but unlike species of *Semotilus*, does not prepare a pebble nest.

Clarification of Terms – There is a need to define and clarify the meanings of words and phrases used to describe structure(s) "used to attach the larvae to the substrate" as stated in the Dictionary of Ichthyology (2017). Definitions of the various attachment mechanisms that have been described in the literature should be based on homologies, which are crucial in phylogenetic reconstructions of species relationships and in identifying developmental homologues of cells, tissues, glands, and organs that have been used to describe attachment of various species to substrates. We identified 10 terms (i.e., cement gland, cement gland apparatus, cement gland-like structure, casquette, temporary adhesive glands, adhesive apparatus, adhesive gland, adhesive organ, attachment organ, and glue secretion and adhesion) that have been used by others to describe how larval and adult fishes, frogs, and barnacles attach themselves to various substrates (Table 1). For example, "adhesive organ" has been used synonymously in four different ways to describe non-homologous attachment mechanisms. The paired anteriodorsal *adhesive organs* (sucking discs) on head of newly hatched larval *A. calva* are endodermal in origin (Eycleshymer and Wilson, 1908). In contrast, the single anterioventral *adhesive organ* of newly hatched larval *L. osseus* is considered as ectodermal in origin (Eycleshymer, 1903; Eycleshymer and Wilson, 1908; Long and Ballard, 2001). Additionally, Meijide and Guerrero (2000) used *adhesive organ* to denote the three to six pairs of glands in newly hatched larval *Cichlasoma dimerus* (Cichlidae) whereas Gomes et al. (2007) described *adhesive organ* as a secretory prismatic epithelial cell in *Hoplias malabaricus* (characiform). More research like those of Retaux and Pottin (2011) and Pottin et al. (2010) who identified the posterior dorsal cephalic cement gland-like structure (casquette) in *A. mexicanus* as homologous to the cement gland in *X. laevis* are warranted to clarify and define the various terms (Table 1) that have been used to describe structures associated with adhesion ability. In this context, "cement" is explicitly used and correctly applied by Retaux and Pottin (2011) and Pottin et al. (2010) to denote a cement-like substance that adheres a newly hatched larva to a substrate, consistent with the definition of "cement" as a noun (i.e., a binding element or agency, such as a substance to make objects adhere to each other) and transitive verb (i.e., to unite or make firm by or as if by cement) in Webster (2016). As such, we disagree with the use of "cement gland" by Snyder et al. (2016), Auer (1982), and Wallus and Simon (2008). We propose "attachment mechanism" is more appropriate for a broad definition of attachment: "discrete or diffuse structures and/or substances which permit a larva to attach and adhere to a substrate." For the test species in our study, attachment mechanism of unculi and mucus is appropriate.

This study has generated new questions and research areas. For example, newly hatched larvae of other ostariophysan fishes, particularly phytophilous spawners, should be examined using SEM to characterize epidermal structures relative to their roles in attachment mechanisms. For example, newly hatched larvae of *Notropis bifrenatus* (Cyprinidae) have been reported to adhere vertically (head up) on their ventral sides to aquarium glass (Harrington, 1947), but no studies have been published on their cephalic and trunk epidermal microstructures that could be associated with adherence. Secondly, is the production of mucus in cephalic epidermal cells of newly hatched larvae controlled by the same or different genes involved in mucus production in trunk epidermis during later stages of larval development?

ACKNOWLEDGEMENTS

We thank Christine Davis, director of microscopy and imaging and Gary Radice, retired professor, University of Richmond for their guidance and assistance in preparation and examination of specimens; Darrel Snyder, Colorado State University and Mark Sabaj, Academy of Natural Sciences of Drexel University for loans of specimens. Both authors prepared and examined specimens and wrote the manuscript.

LITERATURE CITED

Appelbaum, S. and R. Riehl. 1997. Scanning electron microscopic observations of the chemo- and mechanoreceptors of carp larvae (*Cyprinus carpio*) and their relationship to early behaviour, Aquatic Living Resources, 10:1-12.

Arias, A. M. 2011. Larval development of *Hypsophrys nicaraguensis* (Pisces: Cichlidae) under laboratory conditions. Rev. Biol. Trop. 59(4):1679-1684.

Auer, N. A. (Ed.). 1982. Identification of larval fishes of the Greak Lakes Basin with emphasis on the Lake Michigan Drainage. Great Lakes Fisheries Commission, Special Publication 82-3, Ann Arbor, MI. 744 p.

Balon, E. K. 1975. Reproductive guilds of fishes: a proposal and definition. J. Fish. Res. Bd. Canada 32:821-864.

Blaxter, J. H. S. 1969. Development: Eggs and larvae. In "Fish physiology" III, Eds. Hoar W. S. and Randall D. J., Academic Press, New York and London, pp. 177-252.

Bennemann R. and I. Pietzsch-Rohrschneider. 1978. The morphology of the cement gland apparatus of larval *Pterophyllum scalare* Cuv. & Val. (Cichlidae, Teleostei). Cell and Tissue Research. 193(3):491-501.

Boothby, K. M. and A. Roberts. 1992. The stopping response of *Xenopus laevis* embryos: pharmacology and intracellular physiology of rhythmic spinal neurones and hindbrain neurones. J. Exp. Biol. 169:65–86.

Britz, R, F., Kirschbaum, and A. Heyd. 2000. Observations on the structure of larval attachment organs in three species of gymnotiforms (Teleostei: Ostariophysi). Acta Zoologica (Stockholm). 81:57-67.

Eycleshymer, A. C. and J. M. Wilson. 1908. Adhesive organs of *Amia*. Biol. Bull.14:134–149.

Gaur, K. S., V. Sharma, B. K. Verma, and M. S. Sharma. 2013. SEM study of adhesive organ of typical hill stream fish *Garra gotyla* (Teleostei; Cyprinidae). Journal Cell Tissue Research. 13(1):3473-3478.

Gomes, R. Z., Y. Sato, E. Rizzo, and N. Bazzoli. 2011. Early development of *Brycon orthotaenia* (Pisces: Characide). Zygote 21(February):11-20.

Gomes, R. Z., R. S. Scarpelli, F. P. Arentes, Y. Sato, N. Bazzoli, and E. Rizzo 2007. Comparative oocyte morphology and early development in three species of trahiras from the San Francisco River basin, Brazil. Journal of Fish Biology. 70:1412-1429.

Graham, R. J. 1955. Biology of the Utah Chub in Hebgen Lake, Michigan. MS Thesis, Montana State College. 33 p.

Groppelli, S., R. Pennati, C. Sotgia, and F. De Bernardi. 2003. Cement gland apparatus of the angelfish *Pterophyllum scalare* (Teleostei, Cichlidae): Functional morphology in comparison with adhesive organs of other Chordata. Italian Journal of Zoology: 70(2):133-139.

Harrington, R. W. 1947. The early life history of the bridled shiner, *Notropis bifrenatus* (Cope). Copeia 1947(2):97-102.

Horng, J-L., L-Y Lin, and P-P Hwang. 2009. Function regulation of H+-ATPase-rich cells in zebrafish embryos acclimated to an acidic environment. American Journal of Physiology 296(4):C682-C692.

Joshi, S. C., I. Bisht, and S. K. Agarwal. 2012. Study of the "unculi" of *Pseudocheneis sulcatus* (McClelland)(Sisoridae) fish of Kumaun Himalaya. J. American Science 8(2):413-418.

Joshi, S. C., I. Bisht, and S. K. Agarwal. 2011. A comparative surface-architechtural study of some of the hill-stream fishes: A scanning electron microscope investigation. Nature and Science 9(12):109-115.

Kiernan, J. 2008. Histological and Histochemical Methods: Theory and Practice (4th ed.). Scion Publishing Limited. Oxfordshire, Great Britain. 606 p.

Kratochwil, C. F., M. M. Sefton, and A. Meyer. 2015. Embryonic and larval development in the Midas cichlid fish species flock (Amphilophus spp.): a new evo-devo model for the investigation of adaptive novelties and species differences. Developmental Biology 15(12):1-15.

Lee, R. T. H., P. V. Asharani, and T. J. Carney. 2014. Basal keratinocytes contribute to all strata of the adult Zebrafish epidermis. PLOS ONE 9(1):1-11.

Li, Q., M. Frank, M. Akiyama, H. Shimizu, S.Y. Ho, C. Thisse, B. Thisse, E. Sprecher, and J. Uitto. 2011. Abca12-mediated lipid transport and Snap29-dependent trafficking of lamellar granules are crucial for epidermal morphogenesis in a zebrafish model of ichthyosis. Disease Models and Mechanisms. 4:777-785.

Loos, J. J., and L.A. Fuiman. 1978. Subordinate taxa of the genus *Notropis*: a preliminary comparative survey of their developmental traits. Pages 1-50 *in* L.L. Olmsted (ed.). Proceedings of the first symposium from freshwater larval fish. Duke Power Company, Huntersville, NC.

Loos, J. J., L. A. Fuiman, N. R. Foster, and E. K. Jankowski. 1979. Notes on early life histories of cyprinoid fishes of the upper Potomac River. Pages 93-139 *in* R. Wallus and C.W. Voigtlander (eds.). Proceedings of a workshop on freshwater larval fishes. Tennessee Valley Authority, Norris, TN.

Long, Y., Q. Li, B. Zhou, G. Song, T. Lit, and Z. Cui. 2013. De novo assembly of mud loach (*Misgurnus anguillicaudatus*) skin transcriptome to identify putative genes involved in immunity and epidermal mucus secretion. PloS One 8(2):1-14.

Long, W. L. and W. W. Ballard. 2001. Normal embryonic stages of the Longnose Gar, *Lepisosteus osseus*. BMC Develop. Biol. https://doi.org/10.1186/1471-213X-1-6.

Maitland, P. S. and R. N. Campbell. 1992. Freshwater Fishes of the British Isles. Harper Collins. 368 p.

Massar, B. 2015. Scanning electron microscopy of adhesive apparatus of *Garra lissorhynchus* (McClelland) of Meghalaya, India. International Research Journal of Biological Sciences 4(2):48-53.

Maurakis, E. G., W. S. Woolcott, and J. T. Magee. 1990. Pebble-nest microhabitats of *Semotilus* species. Proc. Southeast. Council of Fishes. 22:7-13.

Maurakis, E. G., M. H. Sabaj, and W. S. Woolcott. 1993. Pebble nest-construction and spawning behaviors in *Semotilus thoreauianus* (Pisces: Cyprinidae). Bull. Assoc. Southeast. Biol. 40(2):27-30.

Morrison, C. M., T. Miyake, and J. Wright, Jr. 2001. Histological study of the development of the embryo and early larva of *Oreochromis niloticus* (Pisces: Cichlidae). Journal of Morphology. 247:172-195.

Meijide, F. J. and G. A. Guerrero. 2000. Embryonic and larval development of a substrate-brooding cichlid *Cichlasoma dimerus* (Heckel, 1840) under laboratory conditions. Journal of Zoology 252(4):481-483.

Merriam-Webster. 2016. Merriam-Webster's Dictionary. https://www.merriam-webster.com (2 January, 2018).

Peters, H. M. 1965. Uber larvale *Haftorgane bei* Tilapia (Cichlidae, Teleostei) und ihre Rückbildung in der Evolution. Zool. J. Physiol. 71:287–300.

Pottin, K. H., C. Hyacinthe, and S. Rétaux. 2010. Conservation, development, and function of a cement gland-like structure in the fish *Astyanax mexicanus*. Proc. Nat. Acad. Sci. 107(40):17256-61.

Rao, R. S., S. Patil, B. Majumdar, and R. G. Oswal. 2014. Comparison of special stains for keratin with routine hematoxylin and eosin stain. Journal of International Oral Health 7(3):1-5.

Rétaux, S. and K. Pottin. 2011. A question of homology for chordate adhesive organs. Commun. Integr. Biol. 4(1): 75–77.

Roberts, T. 1982. Unculi (horny projections arising from single cells), an adaptive feature of the epidermis of ostariophysan fishes. Zoological Scripta 11(1):55-76.

Schäperclaus, W. 1962. Traité de pisciculture en étang. Vigot Frères, Paris.

Snyder, D., S. C. Seal, J. A. Charles, and C. L. Bjork. 2016. Cyprinid fish larvae and early juveniles of the Upper Colorado River Basin – morphological descriptions, comparisons, and computer-interactive keys. Colorado Parks and Wildlife Technical Publication 47. 226 p.

Sola, L., S. Cataduella, G. Gentili, and G. Monaco. 1983. An experimental carp x tench hybrid: Karyological analysis and SEM morphological observations, Bolletino di zoologia, 50(3-4):159-171.

Spence, R., G. Gerlach, C. Lawrence, and C. Smith. 2008. The behaviour and ecology of the zebrafish, *Danio rerio*. *Biological Reviews*, 83: 13-34.

Steffens, W. 1980. Der Karpfen. Neue Brehm Bucherei Nr, 203, Ziemsen, Wittenberg, Lutherstadt, Deutschland. 215 p.

Suzuki, N., N. Akiyama, and T. Hibiya. 1985. Development of the bitterling *Rhodeus uyekii* (Cyprinidae), with a note on minute tubercles on the skin surface. Japanese J. Ichthyology 32(1):28-34.

Wallus, R. and T. P. Simon. 2008. Reproductive biology and early life history of fishes in the Ohio River drainage: Elassomatidae and Centrarchidae. Vol. 6. 472 p.

Yap, F. C., W. Wong, A. G. Maule, G. P. Brennan, V. C. Chong, and L. H. S. Lim. 2017. First evidence for temporary and permanent adhesive systems in the stalked barnacle cyprid, *Octolasmis angulata*. Sci. Rep. 7, 44980; doi: 10.1038/srep44980.

Table 1. Diversity of terminology used to describe the attachment mechanisms of larval and adult organisms to substrates.

Name	Species	Stage	Family	Group	Reference
cement gland	*Xenopus laevis*	larvae	Pipidae	Amphibia	Sive & Bradley, 1996
"	*Pterophyllum scalare*	larvae	Cichlidae	Actinopterygii	Bennemann & Pietzsch-Rohrschneider, 1978
"	*Octolasmis angulata*	larvae	Poecilasmatidae	Crustacea	Yap et al., 2017
cement gland apparatus	*Pterophyllum scalare*	larvae	Cichlidae	Actinopterygii	Groppelli et al., 2003
cement gland-like structure	*Astyanax mexicanus*	larvae	Characidae	Actinopterygii	Pottin et al., 2010
casquette	*Astyanax mexicanus*	larvae	Characidae	Actinopterygii	Pottin et al., 2010
temporary adhesive gland	*Octolasmis angulate*	larvae	Poecilasmatidae	Crustacea	Yap et al. 2017
adhesive apparatus	*Pseudocheneis sulcatus*	adult	Sisoridae	Actinopterygii	Joshiet et al., 2011
"	*Glyptothorax pectinopterus*	adult	Sisoridae	Actinopterygii	Joshiet et al., 2011
"	*Garra lissorhynchus*	adult	Cyprinidae	Actinopterygii	Massar, 2015;
adhesive gland	*Cichlasoma dimerus*	larvae	Cichlidae	Actinopterygii	Meijide & Guerrero, 2000
"	*Tilapia marie*	larvae	Cichlidae	Actinopterygii	Retaux & Pottin, 2011
"	*Cyprinus carpio*	larvae	Cyprinidae	Actinopterygii	Applebaum & Riehl, 1997
adhesive organ	*Amia calva*	larvae	Amiidae	Actinopterygii	Eycleshymer & Wilson, 1908
"	*Lepisosteus osseus*	larvae	Lepisosteidae	Actinopterygii	Long & Ballard, 2001; Retaux & Pottin, 2011
"	*Hoplerythrinus unitaeniatus*	larvae	Erythrinidae	Actinopterygii	Gomes et al., 2007
"	*Hoplias lacerdae*	larvae	Erythrinidae	Actinopterygii	Gomes et al., 2007
"	*Hoplias malabaricus*	larvae	Erythrinidae	Actinopterygii	Gomes et al., 2007
"	*Brycon orthotaenia*	larvae	Characidae	Actinopterygii	Gomes et al., 2011
attachment organ	*Apteronotus albifrons*	larvae	Gymnotidae	Actinopterygii	Britz et al., 2000
"	*Apteronotus leptorhynchus*	larvae	Gymnotidae	Actinopterygii	Britz et al., 2000
glue secretion & adhesion	*Pteronotropis hypselopterus*	larvae	Cyprinidae	Actinopterygii	Fletcher & Wilkins, 1999

Figure 1. Epidermis of lateral views of newly hatched larvae of A. *Semotilus atromaculatus* (note abundance of apical pores of goblet cells), B. *Hybognathis hankinsoni* (note abundance of white dots on dorsal, lateral, and ventral cephalic epidermal areas and anterioventral epidermis of yolk sac identified as unculi-like projections under higher magnification), C. *Notemigonus crysoleucas* (note absence of white dots on dorsum but abundance of white dots on lateral and ventral cephalic areas and anterioventral yolk sac epidermis identified as unculi-like projections under higher magnification), D. dorsal cephalic view of newly hatched larva of *Cyprinus carpio* (note nubby unculi-like projections on dorsum and longer ones on lateral cephalic areas), and E. ventral cephalic view of *Gila atraria* (note white dots on ventral cephalic area and on anterioventral yolk sac epidermal areas identified as unculi-like projections under higher magnification).

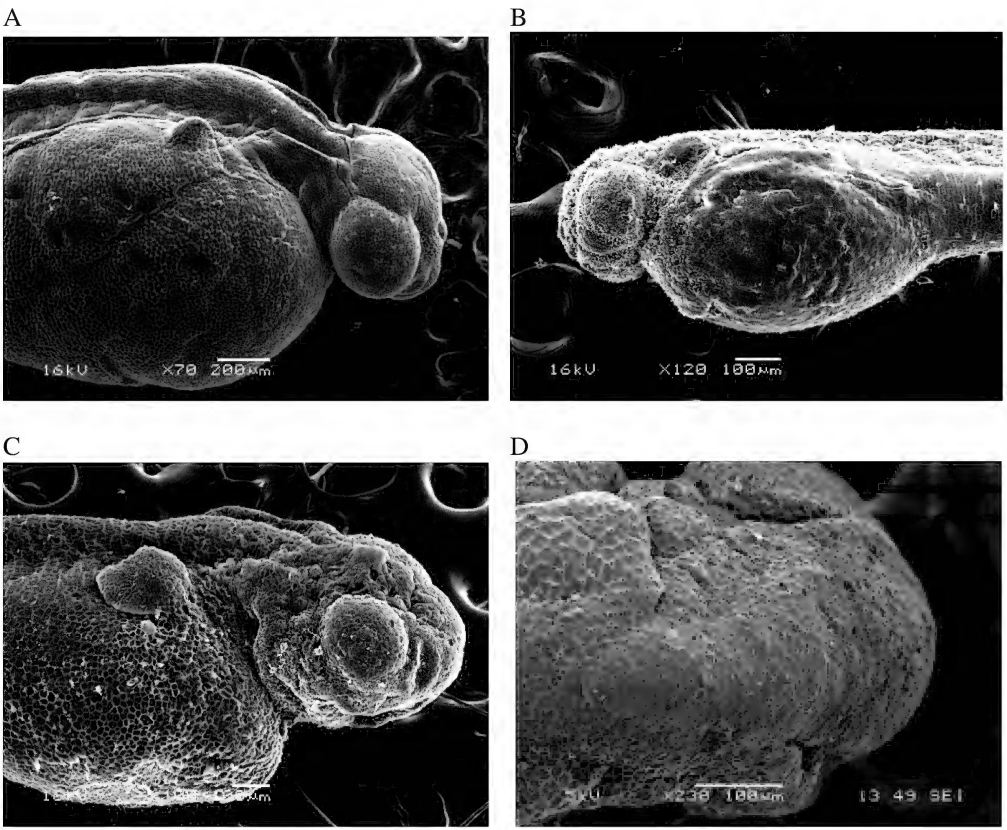

E

Figure 2. Dorsal cephalic epidermal areas of newly hatched larvae. A. *Semotilus atromaculatus* (numerous pores surrounded by hexagonal epidermal cells without unculi-like projections, well-defined microridge (MR) pattern, and free neuromasts (triangle), B. *Hybognathis hankinsoni* with well-defined MR and widespread unculi-like projections, C. *Notemigonus crysoleucas* hexagonal cells with well-defined MR and no unculi-like projections, D. *Cyprinus carpio* with widespread nubby unculi-like projections on dorsum and well defined unculi-like projections on lateral cephalic area, E. *Gila atraria* with short MR, widespread well-defined unculi-like projections on dorsum, and developing olfactory organ (triangle), F. *H. hankinsoni* (thick mucus embedded with debris; note unculi-like projections on lateral cephalic margin), and *G. atraria* (heavy mucus coating embedded with debris on dorsal epidermis).

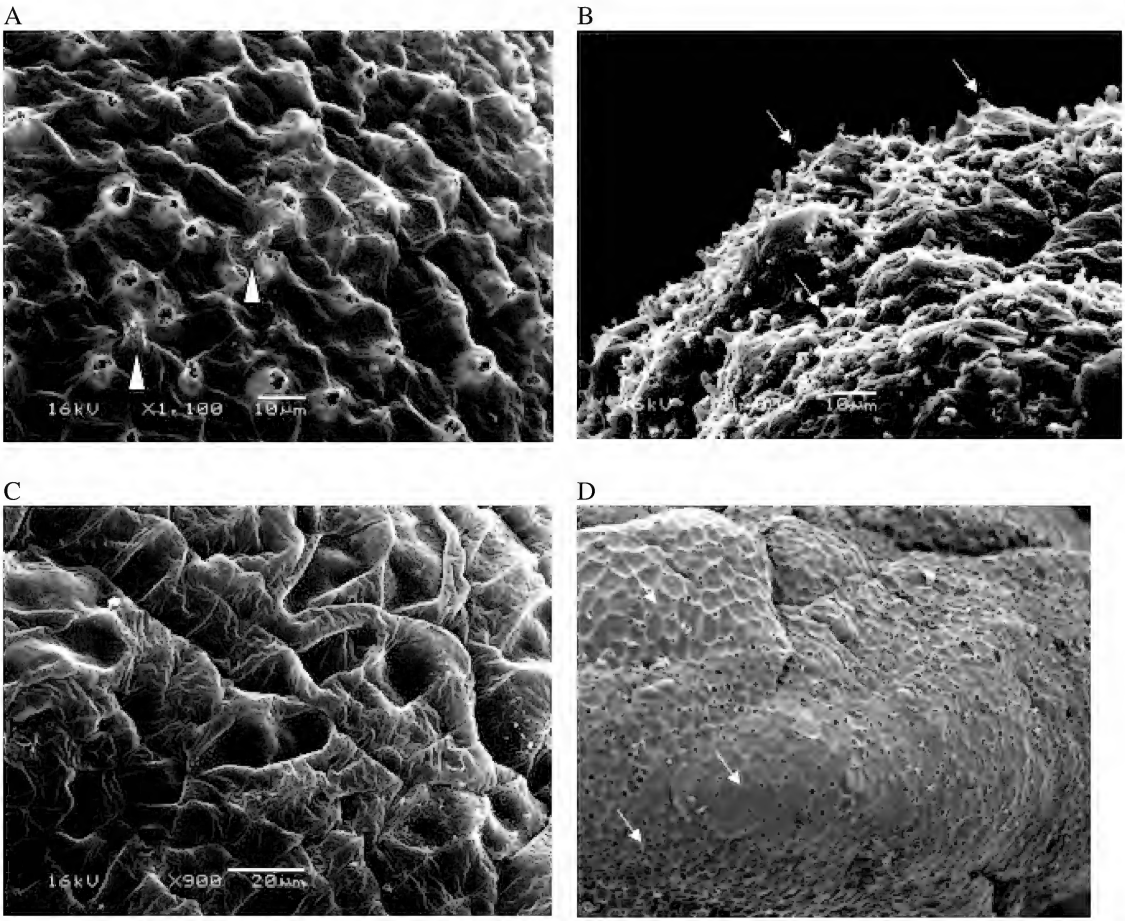

E

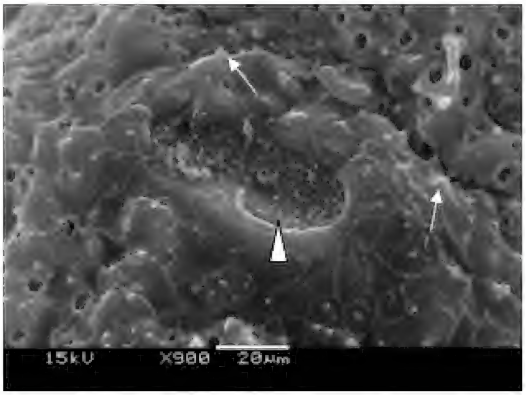

F

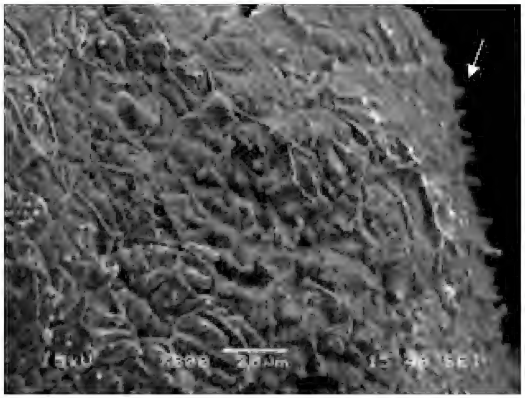

G

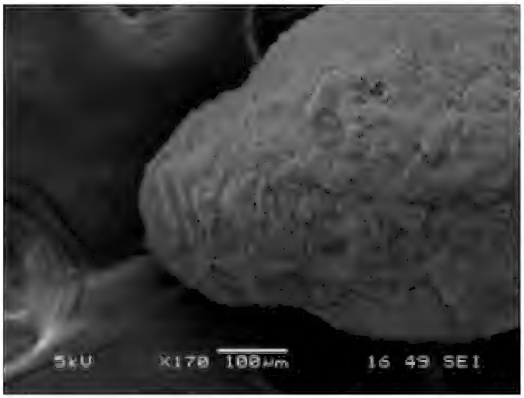

Figure 3. Ventral cephalic epidermal areas of newly hatched larvae. A. *Semotilus atromaculatus* (epidermal cells and apical pores of goblet cells and no unculi-like projections, B. *Hybognathis hankinsoni* (abundant unculi-like projections emanating primarily from cell centers, and apical pores of goblet cells, C. *Notemigonus crysoleucas* (abundant and long unculi-like projections), D. *Cyprinus carpio* (unculi-like projections and apical pores of goblet cells abundant displaying some segregation of cell types), E. *Gila atraria* (abundant unculi-like projections emanating from cell centers and at or near the cell peripheries, and abundant apical pores of goblet cells), F. *N. crysoleucas* (anteriolateral cephalic epidermis contains long unculi-like projections), G. *C. carpio* (mucus covering epidermal unculi-like projections on anterioventral portion of head), and H. *G. atraria* (unculi-like projections emanate from central and at or near cell peripheries).

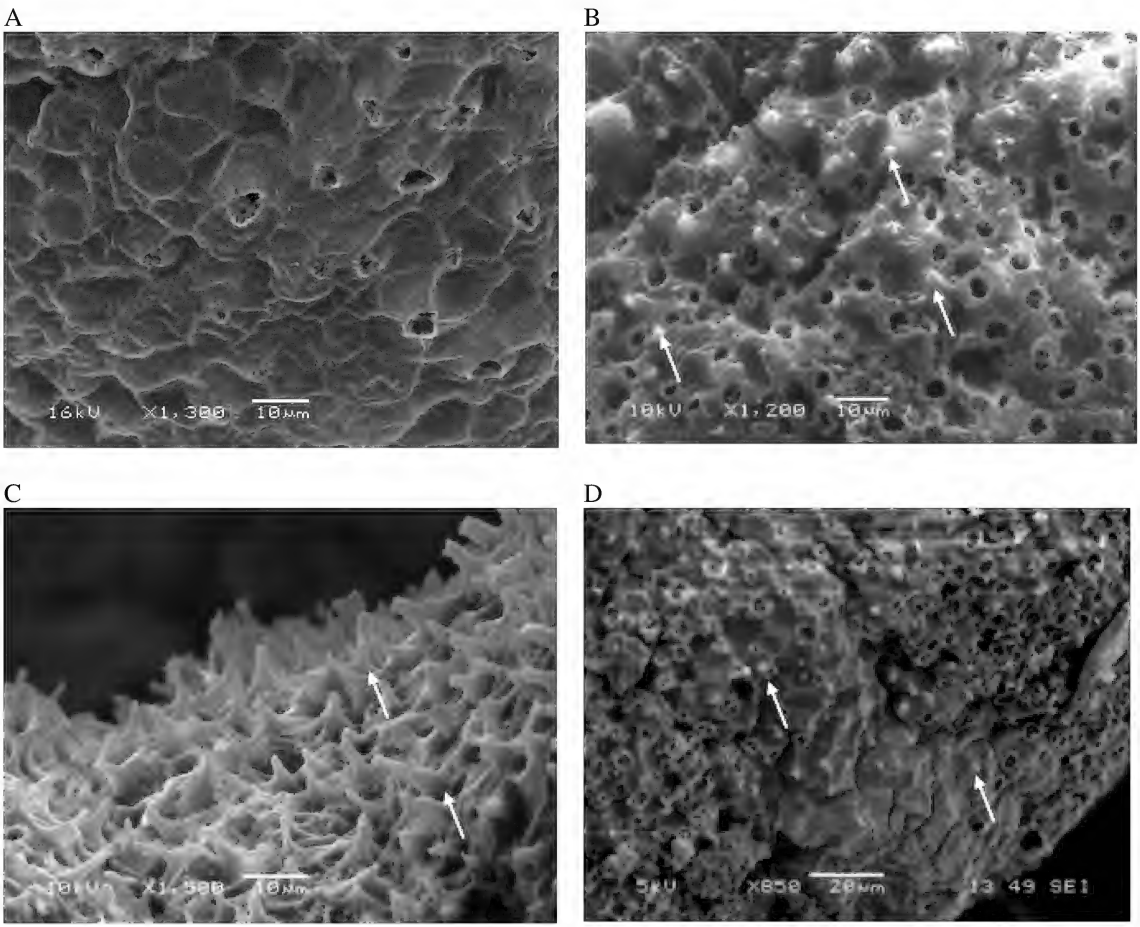

E

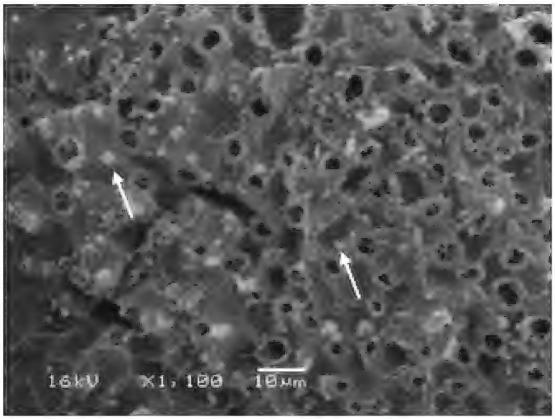
15kV X1,100 10μm

F

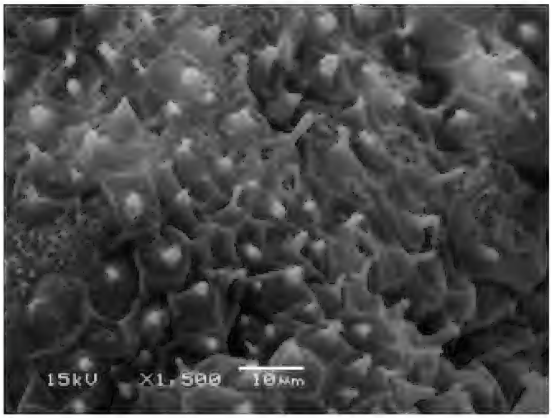
15kV X1,500 10μm

G

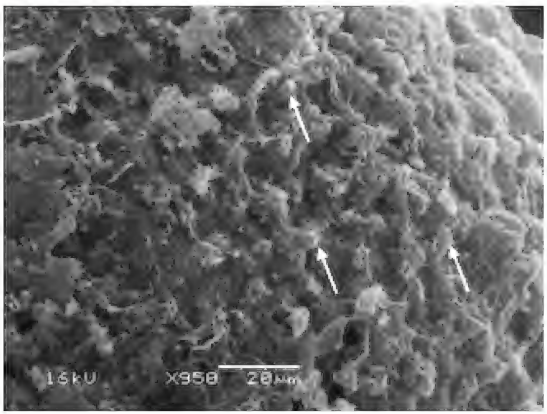
15kV X950 20μm

H

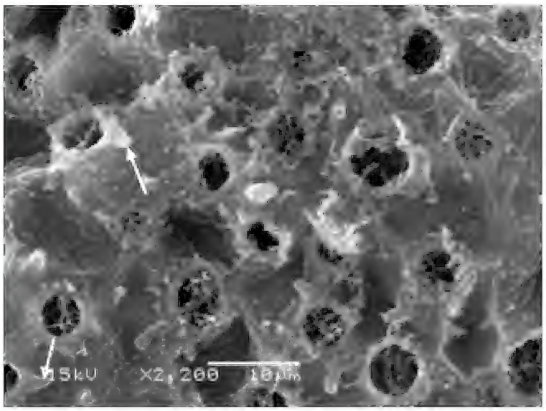
15kV X2,200 10μm

Figure 4. Anterioventral yolk sac epidermal areas of newly hatched larvae. A. *Semotilus atromaculatus* (apical pores and no unculi-like projections), B. *Hybognathis hankinsoni* (long unculi-like projections), C. *Notemigonus crysoleucas* (well developed to nubby unculi-like projections present), D. *Cyprinus carpio* (unculi-like projections present), E. *Gila atraria* (well-developed unculi-like projections and numerous pores present), F. *N. crysoleucas* (well-developed unculi-like projections), and G. *C. carpio* (unculi-like projection magnified at 3,700x).

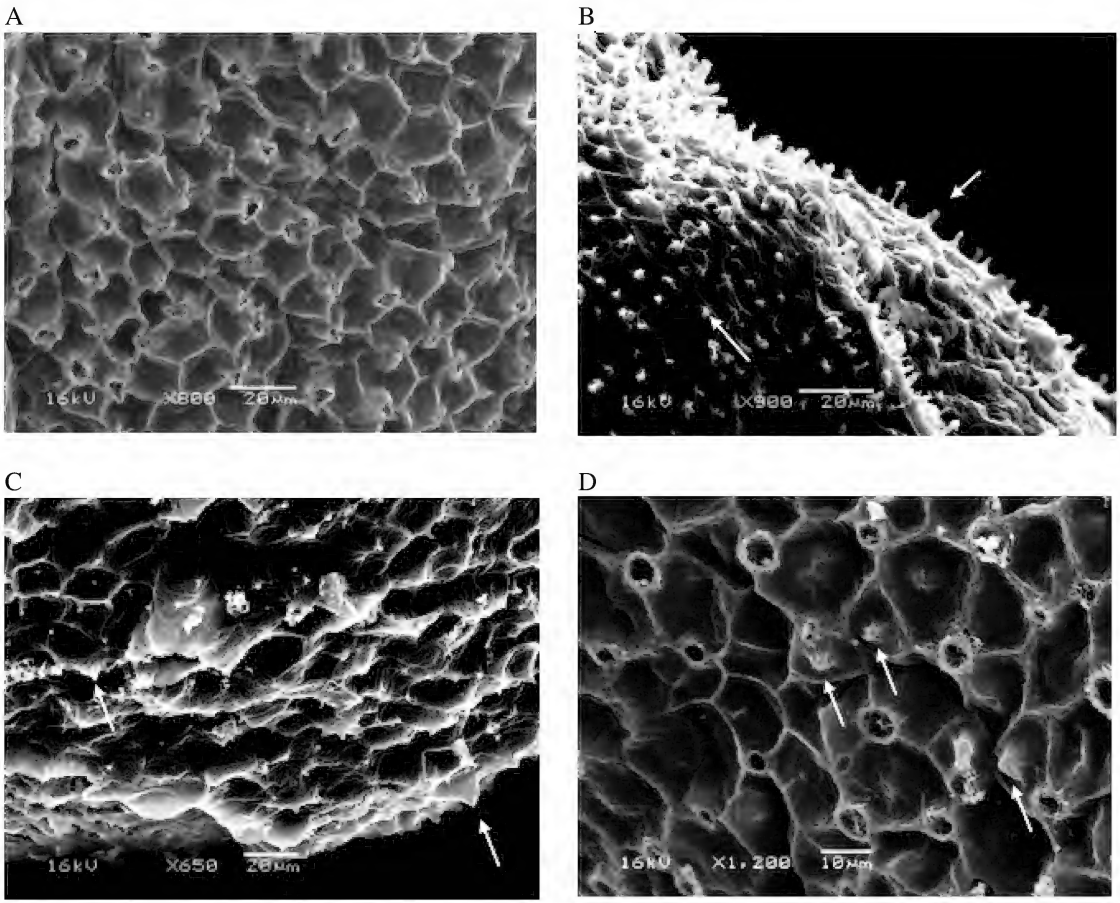

E

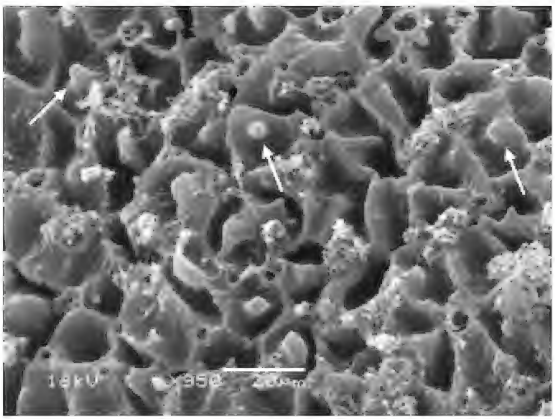

F

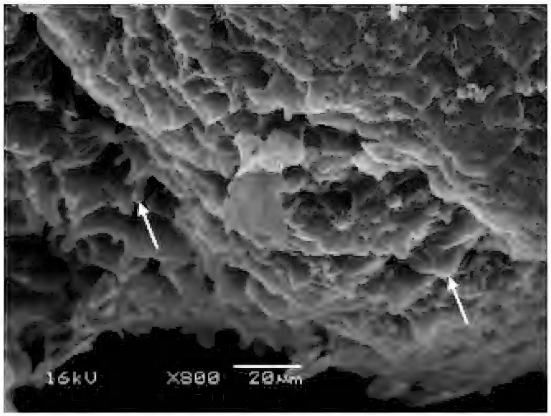

G

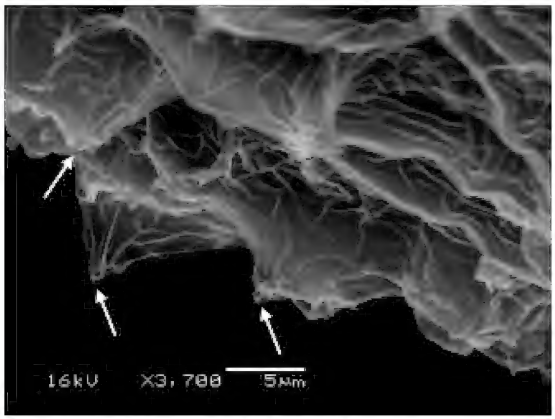

Figure 5. Ventrolateral trunk epidermal areas of newly hatched larvae. A. *Semotilus atromaculatus* (unculi-like projections absent), B. *Hybognathis hankinsoni* (unculi-like projections present), C. *Notemigonus crysoleucas* (unculi-like projections absent on lateral trunk), D. *Cyprinus carpio* (unculi-like projections increase towards ventral finfold), E. *Gila atraria* (few unculi-like projections present on ventrolateral and ventral epidermal cells), and F. *N. crysoleucas* (unculi-like projections present on ventral trunk.

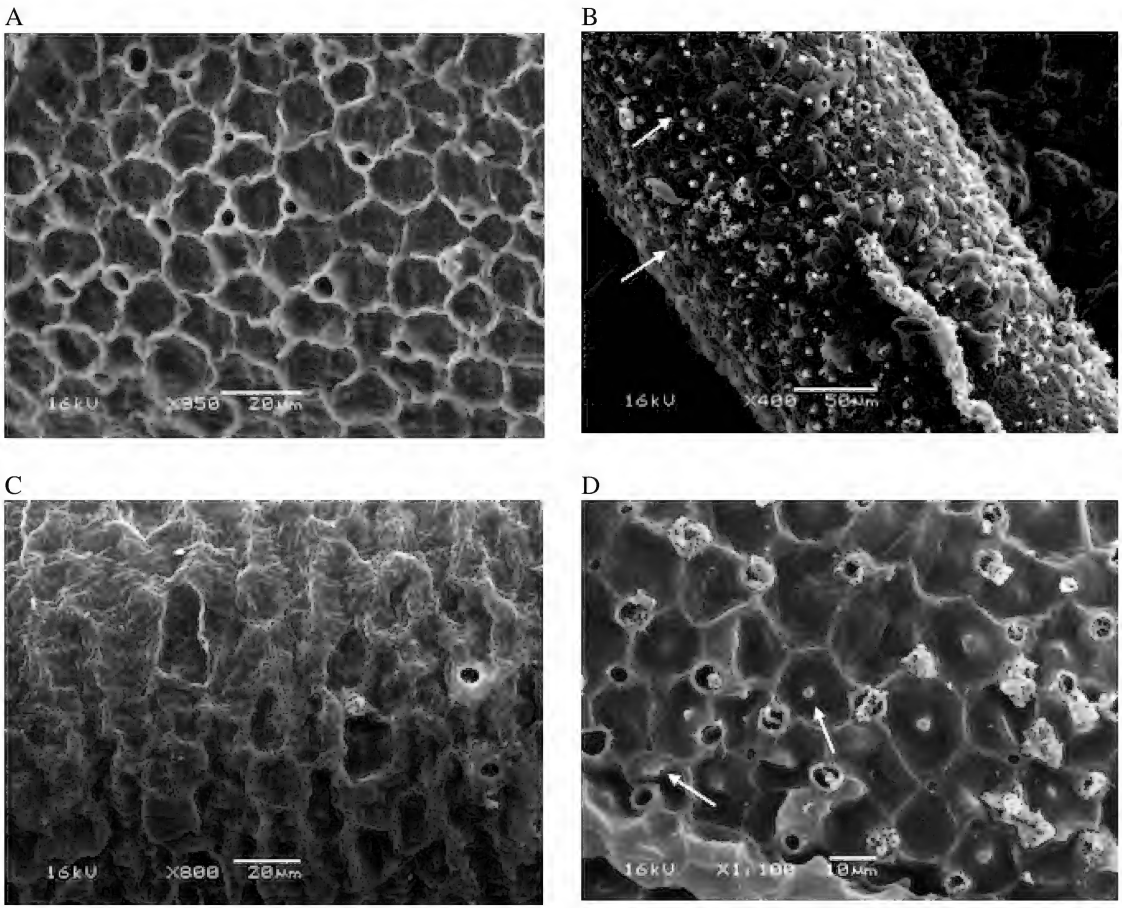

E

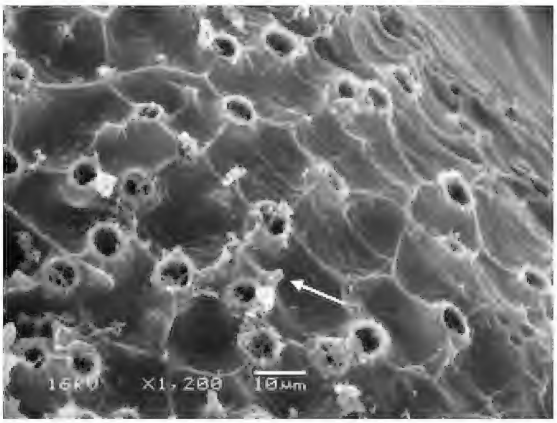

F

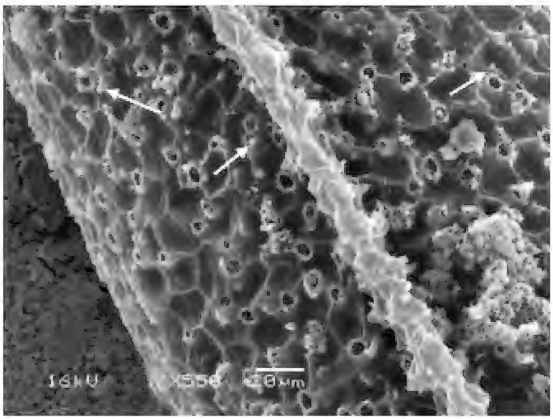

Virginia Journal of Science
Volume 68, Issue 3 & 4
Fall & Winter 2017
doi: 10.25778/WGGY-JY81

Note: This manuscript has been accepted for publication and is online ahead of print. It will undergo copyediting, typesetting, and review of the resulting proof before it is published in its final form.

The Effects of Climate on Radial Growth of Disjunct Northern White Cedar (*Thuja occidentalis L.*) in Virginia

Joshua A. Kincaid

Shenandoah University
1460 University Drive, Winchester, Virginia, USA 22601
Email: jkincaid@su.edu Phone: (540)-665-4909

ABSTRACT

Understanding the geographic range and growth of species is essential for effective land management in a landscape affected by anthropogenic activity and climate change. Climate change is expected to alter the distribution and growth of many tree species in eastern North America, including northern white cedar (*Thuja occidentalis* L.). This research examined the effects of climate on radial growth of *T. occidentalis* in disjunct populations south of its continuous range margin in eastern North America. A *T. occidentalis* tree-ring chronology was developed and examined for growth-climate interactions. Mean sensitivity of the *T. occidentalis* chronology was within the range of values reported for the species in northern portions of its range. Significant positive correlations existed between the *T. occidentalis* chronology and moisture variables late in the growing season of the previous year and current year. The relationship between the *T. occidentalis* chronology and temperature was more variable with significant positive and negative correlations throughout the previous year and current year. The Ordinary Least Squares (OLS) regression model suggested moisture conditions late in the growing season of the previous year and current year had a significant positive influence on the growth of *T. occidentalis*. In contrast, maximum temperature in March of the current year negatively influenced the growth of *T. occidentalis*. While the mean sensitivity of *T. occidentalis* appears similar throughout its range, there is geographic variability in the climate-growth response of *T. occidentalis*. More research is necessary to expand the scope of our knowledge concerning *T. occidentalis* growth throughout its range.

Keywords: *Thuja occidentalis,* Climate, Range, Tree rings, Disjunct

INTRODUCTION

Species located at or beyond the margins of their continuous range are often assumed to be more sensitive to ecological factors such as climate. It is hypothesized that one or more ecological factors become less favorable and more stressful for species located at increasing distances from their range center (Guo et al. 2005; Hart et al. 2010). If disjunct species are indeed more sensitive, then stress should be evident in their growth characteristics. Even if marginal ecological factors remain favorable for a species, conditions may differ from those experienced by more centrally located populations (Lesica and Allendorf 1995; Hardie and Hutchins 2010). Marginal populations are of particular interest to scientists because they may represent hearths for species with unique biological tolerances, variable genotypes, atypical morphologies and life history characteristics (Hardie and Hutchins 2010). With ongoing environmental transformation driven by anthropogenic activity and climate change, it is essential for effective land management that we understand the geographic range and growth characteristics of species. Climate change will likely alter the growth and distribution of many tree species in eastern North America. While climate change will increase the amount of suitable habitat for some species, other species such as *Thuja occidentalis* L. will experience great reductions in habitat (Iverson et al. 2008).

Thuja occidentalis, also known as arborvitae or northern white cedar, is a slow-growing and shade tolerant coniferous tree species native to eastern North America. The continuous range of *T. occidentalis* extends across southeastern Canada to the Great Lakes and New England regions of the United States. Isolated, disjunct populations exist south of the continuous range and throughout the Appalachian Mountains as far south as Tennessee, USA (Caplenor and Speir 1975; Walker 1987). Southern disjunct populations are typically small (0.1 to 1.0 ha) and rare, often restricted to steep, north-facing slopes or cliffs situated in stream or river valleys (Fleming 1999; Fleming and Coulling 2001). It has been suggested that these isolated habitats represented a glacial refugium for *T. occidentalis* and associated species (Larson et al. 1999).

Despite the extensive distribution of *T. occidentalis*, research examining the effects of climate on its growth has been limited in geographic scope, with most studies originating from northern portions of its range (e.g. Kelly et al. 1994; Kelly and Larson 1997; Tardiff and Bergeron 1997; Kipfmueller et al. 2010). Because heterogeneous conditions exist throughout a species range, previous research may be overlooking geographic variation in the growth characteristics of *T. occidentalis*. Previous studies have examined the growth of *T. occidentalis* in disjunct populations near its northern and northwestern range margins in Canada, but no such research originating from southern portions of the range exists (Tardiff and Stevenson 2001; Paul et al. 2014). Research examining *T. occidentalis* in southern disjunct populations has been limited to studies of forest community ecology and population biology (Walker 1987; Young 1996; Fleming 1999; Fleming and Coulling 2001).

The overall purpose of this research is to document the effects of climate on radial growth of *T. occidentalis* in disjunct populations south of its continuous range margin. Two specific objectives are posed by this research: 1) to develop a tree-ring chronology for *T. occidentalis* in Virginia; and 2) to quantify the relationship between *T. occidentalis* radial growth and climate variables.

MATERIALS AND METHODS

Study area

Sampling for this research was conducted in Rockingham County, Virginia, USA (Figure 1). Rockingham County lies predominantly within the Ridge and Valley physiographic province but is bounded by the Appalachian Mountains to the west and Blue Ridge Mountains to the east. Elevation varies within the county from approximately 274 m to 1335 m. Mean annual precipitation in the study area is 852 mm with 61% of it occurring between May and October. The mean annual temperature is 13.3°C with a mean seasonal range of 2.9°C to 23.7°C (SERCC 2016). Frost-free conditions (i.e. the growing season) typically extend from April to October.

The *T. occidentalis* forests examined in this research occurred at a mean elevation of 367 ± 16.3 m. Each forest was located on a steep (31-47%), north to northwest-facing slope with soils derived from calcareous bedrock. The structures and disturbance dynamics of these forests were quantified by Kincaid (2016). *T. occidentalis* was a canopy dominant in the study area, representing > 60% of the basal area at each sample location. Despite its dominant position in the overstory, there were low numbers of *T. occidentalis* stems in the smallest size classes. Other canopy species included *Liriodendron tulipifera* L., *Pinus strobus* L., and *Tilia americana* L. Stand dynamics were characterized by canopy gap-scale processes that generally affected a small number of trees each decade (Kincaid 2016).

Field and Laboratory Methods

Two *T. occidentalis* forest stands were sampled for this study (Kincaid 2016). Increment borers were used to extract cores from canopy trees along a 100-m transect at each site. Each tree was cored at breast height (1.4 m) and parallel to slope contours to avoid reaction wood, which can distort radial growth patterns. Canopy tree selection was accomplished using the point-quarter method every 10 m along transects where slope conditions allowed safe access (Cottam and Curtis 1956). Each transect was situated midslope and parallel to slope contours to avoid forest-environment transitions. A single transect was used at each site because the forests exhibited oblong dimensions and were located on steep slopes.

In preparation for laboratory analyses, all cores were air-dried, glued to wood mounts, and sanded with progressively finer grits of sand paper (Phipps 1985; Stokes and Smiley 1996). The growth rings on all cores were visually enumerated and crossdated using the list method (Yamaguchi 1991). Individual cores were measured to the nearest 0.001 mm using a Velmex measuring stage and Measure J2X software. The accuracy of crossdating was assessed using the computer program COFECHA (Holmes 1983; Grissino-Mayer 2001). COFECHA uses correlation analyses to examine the association between a single measurement series and a master chronology created from the other series. Measurement series that were poorly correlated with the master chronology were checked and corrected or eliminated from further analyses. A total of 42 tree cores were examined in this research (Kincaid 2016).

Radial growth-climate analyses

The computer program ARSTAN was used to standardize the raw tree-ring measurements (Cook 1985). Detrending of the raw tree-ring measurements was accomplished using a 30-year cubic smoothing spline. Standardization reduces the effects of tree age and stand

dynamics, which allows for comparisons among trees with different growth rates. I used the RESIDUAL chronology produced by ARSTAN because autoregressive modelling has removed autocorrelation in the tree-ring data, which can bias the results of statistical tests such as correlation and regression. However, removing autocorrelation from the chronology can make it less sensitive to the signal of interest (Speer 2010).

I evaluated the relationships between monthly climate data and the *T. occidentalis* RESIDUAL chronology using Pearson correlation analysis. Climate data for Virginia Climate Division 5 were obtained from the National Climate Data Center. Virginia Climate Division 5 data were interpolated from stations using a 5 km grid resolution (NCDC 2015). The monthly climate variables examined in this research included total precipitation, Palmer Drought Severity Index (PDSI), mean temperature, maximum temperature, and minimum temperature for the previous year (year t-1) and current year (year t). The RESIDUAL chronology and monthly climate variables were examined using a 17-month window from June of the previous year to October of the current year.

To complement the Pearson correlation analysis, I used ordinary least-squares (OLS) regression to model the overall relationship between the *T. occidentalis* RESIDUAL chronology and climate variables (Chang and Aguilar 1980; Grissino-Mayer and Butler 1993; Parker et al. 2001). OLS regression was used instead of response function analysis because regression explicitly permits interaction among multiple climate variables, providing for an integrative explanatory model (Parker et al. 2001). In addition to examining previous year and current year monthly climate data, I included seasonal variables such as June through August total precipitation and March through May mean temperature. The inclusion of variables representing multiple consecutive months allows for direct examination of the effects of seasonal climate on tree growth and facilitates the estimation of a parsimonious model (Parker et al. 2001). A best subsets regression approach was used to screen all variables and models.

RESULTS

The *T. occidentalis* chronology examined in this research extended from 1895 to 2010 and contained a minimum sample depth of 3 trees. Sample depth consisted of 12 trees by 1929, and increased to 42 trees in 1963 (Figure 2). Intertree and intratree mean correlations were 0.489 and 0.558, respectively. Mean sensitivity of the chronology, which is a measure of the year-to-year variability in tree-rings, was 0.187 ± 0.19. Periods of above mean growth were sustained for 3 to 7 years while below mean growth events spanned 3 to 4 years.

Radial growth of *T. occidentalis* was significantly influenced by monthly precipitation variables. Significant positive relationships ($p < 0.01$) were observed between the *T. occidentalis* chronology and precipitation variables (Figure 3). Increases in *T. occidentalis* radial growth were associated with increases in total precipitation during the previous October and current August-September months. The correlation between *T. occidentalis* growth and monthly PDSI was higher and more significant than with precipitation or temperature. Monthly PDSI values were positively associated with *T. occidentalis* radial growth during the months of July through October of the current year. The PDSI integrates precipitation and temperature data, which may

more closely reflect the conditions significant to tree growth. Positive PDSI values indicate moist conditions, while negative values reflect increasingly dry conditions.

Significant positive and negative relationships ($p < 0.01$) were observed between the *T. occidentalis* chronology and temperature variables (Figure 4). The radial growth of *T. occidentalis* was positively associated with previous August and current August temperatures. Temperatures in March, July, and September of the current year were negatively associated with *T. occidentalis* radial growth.

The OLS model produced an adjusted R^2 value of 0.311, which indicated a moderate amount of explanatory covariance between the climate variables and *T. occidentalis* chronology (Table 1). Two precipitation variables and one temperature variable were included in the final OLS model. Regression coefficients revealed that moisture conditions (i.e. precipitation and PDSI) near the end of the growing season of the previous year and current year positively affected *T. occidentalis* growth. Maximum temperature in March of the current year had a significant negative effect on the radial growth of *T. occidentalis*.

DISCUSSION

Climate was an important influence on the radial growth of *T. occidentalis* in southern disjunct populations. The mean sensitivity of *T. occidentalis* (0.187) in the study area was within the range of values documented for the species (range = 0.13 – 0.255) in northern portions of its range (Kelly et al. 1994; Tardiff and Bergeron 1997; Tardiff and Stevenson 2001; Kipfmueller et al. 2010). The mean sensitivity also was within the range of values expected for trees growing in eastern North America (DeWitt and Ames 1978). It is possible microsite conditions supporting southern disjunct populations of *T. occidentalis* are similar to conditions near the range center; therefore, the species is not necessarily more sensitive to ecological factors south of its continuous range margin (Brown 1984; Hart et al. 2010). Indeed, disjunct *T. occidentalis* populations in Virginia tend to occur along sheltered, north-facing slopes in stream or river valleys with limited solar exposure (Fleming 1999; Fleming and Coulling 2001).

The correlation coefficients and OLS model results revealed that moisture conditions during the late growing season of the previous year and current year were important influences on the radial growth of *T. occidentalis* in southern disjunct populations. Hart et al. (2010) documented a similar relationship between late growing season precipitation during the previous year and the growth of disjunct *Tsuga canadensis* (L.) Carr. south of its continuous range margin in eastern North America. Favorable moisture conditions late in the growing season may promote ongoing cambial activity and the storage of carbohydrates, which will be used to initiate new growth in the spring (Henderson and Grissino-Mayer 2009). The significance of late growing season moisture conditions to *T. occidentalis* growth in the study area contrasted with observations from northern portions of the range where early growing season conditions were more significant (Tardiff and Bergeron 1997; Tardiff and Stevenson 2001; Kipfmueller et al. 2010). The variation in growth responses of *T. occidentalis* to moisture conditions in particular portions of its range is likely related to a latitudinal gradient in growing season initiation and length.

Geographic and seasonal differences were also apparent in the relationship between temperature and *T. occidentalis* radial growth. Maximum temperature in March of the current year appeared to have a significant negative influence on *T. occidentalis* growth. Higher temperatures with limited moisture during the early growing season may facilitate rates of evapotranspiration that favor respiration over carbon assimilation (Henderson and Grissino-Mayer 2009). In contrast, the growth responses of northern populations were positively influenced by early growing season temperatures (Kelly et al. 1994; Tardiff and Bergeron 1997; Tardiff and Stevenson 2001). Prior research from northern portions of the range has also reported negative relationships between previous August temperatures and *T. occidentalis* growth, but this was not evident in the current study (Kelly et al. 1994; Tardiff and Bergeron 1997; Tardiff and Stevenson 2001). The positive association between tree growth and late summer temperatures has been observed in *Chamaecyparis thyoides* L. (Atlantic white cedar; Hopton and Pederson 2005), as well as other conifers in the southern United States (Henderson and Grissino-Mayer 2009). Abundant precipitation and moderate temperatures late in the growing season may facilitate favorable rates of photosynthesis, respiration, and carbohydrate storage for *T. occidentalis* in southern disjunct populations. However, maximum temperatures in July and September of the current year were negatively related to growth, so there appears to be an upper limit, beyond which temperature begins to negatively affect *T. occidentalis* growth.

CONCLUSION

While the sensitivity of *T. occidentalis* growth to climate appears similar throughout its range, there is geographic and seasonal variation in the climate-growth relationships elucidated in this research. These differences in growth responses are likely the result of latitudinal variation in growing season conditions within the geographic range of *T. occidentalis*. Some researchers have suggested that *T. occidentalis* growth at its northern range margin is not significantly limited by climate, particularly temperature (Tardiff and Stevenson 2001; Paul et al. 2014). I hypothesize that maximum temperatures during the early growing season in conjunction with late growing season moisture availability influence the southern extent of *T. occidentalis* in disjunct populations. The current study has elucidated differences in the growth responses of *T. occidentalis* in southern disjunct populations compared to their northern counterparts. More research is clearly necessary to expand the geographic scope of our knowledge concerning *T. occidentalis* ecology and growth, particularly in more southern locations. This additional research should also explore the temporal stability of the climate-growth relationships documented in this research. Indeed, changes in climate have been associated with temporal shifts in the climate-growth relationships of other tree species, including *T. canadensis*, which frequently co-occurs with *T. occidentalis* in the study area (Marcinkowski et al. 2015; Saladyga and Maxwell 2015).

ACKNOWLEDGMENTS

I would like to thank Gary Fleming and Wendy Hochstedler for information regarding the study area. I also thank Angela Felicio, Cory Miller, and Kirby Talbert for assistance in the field and laboratory. This manuscript was improved by comments from Doug Enders and two anonymous reviewers.

LITERATURE CITED

Brown, J. H. 1984. On the relationship between abundance and distribution of species. The American Naturalist 124:255-279.

Caplenor, D. and H. Speir. 1975. *Thuja occidentalis* L. on the Eastern Highland Rim in Tennessee. Journal of the Tennessee Academy of Science 50:74-75.

Chang, M. and G. J. R. Aguilar. 1980. Effect of climate and soil on the radial growth of loblolly pine (*Pinus taeda* L.) in a humid environment of Southeastern USA. Forest Ecology and Management 3:141-150.

Cook, E. R. 1985. A time series analysis approach to tree-ring standardization. Ph.D. thesis, University of Arizona, Tucson.

Cottam, G. and J. T. Curtis. 1956. The use of distance measures in phytosociological sampling. Ecology 37:451-460.

DeWitt, E. and M. Ames. 1978. Tree-ring chronologies of eastern North America, Laboratory of tree-ring research, Chronology series IV, Volume 1. University of Arizona, Tucson.

Fleming, G. P. 1999. Plant communities of limestone, dolomite, and other calcareous substrates in the George Washington and Jefferson national forests, Virginia. Virginia Department of Conservation and Recreation, Division of Natural Heritage, Natural Heritage Technical Report 99-4.

Fleming, G. P. and P. P. Coulling. 2001. Ecological communities of the George Washington and Jefferson national forests, Virginia. Preliminary classification and description of vegetation types. Virginia Department of Conservation and Recreation, Division of Natural Heritage, Natural Heritage Technical report 01-1.

Grissino-Mayer, H. D. 2001. Evaluating crossdating accuracy: a manual and tutorial for the computer program COFECHA. Tree-Ring Research 57:205-221.

Grissino-Mayer, H. D. and D. R. Butler. 1993. Effects of climate on growth of shortleaf pine (*Pinus echinata* Mill.) in northern Georgia: A dendroclimatic study. Southeastern Geographer 33:65-81.

Guo, G. Q., M. Taper, M. Schoenberger and J. Brandle. 2005. Spatial-temporal population dynamics across species range: from centre to margin. Oikos 108:47-57.

Hardie, D.C. and J. A. Hutchings. 2010. Evolutionary ecology at the extremes of species' ranges. Environmental Reviews 18:1-20.

Hart, J. L., S. L. van de Gevel, J. Sakulich and H. D. Grissino-Mayer. 2010. Influence of climate and disturbance on the growth of *Tsuga canadensis* at its southern limit in eastern North America. Trees 24:621-633.

Henderson, J. P. and H. D. Grissino-Mayer. 2009. Climate-tree growth relationships of longleaf pine (Pinus palustris Mill.) in the southeastern Coastal Plain, USA. Dendrochronologia 27:31-43.

Holmes, R.L. 1983. A computer-assisted quality control in tree-ring dating and measurement. Tree-Ring Bulletin 43:69-78.

Hopton, H. M. and N. Pederson. 2003. Climate sensitivity of Atlantic White Cedar at its northern range limit. In: Burke M.K. and P. Sheridan (eds.) Atlantic White Cedar: ecology, restoration, and management. Proceedings of the Arlington Echo Symposium, Millersville, MD.

Iverson L. R., A. M. Prasad, S. N. Matthews, and M. Peters M. 2008. Estimating potential habitat for 134 eastern US tree species under six climate scenarios. Forest Ecology and Management 254:390-406.

Kelly, P. E., E. R. Cook and D. W. Larson. 1994. A 1397-year tree-ring chronology of *Thuja occidentalis* from cliff faces of the Niagara Escarpment, southern Ontario, Canada. Canadian Journal of Forest Research 24:1049-1057.

Kelly, P. E. and D. W. Larson. 1997. Dendroecological analysis of the population dynamics of an old-growth forest on cliff-faces of the Niagara Escarpment, Canada. Journal of Ecology 85:467-478.

Kincaid, J. A. 2016. Structure and dendroecology of *Thuja occidentalis* in disjunct stands south of its contiguous range in the central Appalachian Mountains, USA. Forest Ecosystems 3:25.

Kipfmueller, K. F., G. P. Elliott, E. R. Larson and M. W. Salzer. 2010. An assessment of the dendroclimatic potential of three conifer species in northern Minnesota. Tree-Ring Research 66:113-126.

Larson D. W., U. Matthes-Sears, and P. E. Kelly. 1999. The cliff ecosystem of the Niagara Escarpment. In Anderson R. C., J. S. Fralish, and J. M. Baskin (eds.) Savannas, barrens, and rock outcrop plant communities of North America. Cambridge University Press, New York.

Lesica, P. and F. W. Allendorf. 1995. When are peripheral populations valuable for conservation? Conservation Biology 9:753-760.

Marcinkowski, K., D. L. Peterson, and G. J. Ettl. 2015. Nonstationary temporal response of mountain hemlock growth to climatic variability in the North Cascade Range, Washington, USA. Canadian Journal of Forest Research 45:676-688.

NCDC. 2015. National Climatic Data Center. US Department of Commerce, National Oceanic and Atmospheric Administration, Asheville, North Carolina. http://www.ncdc.noaa.gov.

Paul V., Y. Bergeron and F. Tremblay. 2014. Does climate control the northern range limit of eastern white cedar (*Thuja occidentalis* L.)? Plant Ecology 215:181-194.

Parker A. J., K. C. Parker, T. D. Faust and M. M. Fuller. 2001. The effects of climatic variability on radial growth of two varieties of sand pine (*Pinus clausa*) in Florida, USA. Annals of Forest Science 58:333-350.

Phipps R. L. 1985. Collecting, preparing, crossdating, and measuring tree increment cores. US Geological Survey Water Resources Investigations Report 85-4148.

Saladyga, T. and R. S. Maxwell. 2015. Temporal variability in climate response of eastern hemlock in the central Appalachian Region. Southeastern Geographer 55:143-163.

SERCC. 2016. The Southeast Regional Climate Center. The University of North Carolina, Chapel Hill http://www.sercc.com/climate.

Speer J. H. 2010. Fundamentals of tree-ring research. University of Arizona Press, Tuscon.

Stokes M. A. and T. L. Smiley. 1996. An introduction to tree-ring dating. University of Arizona Press, Tucson.

Tardif J. and Y. Bergeron Y. 1997. Comparative dendroclimatological analysis of two black ash and two white white cedar populations from contrasting sites in the Lake Duparquet region, northwestern Quebec. Canadian Journal of Forest Research 27:108-116.

Tardif J. and D. Stevenson. 2001. Radial growth-climate association of *Thuja occidentalis* L. at the northwestern limit of its distribution, Manitoba, Canada. Dendrochronologia 19:179-187.

Walker G. L. 1987. Ecology and population biology of *Thuja occidentalis* in its southern disjunct range. PhD Dissertation, University of Tennessee, Knoxville.

Yamaguchi D. K. 1991. A simple method for cross-dating increment cores from living trees. Canadian Journal of Forest Research 21:414-416.

Young J. 1996. The cliff ecology and genetic structure of northern white cedar (*Thuja occidentalis* L.) in its southern disjunct range. MS Thesis, University of Tennessee, Knoxville.

Table 1. OLS regression model relating the RESIDUAL tree-ring chronology to temperature and precipitation variables. All variables are significant at $p < 0.01$.

Model summary	Variable	Standardized regression coefficient	Tolerance
$F = 21.84$, $p < 0.01$	September-November Mean PDSI	0.444	0.988
$R^2 = 0.328$	March Maximum Temperature	-0.316	0.988
Adjusted $R^2 = 0.311$	Previous October Precipitation	0.255	0.999

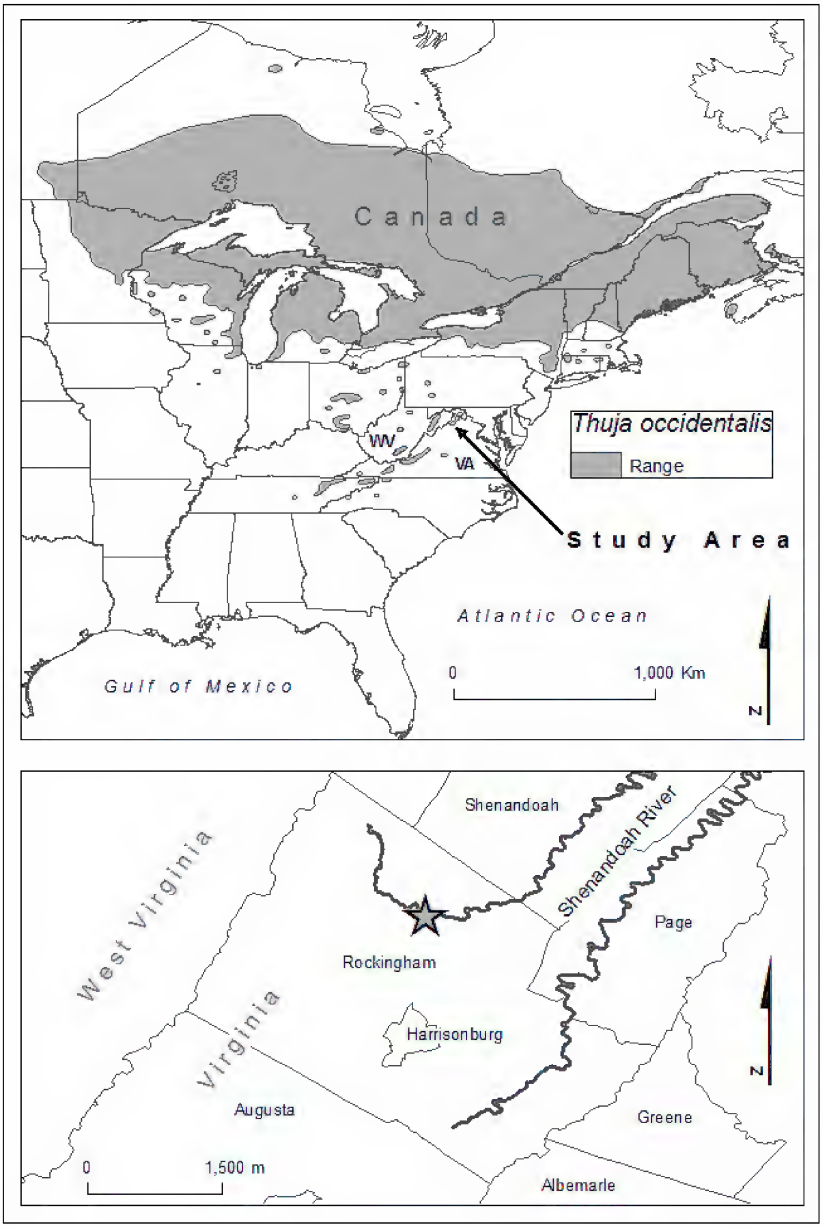

Figure 1. Map showing the range of *Thuja occidentalis* and study area.

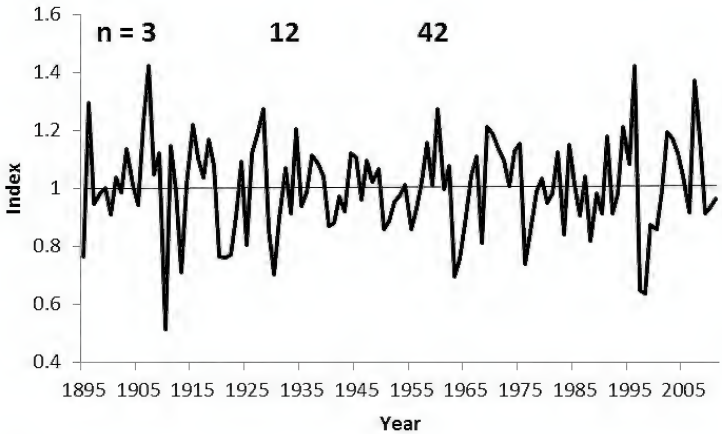

Figure 2. Composite ring-width index for *Thuja occidentalis* in the study area. Mean growth is standardized to 1.0 (n = number of trees represented in the index).

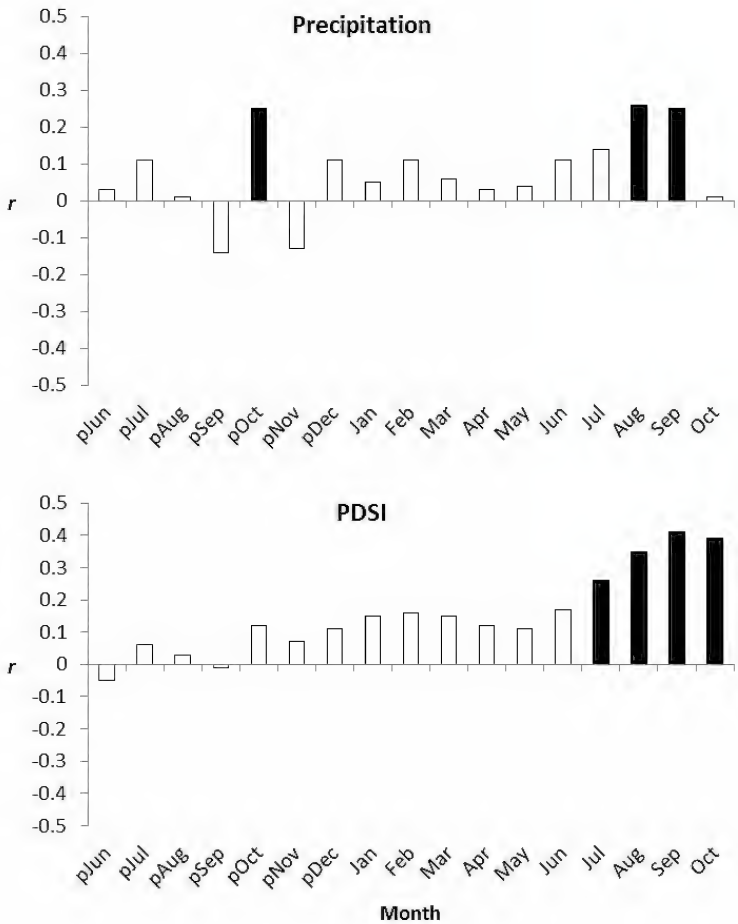

Figure 3. Pearson correlation coefficients showing the relationship between the *T. occidentalis* RESIDUAL chronology and precipitation variables. Black bars indicate a significance level of $p < 0.01$ and grey bars indicate a significance level of $p < 0.05$.

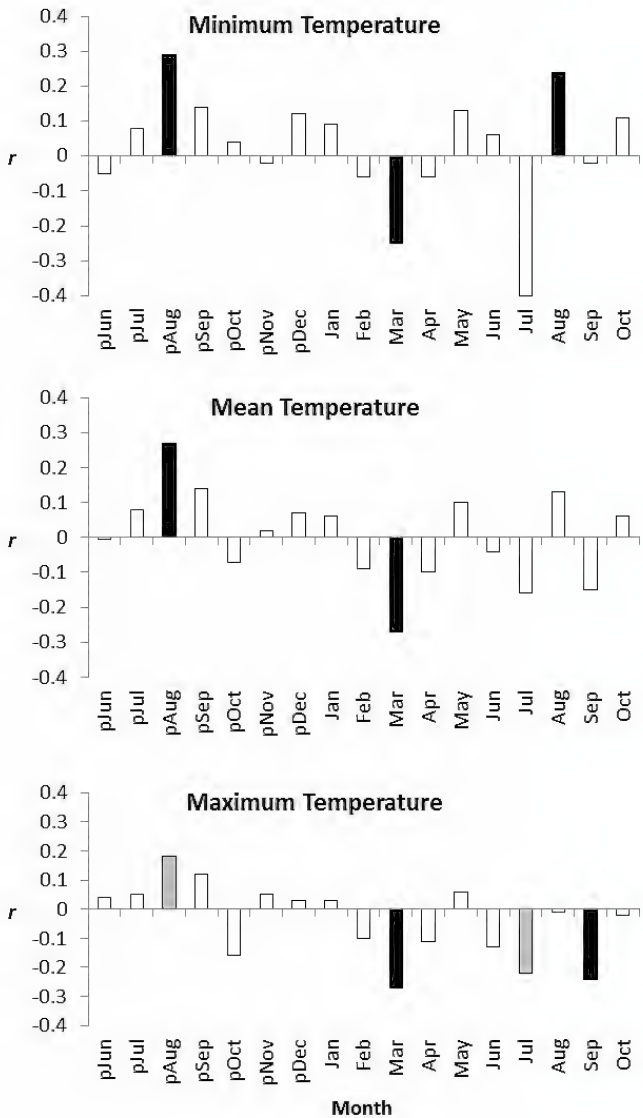

Figure 4. Pearson correlation coefficients showing the relationship between the *T. occidentalis* RESIDUAL chronology and temperature variables. Black bars indicate a significance level of $p < 0.01$ and grey bars indicate a significance level of $p < 0.05$.

Virginia Journal of Science
Volume 68, Issue 3 & 4
Fall & Winter 2018
doi: 10.25778/ ZYS5-H398

Note: This manuscript has been accepted for publication, and is online ahead of print. It will undergo copyediting, typesetting, and review of the resulting proof before it is published in its final form.

Habitat Use by Bats on the Upper Coastal Plain of Virginia

A. Scott Bellows[1, 3, 4] and Joseph C. Mitchell[2]

[1]The Virginia Space Grant Consortium, Hampton, VA 23666
[2]Florida Museum of Natural History, University of Florida, Gainesville, FL 32611-7800
[3]Department of Biological Sciences, Old Dominion University, Norfolk, VA 23529
[4]Corresponding author: Telephone (757) 876-4413, e-mail: abellows@odu.edu

ABSTRACT

We monitored bat activity on the upper Coastal Plain of Virginia using mist nets and acoustic detection (ANABAT) during April-October 2000 and April-August 2001. We classified forty sites into three forest-cover classes (pine forest, mixed pine, and hardwood forest) and three landscape-feature classes (permanent water, riparian corridor, and upland). We captured 406 bats (8 species) in mist nets; red bats (*Lasiurus borealis*; n = 281), big brown bats (*Eptesicus fuscus*; n = 47), and eastern pipistrelles (*Pipistrellus subflavus*; n = 36) were the most commonly captured species. We captured fewer than 30 individuals of five other species. There were no significant differences in captures per 100 net nights for overall captures or for individual species among forest-cover classes. Overall captures per 100 net nights differed significantly among landscape-feature classes; however, *post-hoc* analyses could not tease out significantly different pairs. Captures of *L. borealis* were higher over permanent waters than along riparian corridors or in uplands. Bray-Curtis polar ordination suggested that landscape features such as beaver ponds and impoundments influenced habitat use by bats more than forest-cover type. Discriminant function analysis identified 713 bat calls (≥ 95% confidence) using ANABAT II detectors. *Lasiurus borealis* and *P. subflavus* were more frequently recorded by ANABAT II than northern myotis (*Myotis septentrionalis*) among the three forest-cover classes and among the three landscape-feature classes. Planned, *a priori*, contrast indicated that for 25 nights when mists nets and acoustic detectors were used simultaneously, mean number of bat species detected for the pooled results of both techniques was higher than the average number of species detected by the mean of each of the two techniques separately. Mean number of bat species detected by the ANABAT II system was higher than mean number detected by mist netting.

Keywords: acoustic detection, ANABAT, bats, *Eptesicus fuscus*, habitat use, *Lasiurus borealis*, mist net, *Pipistrellus subflavus*.

INTRODUCTION

Population declines have been documented for many bat species (Rice, 1955; Thomson, 1982; Richter et al., 1993; Dazak et al., 2000; O'Shea et al., 2003) and usually attributed to roost disturbance, habitat loss, inputs of chemical pollution such as insecticides, and introduced pathogens (Clark et al., 1978; Stebbings, 1980; Clark, 1988; Dazak et al., 2000; Frick et al., 2003). Thirteen of the 45 bat species that occur in the United States and Canada are listed as endangered or threatened (U.S. Fish and Wildlife Service, 2017). Recognition of declines and trends towards 'ecosystem management' have increased public and professional interest in bats (Pierson, 1998). Natural resource managers, forest managers, and environmental policy makers traditionally focused their attention on threatened or endangered species or species with limited ranges (Pierson, 1998; Bellows et al., 2001a; Lacki et al, 2007). However, migration patterns and marginal records for many North American bat species suggest large geographic ranges when actual distributions are often disjunct or patchy (Hall, 1981; Pierson, 1998; Ethier and Fahrig, 2011). In addition, bats are difficult to survey accurately because of their secretive, nocturnal, volant, and, in many species, migratory habits (Humphrey and Cope, 1976; Barclay et al., 2003; Gannon et al., 2003). Thus, studies of bats in the field often require specialized monitoring techniques (Kunz and Kurta, 1990; Ministry of Environment, Lands and Parks Resources Inventory Branch, 1998; O'Farrell and Gannon, 1999; O'Shea et al., 2003). As a result, bats are often overlooked in faunal surveys (Jung et al., 1999; Thomas et al., 1999; Tuttle, 2007), and basic knowledge concerning the general ecology of common bat species is lacking (Fenton, 1997; Whitaker and Hamilton, 1998; Tuttle, 2007). An increased understanding of habitat use by bat species in large, relatively undeveloped landscapes (e.g., government installations and regional and national parks) would assist natural resource managers in developing local management strategies that help to maintain large-scale biodiversity.

Compared to the Mountain and Piedmont regions, the Coastal Plain of the mid-Atlantic region offers few natural overwintering locations (e.g., caves). Inventories of and research on bats in this region rely largely on data collected during active seasons, usually March through November for many species. Most recent surveys of bats in Virginia have been conducted in southeastern Virginia in the Great Dismal Swamp and Virginia Beach, along the James River, and in montane regions (e.g., Dalton, 1987; Padgett and Rose, 1991; Hobson, 1998; Rose et al., 2000; Walker, 2000). Our study in Virginia's upper Coastal Plain represents the first examination of chiropterans in a previously unstudied area of the mid-Atlantic region.

Our primary objective was to determine patterns of habitat use by bat species in a previously unstudied area within the upper Coastal Plain. We based habitat use on composition of bat assemblages and species distributions among different forest cover types and different landscape features. Because all local species have distributions far greater than our study area (Hall, 1981; Biggs, 1985; Whitaker and Hamilton, 1998; Wilson and Ruff, 1999), our have management implications at larger spatial scales. A secondary objective was to evaluate and compare the effectiveness and efficacy of two monitoring techniques—mist netting and acoustic detection. Because both techniques have advantages and disadvantages, we hypothesize that these two techniques together will be more effective in explaining habitat-use patterns for a wider suite of species than either technique alone.

MATERIALS AND METHODS

Study Area

We conducted this study on U.S. Army Fort A. P. Hill (APH), Caroline County, Virginia. APH is located on the western side of the Chesapeake Bay and centered at approximately N 77° 15′ and W 38° 05′. It is a military field-training installation with 30,329 ha site mostly in managed forest. With the exception of a few remnant old-growth stands, silvicultural practices on APH have produced a mosaic of successional old fields and forest cover types representative of the region (Mitchell and Roble, 1998; Bellows et al., 2001b).

Mist netting

We monitored bat activity ~ six days/month (70 sampling nights), April-October 2000 and April-August 2001 in 40 sites we selected. We captured bats were using 4-tiered mist nets (50 denier/2ply, 38 mm mesh) that were 3 m in height and ranged in length from 2.6 m to 18.0 m (Avinet, Inc., Dryden, New York, USA). Mist nets were set across openings in interior forests, logging roads, edges of ponds and impoundments, slow-moving woodland creeks with little or no emergent vegetation, small power line openings, over road ruts (puddles), over and under bridges, and other likely corridors of bat movement. Vertical coverage of mist nets ranged from ground or water level to heights of ~ 10 m.

Mist nets were deployed shortly after sunset after diurnal bird activity ended and monitored continuously for ~ 7 hours. One net night (NN) equals one 6x3-m area of mist net/sampling night, regardless of vertical placement. For example, a set consisting of two 9x3 m nets equals 3.0 NN. Bats were lightly marked with a black felt pen on their dorsal pelage to identify recaptures and then released unharmed. Recaptured individuals were not included in analyses.

Acoustic Detection

We used an ANABAT II bat detector (Titley Electronics, Ballina, New South Wales, Australia) to record bat calls using ANABAT software (version 5.7i). This system supplemented our mist netting efforts on 25 sampling nights during 2000 (10 sites) and 2001 (15 sites of which 10 were new). We did not deploy ANABAT II on rainy nights.

ANABAT II enabled remote identification of bats based on diagnostic characteristics (e.g., variations in frequency/time) of echolocation calls (sequence recordings—Corben and O'Farrell, 1999). Sequence recordings were passively collected (i.e., "monitor" mode) by directing the ANABAT II detector over likely corridors of bat movement (e.g., openings under the forest canopy, over riparian corridors, impoundments and beaver ponds, logging roads). Detectors were positioned such that recordings did not include distress calls from bats entangled in mist nets. We assumed that all species were equally susceptible to acoustic detection when calling in range of a detector. ANABAT receiver sensitivity was set the same throughout the study. A sampling unit (night) consisted of the data collected by a single ANABAT II detector, for one night, at one location. Sequence recordings were downloaded directly to a laptop

computer in the field using a Zero Crossing Analysis Interface Module (Titley Electronics, Ballina, New South Wales, Australia). Sampling night duration was the same as mist netting (~ 7 hours).

Raw sequence recordings were processed using ANALOOK software (version 3.5) to cull non-bat recordings (e.g., insects, human activity) and remove background noise from potentially identifiable recordings. We also culled all remaining recordings with fewer than six echolocation pulses. Methods of analysis and identification of cleaned sequence recordings are discussed in the *Statistical Analyses* section below.

Study Sites

Each of the 40 study sites was classified into one of three general forest-cover classes (FCC), pine forest (PN), mixed pine and hardwood forest (MX), or hardwood forest (HW), based on dominant canopy tree species. Loblolly pine (*Pinus taeda*) and Virginia pine (*P. virginiana*) dominated PN sites and were the only pine species in MX sites. Hardwood species composition of MX and HW sites varied from red maple (*Acer rubrum*) and river birch (*Betula niger*) in bottomland forest to American beech (*Fagus grandifolia*), hickories (*Carya* spp.) and oaks (*Quercus* spp.) in upland forest. Each study site was also classified into one of three landscape-feature classes (LFC): permanent water (e.g., impoundments, beaver ponds) (PW), riparian corridor (RC), or upland (UP). For more comprehensive descriptions of habitat types on APH refer to Mitchell and Roble (1998) and Bellows et al. (2001b).

Statistical Analyses

Replication of both mist netting and acoustic detection for sampling sites was often difficult because of military-training activities and restricted access. We used captures/100 NN for mist netting analyses because effort among sampling sites varied (i.e., variation in the number and sizes of nets set). We used a significance level of $\alpha < 0.05$ for all univariate tests.

Captures/100 NN for individual species for a given FCC or LFC class were calculated using the following equation:

$$C_{ij} = N_{ij} / M_j \qquad \text{(Equation 1.0)}$$

Where C_{ij} = captures/100 NN for the ith species in the jth class (i.e., j^{th} class = Forest Cover or Land Cover class (FCC or LFC), N_{ij} = total number of the ith species captured in the jth FCC or LFC, and M_j = total number of mist-net sampling nights for the jth class. Overall captures/100 NN for individual classes of FCCs and LFCs was calculated using the following equation:

$$C_j = \sum C_{ij} / R_n \qquad \text{(Equation 1.1)}$$

Where C_j = overall captures/100 NN for the jth FCC or LFC, C_{ij} = captures/100 NN for the ith species captured in the jth FCC or LFC (as per Equation 1.0), and R_n = total number of species captured using mist nets.

Single-factor ANOVA was used to test the null hypotheses of no FCC effect on mean overall captures/100 NN among the three FCCs and of no LFC effect on mean overall captures/100 NN among the three LFCs (Equation 1.1; Zar, 1996). We used single-factor ANOVA to test null hypotheses of no differences in mean captures/100 NN among FCCs and no

differences in mean captures/100 NN among LFCs for each bat species represented by ≥ 30 captures (Equation 1.0) where the assumptions of normal distributions and equality of variances were met. We used Student-Newman-Keuls multiple comparison procedure to isolate significant differences in mean captures/100 NN among FCCs and mean captures/100 NN among LFCs in these ANOVAs (Zar 1996). Were used either Kruskal-Wallis one-way ANOVA on ranks (three treatments; critical statistic = H) or Mann-Whitney rank-sum tests (two treatments; critical statistic = U) to test null hypotheses of similar captures/100 NN for FCCs and of similar captures/100 NN for LFCs for each bat species represented by ≥ 30 captures (Equation 1.0) when the assumptions of normality and equal variance were not met (Zar, 1996).

We used Bray-Curtis polar ordination (a Euclidean distance measure) to identify subtle patterns in bat species use of LFC represented by mist net captures among the 40 study sites (Ludwig and Reynolds, 1988). Bray-Curtis was selected because it is relatively insensitive to the nonlinear relationships common in most ecological data sets (Gauch and Whitaker, 1972) and, as an indirect gradient analysis, results are based solely on species distributions among study sites and not on environmental data (Gauch, 1984). Euclidean distance among sites in relation to each ordination axis correlates with general similarity of species composition among sites—shorter distance represents increased similarity (Ludwig and Reynolds, 1988). We overlaid captures/100 NN for each species (from Equation 1.0) for each study site on the main matrix to correlate explained variance for the first three ordination axes to the distribution of individual species (McCune and Mefford, 1995). We used Pearson's correlation coefficient (r) for species where parametric assumptions were met or Kendall's rank correlation coefficient (τ) for species where assumptions were not met to numerically describe relationships between species distributions and positions of study sites along ordination axes (McCune and Mefford, 1995).

Cleaned sequence recordings collected by ANABAT II were compared to bat calls of known origin (vouchers) in the Virginia Department of Game and Inland Fishery's (VDGIF) bat call library using discriminant function analysis (DFA: SPSS version 7.5). We selected within-group covariance matrices and prior probabilities assuming all groups equal (after Walker, 2000). We used only sequence recordings classified to species by DFA with ≥ 95% confidence in acoustic detection analyses.

We made no assumptions regarding the numbers of individuals for each species detected on a single night because of the difficulties associated with estimating population abundance using acoustic detection (Hayes, 1997). As a result, we considered only the use (occurrence) by individual species during a sampling night at a sampling site (i.e., use or nonuse of a FCC and LFC type). We calculated frequency of occurrence for individual species for a given FCC or LFC class using the following equation:

$$F_{ij} = N_{ij} / A_j \qquad \text{(Equation 2.0)}$$

where F_{ij} = frequency of occurrence for the ith species in the jth class (i.e., j^{th} class = FCC or LFC class), N_{ij} = total number of nights the ith species was acoustically detected in the jth FCC or LFC, and A_j = total number of ANABAT II sampling nights for the jth class. Overall frequency of occurrence for individual classes of FCCs and LFCs was calculated using the following equation:

$$F_j = \sum F_{ij} / R_j \qquad \text{(Equation 2.1)}$$

where F_j = overall frequency of occurrence for the jth FCC or LFC, F_{ij} = frequency of occurrence for the ith species detected in the jth FCC or LFC (as per Equation 2.0), and R_j = total number of species identified using acoustic detection.

We used single-factor ANOVA to test null hypotheses of no FCC effect on overall frequencies of presence among the three FCCs for the six species identified by DFA and of no LFC effect on overall frequencies of presence among LFCs for the six species identified by DFA (Equation 2.1—Zar, 1996). We used single-factor ANOVA to test null hypotheses of similar frequencies of occurrence for FCCs and of similar frequencies of occurrence for LFCs among the six bat species represented in the DFA model (Equation 2.0—Zar, 1996).

We used ANOVA with two planned, *a priori*, contrasts (critical statistic = *t*: Sokal and Rohlf, 1981) to test the following two null hypotheses. The first hypothesis (A) is of no difference in mean nightly species richness obtained by pooling mist netting and ANABAT II (-2) and the average species richness for the two techniques, mist netting (1) and ANABAT II (1), for the 25 nights when both techniques were used simultaneously within the same sampling area—planned contrast A (-2, 1, 1). Pooled results did not include replicate species detected by both techniques; thus, a species captured in mist nets and recorded with ANABAT II on the same night represents occurrence of a single species. The second hypothesis is of no difference in mean species richness obtained by mist netting (-1) and ANABAT II (1)—planned contrast B (0 [both], -1, 1). We did not compare numbers of sequence recordings among sites or compare them to numbers of captures because of the difficultly of accurately determining relative abundance using acoustic detection (Hayes, 1997); multiple calls could be a single bat circling over the detector.

RESULTS

Mist netting

We captured a total of 406 bats in mist nets representing 8 species in 733.5 NN from April-October 2000 and April-August 2001 (Tables 1 and 2). The most commonly captured species were red bats (*Lasiurus borealis*; $n = 281$), big brown bats (*Eptesicus fuscus*; $n = 47$), and eastern pipistrelle (*Pipistrellus subflavus*, $n = 36$). Captures for the remaining five species were all ≤ 13 individuals (Tables 1 and 2).

Bats were captured at all but two of the 40 sites sampled during 70 sampling nights. Number of species captured at each site ranged from zero to five (mean = 2.4 ± 1.4). Overall captures/100 NN averaged 54.6 ± 39 bats. Mean overall captures/100 NN were not significantly different among forest-cover classes (FCCs) ($F = 0.64$, $P = 0.535$; Table 3), and ranged from 39.2 ± 36.3 for PN to 59.8 ± 53.7 for MX (Table 1). There were significant differences in mean overall captures/100NN ($F = 3.31$, $P = 0.048$) among landscape-feature classes (LFCs); however, *post-hoc* analyses could not tease out significantly different pairs (Table 3). Mean overall captures/100 NN for LFCs ranged from 71.3 ±44.4 for RC to 36.0 ± 36.7 for UP (Table 2).

Lasiurus borealis, captured at 35 of the 40 study sites, was the sole species at nine of these sites. *Eptesicus fuscus*, *P. subflavus*, and northern myotis (*Myotis septentrionalis*) were

captured at 19, 16, and 6 sites, respectively. The remaining four species were captured at 1 to 4 sites. There were no significant differences in mean captures/100 NN for *L. borealis* ($F = 0.86$, P = 0.432), *P. subflavus* ($H = 1.86$, P = 0.394), or *E. fuscus* ($H = 1.54$, P = 0.463) among FCCs (Table 3). Comparisons of captures for FCCs and LFCs for the remaining five species, $n \leq 30$ (Tables 1 and 2), were not conducted because of small sample sizes.

Mean captures/100 NN for *L. borealis* was significantly higher ($F = 3.92$, P = 0.029) in PW (54.2 ±33.4) than in RC (27.3 ±24.0) and UP (26.6 ±26.5; Tables 2 and 3). There was no significant difference ($U = 180.50$, P = 0.279) in captures/100 NN of *P. subflavus* between PW and RC (Table 3); however, none was captured in UP (Table 1). There were no significant differences ($H = 0.07$, P = 0.966) in captures/100 NN of *E. fuscus* among the three LFCs (Table 3).

The first three Bray-Curtis polar-ordination axes explained 97.53% of the variation in bat assemblages among study sites. For bats as a group, no clear-cut patterns of LFC use were apparent. PW sites tended to be more diversely distributed than RC and UP, and RC more so than UP. Sites positioned near endpoints of each of the three axes were generally PW and RC (Figures 1 - 3).

Variation in bat species composition among the 40 study sites described by the first three polar-ordination axes was largely explained by one species for each axis. Variation for Axis I (74.96%) was best explained ($r = 0.998$) by the distribution (abundances) of *L. borealis* among study sites (Figure 1); for all other species r or τ was < 0.089. Variation in the second ordination axis (12.64%) was best explained by the abundances of *P. subflavus* among sites ($\tau = 0.554$) (Figure 2); for all other species r or τ was < 0.016. Variation in the third axis (9.92%) was best explained by the abundances of *E. fuscus* among sites ($\tau = 0.943$; Figure 3); r for all other species r or τ was < 0.243.

Acoustic Detection

We collected 2,187 raw sequence recordings during 25 sampling nights, 342 of which were non-bat calls and 698 had fewer than six pulses, thus, leaving 1,147 sequence recordings to be identified. Of these, DFA was able to identify 713 (~ 62%) to species with ≥ 95% confidence. Our DFA model included voucher calls of six species from the VDGIF's bat call library: *E. fuscus* (23 voucher calls), *L. borealis* (15), hoary bats (*Lasiurus cinereus*: 15), little brown bats (*Myotis lucifugus*: 29), *M. septentrionalis* (11) and, *P. subflavus* (13). Calls of two species we captured, evening bats (*Nycticeius humeralis*) and silver-haired bats (*Lasionycteris noctivagans*), were not in the VDGIF's bat call library at the time of our analysis; thus, these species were not considered in our current DFA model.

All six species identified by the DFA model were detected in all three FCCs (Table 1). There was no significant effect among the three FCCs on overall mean frequencies of presence for the six species identified (by DFA; $F = 1.03$, P = 0.358; Table 3), with mean frequency of presence ranging from 0.42 ± 0.20 for PN to 0.65 ± 0.33 for MX (Table 1). Significant differences in mean frequencies of occurrence were detected among the six species (DFA) for FCCs ($F = 4.15$, P = 0.020); *L. borealis* (0.77 ± 0.23) and *P. subflavus* (0.81 ± 0.16) were recorded more frequently than *M. septentrionalis* (0.19 ± 0.10) (P < 0.05; Tables 1 and 3).

Four of the six species identified by the DFA model were detected in all three LFCs. *Lasiurus cinereus* and *M. septentrionalis* were not recorded in UP, but were recorded in PW and RC (Table 2). There was no significant effect among the three LFCs on overall frequencies of presence for the six species identified by DFA ($F = 2.08$, $P = 0.380$; Table 3), with mean overall frequencies of presence/sampling night among the three LFCs ranging from 0.35 ± 0.20 for RC to 0.57 ± 0.29 for PW (Table 2). Significant differences in mean frequencies of presence were seen among the six species (DFA) for LFCs ($F = 4.91$, $P = 0.011$); as for FCCs, *L. borealis* and *P. subflavus* were recorded more frequently in than *M. septentrionalis* ($P < 0.05$; Tables 2 and 3).

Significant differences in species richness/sampling night were obtained among the three protocols: both mist netting and ANABAT II, mist netting alone, and ANABAT II alone ($F = 11.64$, $P = 0.000042$) (Table 4). Mean combined, or "pooled," species richness/sampling night for the pooled mist netting and ANABAT II treatment was significantly higher than the average species richness/sampling night achieved for either technique (Contrast A; $t = 3.65$, $P = 0.0005$), and species richness for ANABAT II was significantly higher than for mist netting (Contrast B; $t = 3.16$, $P = 0.0023$, Table 4).

DISCUSSION

Four species (*L. cinereus*, *M. lucifugus*, *M. septentrionalis*, *N. humeralis*) were not captured in pine forest (PN), and *L. cinereus* was not captured in mixed hardwood and pine forest (MX). None of these five species was well represented in mist net captures; however, calls for these species, except *N. humeralis* (not in DFA model), were recorded in all forest-cover classes (FCCs). In fact, all of the six species in our DFA model were recorded in all FCCs (Table 1). By comparison, captures/100 NN for the three most abundant species (*L. borealis*, *E. fuscus*, *P. subflavus*) were similar among FCCs (Ho_3), and their influence, in part, caused the lack of a significant difference in overall captures/100 NN among FCCs (Ho_1). ANABAT results for FCCs were similar to capture results for FCCs in two respects: 1) similar to overall captures/100 NN, overall frequencies of presence were similar and not significantly different among FCCs ($Ho:_5$), and 2) species with high captures/100NN generally had higher frequencies of occurrence than those species with lower captures/100 NN (Ho_7; Table 3). Although the importance of forest-cover type for bats has been well documented (Pierson, 1998; Jung et al., 1999; Elmore et al., 2005; Lacki et al., 2007), no abundant bat species was significantly associated with any particular FCC in our study.

Unlike FCCs, species composition based on mist net captures/100 NN varied among the three landscape-feature classes (LFCs; Table 3; Ho_2). *Myotis septentrionalis* was captured in mist nets in upland forest (UP), but never recorded there. Three of the eight species were not captured in all LFCs. *Pipistrellus subflavus* was not captured in UP, but it was usually acoustically detected there (Table 2). This is interesting because the number of mist-net captures for this species (36) should have been sufficient to determine patterns of forest-cover use at our relatively coarse-grained classification scheme. *Lasiurus noctivagans* was not captured near permanent water (PW) and *L. cinereus* was not captured or acoustically detected in UP. *Lasionycteris noctivagans* regularly feed adjacent to bodies of water (Kunz, 1982) and *L. cinereus* occur in wet and dry habitats (Shump and Shump, 1982). We suggest that the absence

of *L. noctivagans* in PW and the absence of *L. cinereus* UP are indirect results of seasonal migration habits that largely limited the presence of these species within the region to spring and fall and that *L. cinereus* regularly frequently travels higher than mist nets can be effectively set (Ministry of Environment, Lands and Parks Resources Inventory Branch, 1998; MacCarthy et al., 2006). Solitary habits and sporadic abundance during migrations further reduced our ability to capture these two species (Kunz, 1982; Shump and Shump, 1982). However, we believe that with further effort in spring and fall, *L. noctivagans* would be captured over or near water and *L. cinereus* would be captured or recorded in UP.

Justification for our use of polar ordination was twofold. First was the inability of *post-hoc* analysis to isolate significantly different overall captures/100 NN between pairs of LFCs following ANOVA ($P = 0.048$, Table 3; Ho_2). Polar ordination illustrated subtle patterns of LFC use by bats as a group; PW and riparian corridors (RC) were used more frequently than UP (Figures 1–3). Second, use of LFCs by bats was largely influenced by the most abundant species. A single abundant species largely explained the variation in species composition for each of the first three polar ordination axes, with most of the more dissimilar (extreme) sites along all three axes being PW or RC (Figures 1–3). Collectively, these findings indicate a tendency for these abundant species, *L. borealis* and *E. fuscus,* and to a lesser degree, *P. subflavus*, to use mesic to hydric habitats.

Mist nets sample an extremely small area (volume) relative to that used by bats (O'Farrell and Gannon, 1999; Flaquer et al., 2007). Within this small area, proper net placement is critical to capture success (Kunz and Kurta, 1990; Jones et al., 1996), and effective mist net placement is limited to situations where bat movement is restricted, e.g., under overhanging branches over roadways and creeks (Barbour and Davis, 1969; Kunz, 1973; Jones et al., 1996). In contrast, ANABAT II samples a larger proportion of area than mist nets (O'Farrell and Gannon, 1999) and is not as limited to situations where bat flight is restricted. In addition, it is more effective to capture bats in mist nets set along travel corridors than in foraging areas (e.g., over ponds or old fields) because sensory perception in the latter areas is usually more acute (Black, 1974; Kunz and Kurta, 1990; Kunz and Fenton, 2005). We occasionally set nets over foraging areas, but the most successful nets were those across travel corridors as they opened into foraging sites.

Standard mist-netting techniques are also limited by the maximum heights to which nets can be deployed (Kunz and Kurta, 1990; Munn, 1991; Jones et al., 1996). Many species routinely fly above the highest mist nets (O'Farrell and Gannon, 1999). There is also variation among and within species in their ability to avoid even well-placed nets (Cockrum and Cross, 1964; Kunz and Kurta, 1990; MacCarthy et al., 2006). Because ANABAT II data were collected remotely, with no physical impediment, and this technique is capable of functioning over a relatively broad area, our findings are based on the assumptions of no detectability and that all species are equally susceptible to data collection when passing within range of a detector.

Our findings indirectly supported these assumptions; only two of the 11 'species absences' among FCCs and LFCs were with ANABAT II methods, compared to nine of the absences using mist nets (Tables 1 and 2). In addition, we were able to significantly increase the number of species detected/sampling night an average of one species when using both methods simultaneously (Table 4). This increase is likely a function of differences in the spatial nature in

which these two methods collect data and variation in the detectability of mist nets by each species. We suggest that these results are affected by the potential biases and shortcomings of mist netting described above. However, unlike mist netting, ANABAT II is generally not used to determine relative abundance of species because it does not provide a one-to-one correlation between recorded calls and the number of individuals present (Thomas and LaVal, 1990; Rudran et al., 1996). ANABAT II is also unable to determine sex ratios. Thus, we concur with O'Farrell and Gannon (1999) and Weller (2007) that no single technique provides a complete inventory.

Records from Hall (1981), Whitaker and Hamilton (1998), and others suggest that with the exception of a few extralimital records (described below), our efforts on APH have recorded most of the bat species that should occur in the region. Our captures of two *L. cinereus* in July (adult male) and August (juvenile female) of 2000 are the first records for this species on Virginia's Coastal Plain during the summer (Bellows and Mitchell, 2002), indicating the likelihood of breeding here. Despite our use of two methods of survey, we cannot be certain that no other species of bats occur on APH. There are extralimital records for other bat species that potentially include the study region (Rageot, 1955; Cranford and Fortune, 1994; Webster, 2002). In brief, we believe our surveys revealed all the common resident and migratory species for the region.

Our findings suggest that landscape features such as bottomland and upland areas have a greater influence on patterns of habitat use by bats in fragmented landscapes than the composition of tree species within these areas. We attribute these patterns to the propensity of many bat species to forage over or near a wide variety of mesic and hydric habitats (Barbour and Davis, 1969; Pierson, 1998; Erickson and West, 2002). We present these suggestions with caution because we are aware that habitat fragmentation of our study area has likely affected our results. Day roosts are often located many km away from foraging sites. As bats move from day roosts to foraging areas, the number of habitat types they pass through will increase as fragmentation and fractal dimensions of FCC and LFCs patches increase. Thus, increased fragmentation would increase the likelihood of individuals being captured or recorded as they pass through a habitat for which they have no or only marginal affinity. Because each of the 40 sample sites was assigned to a FCC class and a LFC class, the collective effectiveness of acoustic detectors to provide accurate results is exactly the same for FCCs as it is for LFCs—logic says the same must be true for mist nets. Therefore, it might be expected that differences among FCCs and among LFCs in acoustic detection results should be mirrored in mist-netting results, but this was not true. Our acoustic detection findings of similar, non-significant overall frequencies of occurrence among FCCs (Ho_5) and among LFCs (Ho_6) were contradicted with significant differences in overall captures/100 NN among LFCs (Ho_2), but no differences in overall captures/100 NN among FCCs (Ho_1). Spatially related differences in the abilities of acoustic detectors and mist nets to collect data (e.g., effective heights and ranges, detectability) provide different findings for each technique. Thus, if the activities, e.g., foraging (relatively high sensory perception) vs. traveling to and from roosts (relatively low sensory perception), within the various FCCs were not the same as within LFCs, then the above contradiction suggest that habitat utilization by bats is different with regard to LFC attributes than for FCC attributes. We realize such conclusions cannot be drawn from our current sampling design; however, this does provide sufficient justification for additional hypotheses. Further study on roosting habits

and daily movements (i.e., radio tracking and simultaneous monitoring stations) is needed to achieve a fine-grained resolution of spatial habitat and landscape use by bats.

Studies of chiropterans on this and other government installations should be an ongoing focus of natural resource managers because such relatively undeveloped landscapes are quickly disappearing. Trends in the ecological conditions in these "refuge-like islands" should be used to quantify regional effects of landscape-level anthropogenic changes such as deforestation and urban sprawl on chiropterans and other environmentally sensitive taxa. Although our results describe local habitat use patterns, the species we studied have regional to continental distributions. As a result, management at a local scale may provide critical links of protection for vulnerable species with relatively large population ranges. Our results can be used to encourage management efforts that target protection and conservation of the current regional diversity of chiropterans. Conservation efforts should include provisions for common and widely distributed species, as well as endangered and threatened species, because they are all key components of regional biodiversity.

ACKNOWLEDGMENTS

We thank C.T. Georgel and K.D. Walters for field assistance. Rick Reynolds (VDGIF) and T.W. Walker (World Resources Institute, Washington, D.C.) helped with analysis of our ANABAT II results. We thank R.K. Rose (Old Dominion University, Norfolk, Virginia) for his review of drafts of this manuscript. Funding for this study was provided by the Environmental and Natural Resources Division of APH through the US Army Corps of Engineers and administered by the Conservation Management Institute, Virginia Tech (for 2000) and AH Environmental Consultants, Inc. Newport News, Virginia (for 2001).

LITERATURE CITED

Barbour, R.W., and W.H. Davis. 1969. Bats of America. University Press of Kentucky, Lexington. 286 pp.

Barclay, R.M., L.D. Harder, T.H. Kunz, and M.B. Fenton. 2003. Life histories of bats: life in the slow lane. Pp. 209–253 in T.H. Kunz, and M.B. Fenton, eds., Bat Ecology. University of Chicago Press.

Bellows, A.S., and J.C. Mitchell. 2002. Summer records for the hoary bat, *Lasiurus cinereus* (Chiroptera: Vespertilionidae), on the Coastal Plain of Virginia. Journal of the North Carolina Academy of Science 118: 54–56.

Bellows, A.S., and J.C. Mitchell, and J.F. Pagels. 2001a. Macrohabitat and microhabitat affinities of small mammals in a fragmented landscape on the upper Coastal Plain of Virginia. American Midland Naturalist 146: 345–360.

Bellows, A.S., J.C. Mitchell, J.F. Pagels, and H.N. Mansfield. 2001b. Mammals of Fort A. P. Hill, Caroline County, Virginia and vicinity. Virginia Journal of Science 52: 163–226.

Biggs, W.C., Jr. 1985. Mammals of the Carolinas, Virginia, and Maryland. University of North Carolina Press, Chapel Hill. 255 pp.

Black, H.L. 1974. A north temperate bat community: structure and prey populations. Journal of Mammalogy 55: 138–155.

Cockrum, E.L., and S.P. Cross. 1964. Time of bat activity over water holes. Journal of Mammalogy 45: 635–636.

Clark, D.R., Jr., R.K. LaVal, and D.M. Swineford. 1978. Dieldrin-induced mortality in an endangered species, the gray bat (*Myotis grisescens*). Science 199: 1357–1359.

Clark, D.R., Jr. 1988. How sensitive are bats to insecticides? Wildlife Society Bulletin 6: 399–403.

Corben, C., and M.J. O'Farrell. 1999. ANABAT system manual: techniques for the effective use of ANABAT in identifying free-flying bat species. Copyright by Chris Corben and Michael J. O'Farrell, Titley Electronics, Ballina, New South Wales, Australia.

Cranford, J.A., and D.S. Fortune. 1994. Mexican free-tailed bats at Mt. Lake Biological Station! Virginia Journal of Science 54: 111.

Dalton, V.M. 1987. Distribution, abundance, and status of bats hibernating in caves in Virginia. Virginia Journal of Science 38: 369–379.

Daszak, P., A.A. Cunningham, and A.D. Hyatt. 2000. Emerging infectious diseases of wildlife--threats to biodiversity and human health. Science 287: 443–449.

Elmore, L.W., D.A. Miller, and F.J. Vilella. 2005. Foraging area size and habitat use by red bats (*Lasiurus borealis*) in an intensively managed pine landscape in Mississippi. American Midland Naturalist 153: 405–417.

Erickson, J.L., and S.D. West. 2002. The influence of regional climate and nightly weather conditions on activity patterns of insectivorous bats. Acta Chiropterologica 4: 17–24.

Ethier, K., and L. Fahrig. 2011. Positive effects of forest fragmentation, independent of forest amount, on bat abundance in eastern Ontario, Canada. Landscape Ecology 26: 865–876.

Flaquer, C., I. Torre, and A. Arrizabalaga. 2007. Comparison of sampling methods for inventory of bat communities. Journal of Mammalogy 88: 526–533.

Fenton, M.B. 1997. Science and the conservation of bats. Journal of Mammalogy 78:1–14.

Frick, W.F., J.F. Pollock, A.C. Hicks, K.E. Langwig, D.S. Reynolds, G.G. Turner, C.M. Butchkoski, and T.H. Kunz. 2010. An emerging disease causes regional population collapse of a common North American bat species. Science 329: 679–682.

Gannon, W.L., R.E. Sherwin, and S. Haymond. 2003. On the importance of articulating assumptions when conducting acoustic studies of habitat use by bats. Wildlife Society Bulletin 31: 45–61.

Gauch, H.G., Jr. 1984. Multivariate Analysis in Community Ecology. Cambridge University Press, United Kingdom. 298 pp.

Gauch, H.G., Jr., and R.H. Whittaker. 1972. Comparison of ordination techniques. Ecology 53: 868–875.

Hall, E.R. 1981. The Mammals of North America. John Wiley & Sons, New York. 1280 pp.

Hayes, J.P. 1997. Temporal variation in activity of bats and the design of echolocation monitoring studies. Journal of Mammalogy 78: 514–524.

Hobson, C.S. 1998. Bat records from southeastern Virginia, including a new resident species, *Myotis austroriparius* (Chiroptera: Vespertilionidae). Banisteria 12: 18–23.

Humphrey, S.R., and J.B. Cope. 1976. Population ecology of the little brown bat, *Myotis lucifugus*, in Indiana and North-Central Kentucky. Special Publication No. 4, American Society of Mammalogists. 81 pp.

Jones, C., W.J. McShea, M.J. Conroy, and T.H. Kunz. 1996. Capturing mammals. Pp. 115–155 in D.E. Wilson, F.J. Cole, J.D. Nichols, R. Rudran, and M.S. Foster, eds., Measuring and Monitoring Biological Diversity, Standard Methods for Mammals. Smithsonian Institution Press, Washington, D.C.

Jung, T.S., I.D. Thompson, R.D. Titman and A.P. Appleton. 1999. Habitat selection by forest bats in relation to mixed-wood stand types and structure in central Ontario. Journal of Wildlife Management 63: 1306–1319.

Kunz, T.H. 1973. Resource utilization: temporal and spatial components of bat activity in central Iowa. Journal of Mammalogy 54: 14–32.

Kunz, T.H. 1982. *Lasionycteris noctivagans*—Mammalian Species No. 172. Special publication of the American Society of Mammalogists.

Kunz, T.H. and Fenton, M.B., eds. 2005. Bat Ecology. University of Chicago Press. 978 pp.

Kunz, T.H., and A. Kurta. 1990. Capture methods and holding devices. Pages 1–29 *In* Kunz, T.H., ed. Ecological and Behavioral Methods for the Study of Bats. Smithsonian Institution Press, Washington, D.C. 533 pp.

Lacki, Michael J., John P. Hayes, and Allen Kurta, eds. 2007. Bats in Forests: Conservation and Management. Johns Hopkins University Press, Baltimore, Maryland. 352 pp.

Ludwig, J.A., and J.F. Reynolds. 1988. Statistical Ecology—A Primer on Methods and Computing. John Wiley and Sons, New York. 337 pp.

MacCarthy, K.A., T.C. Carter, B.J. Steffen, and G.A. Feldhamer. 2006. Efficacy of the mist-net protocol for Indiana bats: A video analysis. Northeastern Naturalist 13: 25–28.

McCune, B., and M.J. Mefford. 1995. PC-ORD: Multivariate Analysis of Ecological Data. MjM Software Design, Gleneden Beach, Oregon.

Ministry of Environment, Lands and Parks Resources Inventory Branch. 1998. Inventory methods for bats: standards for components of British Columbia's biodiversity. No. 20. Vancouver, British Columbia.

Mitchell, J.C., and S.M. Roble. 1998. Annotated checklist of the amphibians and reptiles of Fort A.P. Hill, Virginia, and vicinity. Banisteria 11: 19–31.

Munn, C.A. 1991. Tropical canopy netting and shooting lines over tall trees. Journal of Field Ornithology 62: 454–463.

O'Farrell, M.J., and W. L. Gannon. 1999. A comparison of acoustic versus capture techniques for the inventory of bats. Journal of Mammalogy 80: 24–30.

O'Shea, T.J., M.A. Bogan, and L.E. Ellison. 2003. Monitoring trends in bat populations of the United States and territories: status of the science and recommendations for the future. Wildlife Society Bulletin 31: 16–29.

Padgett, T.M., and R.K. Rose. 1991. Bats (Chiroptera: Vespertilionidae) of the Great Dismal Swamp of Virginia and North Carolina. Brimleyana 17: 17–26.

Pierson, E.D. 1998. Tall trees, deep holes, and scarred landscapes: Conservation biology of North American bats. Pages 309–325 *In* T.H. Kunz, and P.A. Racey, eds. Bat Biology and Conservation. Smithsonian Institution Press, Washington, D.C. 365 pp.

Rageot, R.H. 1955. A new northernmost record of the yellow bat, *Dasypterus floridanus*. Journal of Mammalogy 36: 456.

Rice, D.W. 1955. Status of *Myotis grisescens* in Florida. Journal of Mammalogy 36:384–388.

Richter, A.R., S.R. Humphrey, J.B. Cope, and V. Black, Jr. 1993. Modified cave entrances: thermal effect on body mass and resulting decline of endangered Indiana bats (*Myotis sodalis*). Conservation Biology 7: 407–415.

Rose, R. K., C. S. Hobson, T. M. Padgett and D. A. Schwab. 2000. Dismal swamp bats. Pp. 235–239 *In* Rose, R.K., ed. The Natural History of the Great Dismal Swamp. Omni Press, Madison, Wisconsin. 301 pp.

Rudran, R., T.H. Kunz, C. Southwell, P. Jarman, and A.P. Smith. 1996. Observational techniques for nonvolant mammals. Pp. 81–114 in D.E. Wilson, F.J. Cole, J.D. Nichols, R. Rudran, and M.S. Foster, eds., Measuring and Monitoring Biological Diversity, Standard Methods for Mammals. Smithsonian Institution Press, Washington, D.C.

Shump, K.A., Jr., and A.U. Shump. 1982. *Lariurus borealis*—Mammalian Species No. 183. Special publication of the American Society of Mammalogists.

Sokal, R.R., and F.J. Rohlf. 1981. Biometry: the Principles and Practice of Statistics in Biological Research, 2nd edition. W.H. Freeman and Company, New York. 859 pp.

Stebbings, R.E. 1980. An outline global strategy for the conservation of bats. Pages 173–178 *In* Wilson, D.E. and A.L. Gardner, eds. Proceedings, 5th International Bat Research Conference. Texas Tech Press, Lubbock. 434 pp.

Thomas, D.W., and R.K. LaVal. 1990. Survey and census methods. Pages 77–89 In T.H. Kunz, ed. Ecological and Behavioral Methods for the Study of Bats. Smithsonian Institution Press, Washington, D.C. 533 pp.

Thomas, S.J., I.D. Thompson, R.D. Titman, and A. P. Applejohn. 1999. Habitat selection by forest bats in relation to mixed-wood stand types and structure in central Ontario. Journal of Wildlife Management 63: 1306–1319.

Thomson, C.E. 1982. *Myotis sodalis*—Mammalian Species No. 163. Special publication of the American Society of Mammalogists.

Tuttle, M.L. 2007. Foreword. Pp. ix–x in M.J. Lacki, J.P. Hayes, and A. Kurta, eds. Bats in Forests: Conservation and Management. Johns Hopkins University Press, Baltimore, Maryland.

U.S. Fish and Wildlife Service. 2017. Endangered Species Database. https://www.fws.gov/endangered/species/us-species.html, Accessed 17 September 2017.

https://www.fws.gov/endangered/species/us-species.html

Walker, T.W. 2000. Allegheny bats: a study of species richness, activity, and distribution in Virginia. Master's Thesis, Virginia Commonwealth University, Richmond, Virginia, 48 pp.

Webster, W.D. 2002. Northern yellow bat (*Lasiurus intermedius*) in North Carolina. Journal of the North Carolina Academy of Science 118: 61–62.

Weller, T.J. 2007. Assessing population status of bats in forests: challenges and opportunities. Pp. 263–291 in M.J. Lacki, J.P. Hayes, and A. Kurta, eds. Bats in Forests: Conservation and Management. Johns Hopkins University Press, Baltimore, Maryland.

Whitaker, J.O., Jr. and W.J. Hamilton, Jr. 1998. Mammals of the Eastern United States. 3rd edition. Cornell University Press, Ithaca, New York. 583 pp.

Zar, J.H. 1996. Biostatistical Analysis, 3rd edition. Prentice Hall, Upper Saddle River, New Jersey. 662 pp.

Table 1. Mist net (MN) and ANABAT II (AB) effort and results (2000 and 2001) for 8 bat species (and the total number captured for each) for FCCs. ANABAT II values represent the frequency of presence (Equation 2.0) for each FCC where each species in the DFA model. Mist net values represent captures/100 NN (Equation 1.0). Forest-cover classes (FCCs) = pine forest (PN), mixed hardwood and pine forest (MX), and hardwood forest (HW).

		FCC (Total Net Nights and ANABAT II nights)								
		PN (71.5, 4)			MX (274.5, 8)			HW (387.5, 13)		
Species (Number captured)	Device	mean[a] median[b]	SD[c] min, max[d]	Freq	mean[a] median[b]	SD[c] min, max[d]	Freq	mean[a] median[b]	SD[c] min, max[d]	Freq
E. fuscus	AB			0.25			0.88			0.54
(47)	MN	0.0[b]	0.0, 38.1[d]		0.0[b]	0.0, 26.3[d]		4.4[b]	0.0, 52.4[d]	
L. noctivagans[e]	MN	0.0[b]	0.0, 17.4[d]		0.0[b]	0.0, 3.8[d]		0.0[b]	0.0, 17.4[d]	
(9)										
L. borealis	AB			0.50			0.88			0.92
(281)	MN	25.5[a]	19.9[c]		44.7[a]	40.5[c]		39.4[a]	27.5[c]	
L. cinereus	AB			0.25			0.63			0.15
(3)	MN	NC[f]			NC[f]			0.0[b]	0.0, 3.1[d]	
M. lucifugus	AB			0.50			0.25			0.31
(12)	MN	NC[f]			0.0[b]	0.0, 7.1[d]		0.0[b]	0.0, 7.1[d]	
M. septentrionalis	AB			0.25			0.25			0.08
(13)	MN	NC[f]			0.0[b]	0.0, 13.3[d]		0.0[b]	0.0, 13.3[d]	
N. humeralis[e]	MN	NC[f]			NC[f]			0.0[b]	0.0, 5.9[d]	
(5)										

P. subflavus		AB			0.75			1.00			0.69
	(36)	MN	0.0[b]	0.0, 19.1[d]		0.0[b]	0.0, 80.0[d]		2.5[b]	0.0, 17.4[d]	
Means		AB			0.42			0.65			0.45
		MN	39.2[a]	36.3[c]		59.8[a]	53.7[c]		56.5[a]	30.7[c]	

[a]mean captures/100 NN (species where basic parametric assumptions were met)

[b]median captures/100 NN (species where basic parametric assumptions were not met)

[c]standard devation for mean captures/100 NN (species where basic parametric assumptions were met)

[d]minimum, maximum captures/100 NN (species where basic parametric assumptions were not met)

[e]indicates species not in the VDGIF's library of ANABAT calls at the time of analysis

[f]not captured

Table 2. Mist net (MN) and ANABAT II (AB) effort and results (2000 and 2001) for 8 bat species (and the total number captured for each) for LFCs. ANABAT II values represent the frequency of presence (Equation 2.0) for each LFC where each species in the DFA model. Mist net values represent captures/100 NN (Equation 1.0). Landscape features (LFCs) = permanent water (PW), riparian corridor (RC), upland (UP).

		LFC (Total Net Nights and ANABAT II nights)								
		PW (370.5, 12)			RC (236.0, 10)			UP (127.0, 3)		
Species (Number captured)	Device	mean[a] median[b]	SD[c] min, max[d]	Freq	mean[a] median[b]	SD[c] min, max[d]	Freq	mean[a] median[b]	SD[c] min, max[d]	Freq
E. fuscus	AB			0.70			0.50			0.33
(47)	MN	0.6[b]	0.0, 38.1[d]		0.0[b]	0.0, 52.4[d]		0.0[b]	0.0, 14.3[d]	
L. noctivagans[e] (9)	MN	NC[f]			0.0[b]	0.0, 17.4[d]		0.0[b]	0.0, 14.3[d]	
L. borealis	AB			0.90			0.58			0.67
(281)	MN	52.9[a]	33.4[c]		27.3[a]	24.0[c]		26.6[a]	26.5[c]	
L. cinereus	AB			0.50			0.17			0.00
(3)	MN	0.0[b]	0.0, 10.0[d]		0.0[b]	0.0, 3.9[d]		NC[f]		
M. lucifugus	AB			0.40			0.17			0.67
(12)	MN	0.0[b]	0.0, 7.1[d]		0.0[b]	0.0, 3.6[d]		0.0[b]	0.0, 16.1[d]	
M. septentrionalis	AB			0.10			0.17			0.00
(13)	MN	0.0[b]	0.0, 7.7[d]		0.0[b]	0.0, 13.3[d]		0.0[b]	0.0, 9.2[d]	
N. humeralis[e] (5)	MN	0.0[b]	0.0, 5.8[d]		0.0[b]	0.0, 7.7[d]		0.0[b]	0.0, 4.6[d]	
P. subflavus	AB			0.80			0.50			0.67

	(36)	MN	5.4[b]	0.0, 80.0[d]		0.0[b]	0.0, 8.2[d]		NC[f]	
Means		AB			0.57			0.35		0.39
		MN	71.3[a]	44.7[c]		44.2[a]	27.1[c]		36.0[a]	36.7[c]

[a]mean captures/100 NN (species where basic parametric assumptions were met)

[b]median captures/100 NN (species where basic parametric assumptions were not met)

[c]standard devation for mean captures/100 NN (species where basic parametric assumptions were met)

[d]minimum, maximum captures/100 NN (species where basic parametric assumptions were not met)

[e]indicates species not in the VDGIF's library of ANABAT calls

[f]not captured

Table 3. Results of mist netting and ANABAT II univariate analyses (i.e., ANOVA [*F*], Kruskal-Wallis ANOVA on ranks [*H*], and Mann-Whitney rank sum test [*U*]). Numbers in the Ho: column refer to the numbered null hypotheses below. "ALL" species include all 8 species captured. Individual species include: *L. borealis* (*LB*), *P. subflavus* (*PS*), and *E. fuscus* (*EF*). "DFA" includes the six species modeled in our DFA analysis.

			Critical Statistic				
Ho:	Species	*df*	*F*	*H*	*U*	P	Significant Pairs
1	ALL	2	0.64			0.535	-
2	ALL	2	3.31			0.048†	none
3	*LB*	2	0.86			0.432	-
3	*PS*	2		1.86		0.394	-
3	*EF*	2		1.54		0.463	-
4	*LB*	2	3.92			0.029†	PW > RC, UP
4	*PS*	2			180.5	0.279	n/a
4	*EF*	2		0.07		0.966	-
5	DFA	2	1.10			0.358	-
6	DFA	2	1.03			0.380	-
7	DFA	5	4.14			0.020†	*LB*, *PS* > *MS*
8	DFA	5	4.91			0.011†	*LB*, *PS* > *MS*

† term significant at $\alpha = 0.05$

1) no FCC effect on mean overall mist net captures/100 NN

2) no LFCs effect on mean overall mist net captures/100 NN

3) similar mean captures/100 NN among FCCs for an individual species

4) similar mean captures/100 NN among LFCs for an individual species

5) no FCC effect on overall frequencies of presence for the six species identified (by DFA)

6) no LFC effect on overall frequencies of presence for the six species identified (by DFA)

7) similar frequencies of presence among FCCs among species represented in DFA

8) similar frequencies of presence among LFCs among species represented in DFA

Table 4. Analysis of Variance with planned contrasts testing the null hypotheses: A) no difference in mean nightly species richness obtained by pooling mist netting and ANABAT II (-2) and the average species richness for the two techniques, mist netting (1) and ANABAT II (1)—*a priori* contrast A (-2, 1, 1); B) no difference between mean species richness obtained by mist netting (-1) and ANABAT II (1)—*a priori* contrast B (0 [both], -1, 1).

Source	*df*	SS	MS	*F*	P
Treatments	2	26.8	13.4	11.64	0.000042*
Error	72	83.2	1.2		
Total (Adjusted)	74	110.0			

Planned contrast A: $df = 72$, $t = 3.65$, P = 0.0005*

Group	Comparison Coefficient	Count	Mean
Both	-2	25	3.44
ANABAT II	1	25	2.96
Mist netting	1	25	2.00

Planned contrast B: $df = 72$, $t = 3.16$ P = 0.0023*

Group	Comparison Coefficient	Count	Mean
Both	0	25	3.44
ANABAT II	-1	25	2.96
Mist netting	1	25	2.00

* Term significant at alpha < 0.05

FIGURE LEGENDS

Figure 1. Graphic overlay of *Lasiurus borealis* on Bray-Curtis polar ordination plot. Size of the circles indicates proportion of captures/100 net nights for *L. borealis* for that site among the 40 study sites. Scatterplots depict the relationship between *L. borealis* and the explained variance for each axis represented. Pearson's correlation coefficients (r) are provided. PW = permanent water body; RC = riparian corridor.

Figure 2. Graphic overlay of *Pipistrellus subflavus* on Bray-Curtis polar ordination plot. Size of the circles indicates proportion of captures/100 net nights for *P. subflavus* for that site among the 40 study sites. Scatterplots depict the relationship between *P. subflavus* and the explained variance for each axis represented. Kendall's correlation coefficients (τ) are provided. PW = permanent water body.

Figure 3. Graphic overlay of *Eptesicus fuscus* on Bray-Curtis polar ordination plot. Size of the circles indicates proportion of captures/100 net nights for *E. fuscus* for that site among the 40 study sites. Scatterplots depict the relationship between *E. fuscus* and the explained variance for each axis represented. Kendall's correlation coefficients (τ) are provided. PW = permanent water body; RC = riparian corridor.

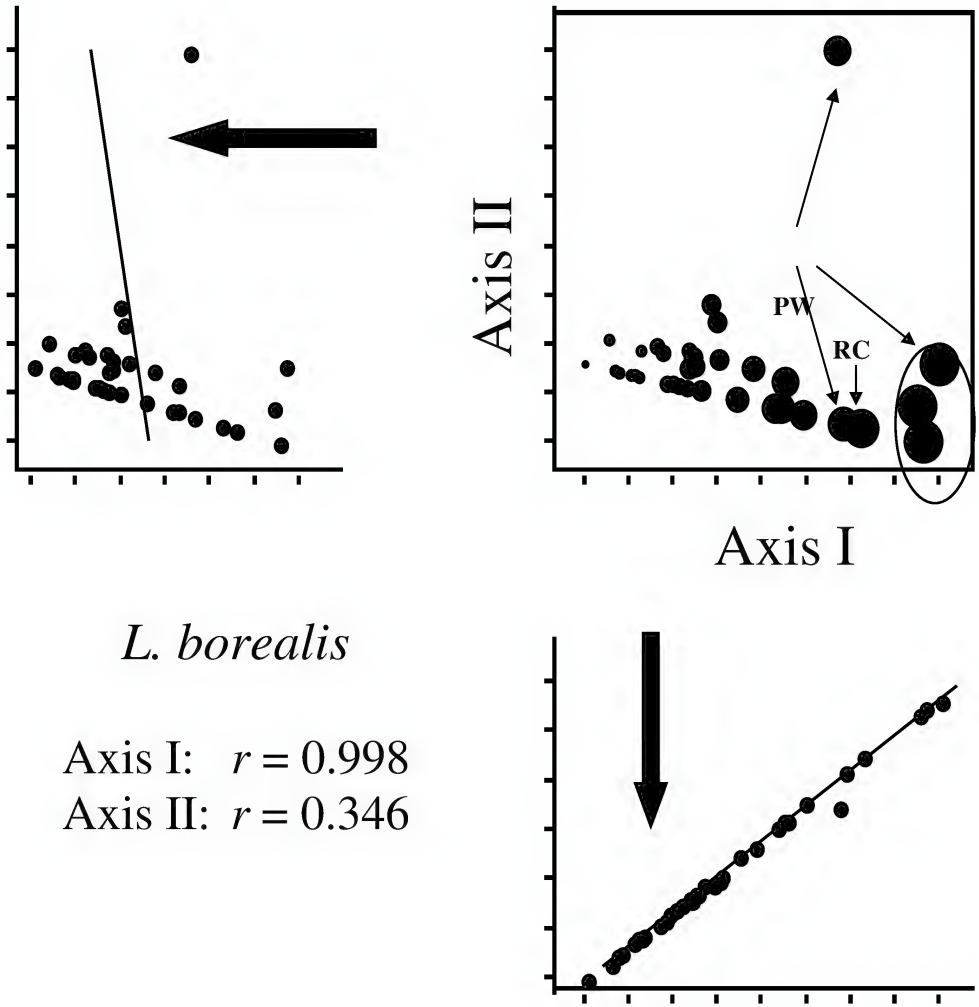
Axis II
PW
RC
Axis I
L. borealis
Axis I: $r = 0.998$
Axis II: $r = 0.346$

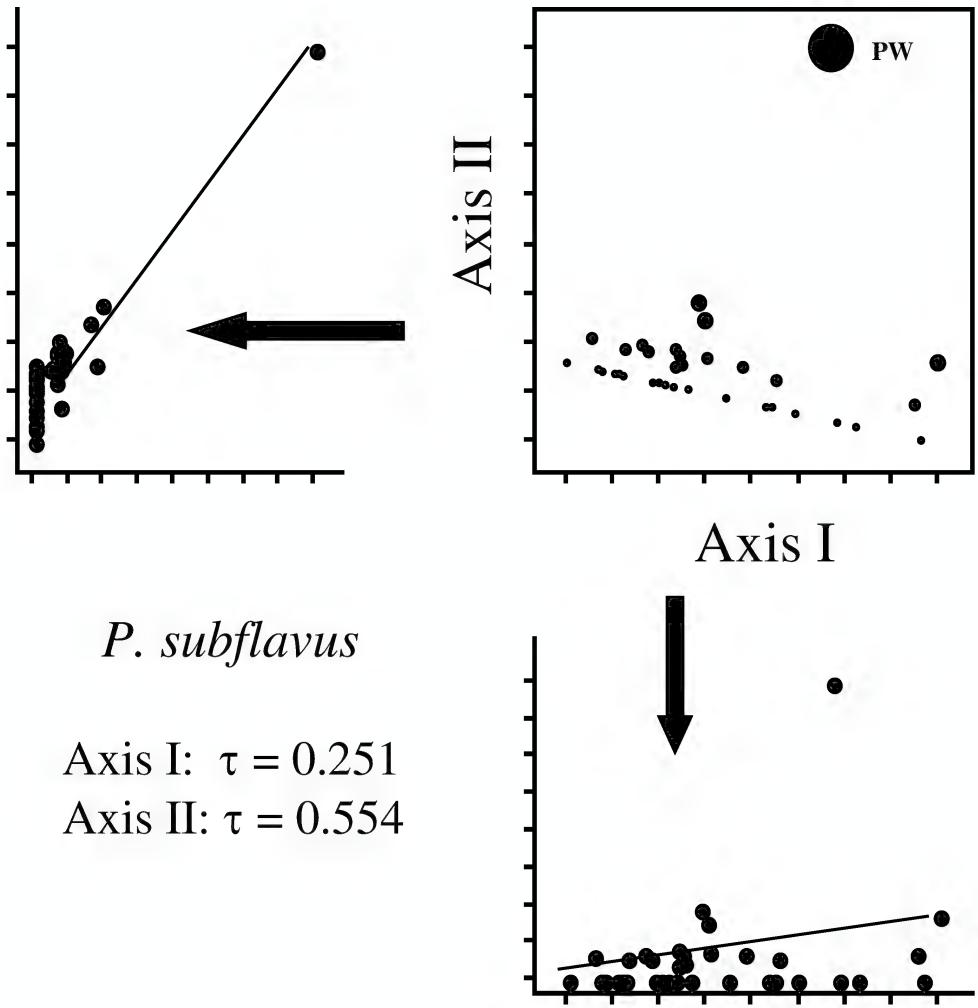
PW
Axis II
Axis I
P. subflavus
Axis I: τ = 0.251
Axis II: τ = 0.554

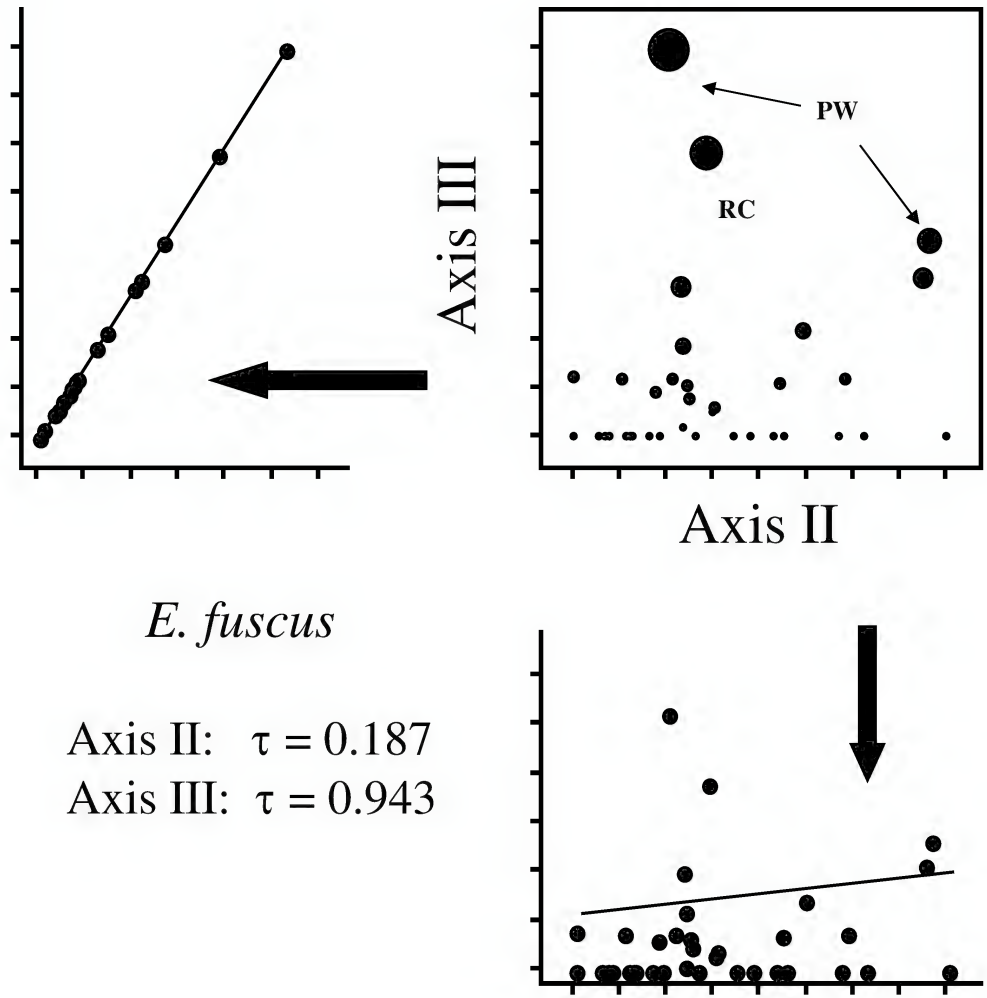
PW
RC
Axis III
Axis II
E. fuscus
Axis II: τ = 0.187
Axis III: τ = 0.943

Virginia Journal of Science
Volume 68, Issue 3 & 4
Fall & Winter 2017
doi: 10.25778/PEXS-2309

Note: This manuscript has been accepted for publication, and is online ahead of print. It will undergo copyediting, typesetting, and review of the resulting proof before it is published in its final form.

A Comparative Study on Machine Learning Algorithms for Network Defense

Abdinur Ali, Yen-Hung Hu, Chung-Chu (George) Hsieh, Mushtaq Khan
Norfolk State University, Center of Excellence in Cyber Security
700 Park Avenue, Norfolk, VA, 23504, USA
{amali, yhu, ghsieh, mkhan}@nsu.edu

ABSTRACT

Network security specialists use machine learning algorithms to detect computer network attacks and prevent unauthorized access to their networks. Traditionally, signature and anomaly detection techniques have been used for network defense. However, detection techniques must adapt to keep pace with continuously changing security attacks. Therefore, machine learning algorithms always learn from experience and are appropriate tools for this adaptation. In this paper, ten machine learning algorithms were trained with the KDD99 dataset with labels, then they were tested with different dataset without labels. The researchers investigate the speed and the efficiency of these machine learning algorithms in terms of several selected benchmarks such as time to build models, kappa statistic, root mean squared error, accuracy by attack class, and percentage of correctly classified instances of the classifier algorithms.

Keywords: Machine learning, KDD dataset, network defense

INTRODUCTION

The number of Internet security threats are growing astronomically. In 2016, the report (Symantec, 2016) revealed that, more than 430 million new malwares were discovered in 2015, up 36 percent more from the year before; a new zero day vulnerability was discovered on average each week in 2015, up 125 percent from the year before; more than 429 million personal identities were stolen in 2015, up 23 percent from the year before; over one million web attacks each and every day in 2015; spear-phishing attacks increased 55 percent in 2015; ransomware increased 35 percent in 2015; and more than 100 million fake technical support scams were blocked in 2015. Meanwhile, in 2016, the report (FBI, 2016) from the FBI disclosed that approximately 300 thousand cybercrime complaints were filed and the total loss of those victims was about 1.33 billion dollars. These data demonstrate that it is crucial and very challenging to protect end users from security threats and cybercrimes while they are connecting to the Internet via private or public networks.

Many approaches have been developed in the past few years for defending networks against security threats. Such technologies include IP traceback (Gong & Sarac, 2008) (Murugesan, Shalinie, & Neethimani, 2014) (Song & Perrig, 2001), IP traffic classification (Crotti, Gringoli, Pelosato, & Salgarelli, 2006) (Nguyen & Armitage, 2008) (Callado, et al., 2009), intrusion detection (Zhou & Lang, 2003) (Dharmapurikar & John W. Lockwood, 2006)

(Chen & Leneutre, 2009) (Das, Nguyen, Zambreno, Memik, & Choudhary, 2008) (Hu, Hu, & Maybank, 2008) (Mabu, Chen, Lu, Shimada, & Hirasawa, 2011) having been widely discussed and implemented. Their performance, advantages and disadvantages have been thoroughly investigated as well. In addition, cybersecurity issues caused by human factors are also addressed and discussed (Hadlington, 2017). Recently, machine learning technology has been used to detect network threats and malicious executables (Kolter & Maloof, 2006) (Siddiqui, Khan, Ferens, & Kinsner, 2016). Machine learning gives computers the ability to learn without being explicitly programmed (Samuel, 1959). In 1997, Tom Mitchell (Tom Mitchell, 1997) gave the definition: "*A computer program is said to learn from experience E with respect to some task T and some performance measure P, if its performance on T, as measured by P, improves with experience E.*" Furthermore, machine learning is a data analysis approach that builds automatic models for processing, predicting data, and decision making (Mannila, 1996) (Chandiok & Chaturvedi, 2015).

We focus on applying machine learning algorithms for network defense. However, the efficiencies of those algorithms vary quite a bit. In this paper, we investigate various machine learning algorithms. Our goal is to help researchers to select the appropriate algorithm based on speed and efficiency. In this research, we have used the KDD99 dataset (KDD Cup 1999 Data, n.d.) and the Weka software (Weka 3: Data Mining Software in Java, n.d.). A number of authors have pointed out some drawbacks of the KDD99 dataset (A. Olusola, S. Oladele, & O. Abosede, 2010) (Tavallaee, Bagheri, Lu, & Ghorbani, 2009) (McHugh, 2000) (Kayacik & Zincir-Heywood, 2005). Each of the proposals has its merits and demerits. However, we have used the original KDD99 dataset for training and testing the classifier algorithms. The focus of our research is benchmarking the machine learning algorithms used for network defense.

The remainder of this paper is organized as follows: Section 2 reviews related literature. Section 3 introduces research materials and methods. Section 4 discusses our research results. Section 5 concludes this paper and points out future work. Section 6 expresses our thanks to the research sponsors.

LITERATURE REVIEW

Several articles have studied and investigated machine learning algorithms. In (Solanki & Dhamdhere, 2015), the authors compared the performance of the support vector machines (SVM) and the C 4.5 algorithm. Accuracy of the two algorithms was tested for four different computer network attacks. The findings indicate that C 4.5 outperforms SVM. This finding agrees with the result we obtained with the J48 tree which is a Weka implementation of the C 4.5 algorithm.

In (Nguyen & Choi, 2008), the authors investigated a set of classifier algorithms for denial of service (DoS), remote to local (R2L), user to root (U2R), and surveillance (PROBE) attacks. The authors tried to determine the best algorithms for each attack category. The results show that Naïve Bayes, Bayes Net, One-R are the best algorithms for PROBE, U2R, and R2L attacks, respectively. Most of the algorithms were reported to have significant performance for DoS attack category.

Hidden Markov models are usually used for speech recognition (Rabiner, 1989). However, Gao, Ma and Yang have used hidden Markov models to model the normal and abnormal behavior of computer networks to detect network intrusions (Gao, Ma, & Yang, 2002). Comparing detection anomalies of different experiments, the highest accuracy achieved was 63.2% detection. Some other authors (Zhou & Lang, 2003) have used Fourier series methods for network intrusion detection. They used such methods to extract network traffic periodic patterns from raw network traffic and classify those periodic patterns as normal or abnormal traffic behavior. Gomez and Dasgupta (Gomez & Dasgupta, 2001) have proposed the use of fuzzy logic for network intrusion detection. The authors claim that their results are comparable to 95.4% detection rate.

Unlike most researchers who focused on a single audit of the data, Ye et. al. (Ye, Li, Chen, Emran, & Xu, 2001) introduced a multiple audit method based on frequency properties of the traffic data. However, the data they used for testing was "pure data" which was not noisy network data and did not reflect real case scenario of network traffic. In addition, Goonatilake, et. al. (Goonatilake, Herath, Herath, Herath, & Herath, 2007) used Chi-square goodness of fit tests for network intrusion detection. They used the test to determine abnormal network traffic activities which deviate from normal traffic patterns. Related research shows that all the existing algorithms found in the literature have challenges to determine and estimate the optimal parameters which will give us the highest detection rates within the fastest time. However, the goal for network security is still better profiling, better classification and better prediction (Wang, 2008).

In (Dao & Vemuri, 2002), the authors compared and analyzed the performance measures for five neural networks. The result of the study indicates quasi-Newton and conjugate gradient descent produced better detection rates. Our contribution is to use rigorous statistical analysis such as tests of normality, hypothesis testing, and nonparametric tests of statistical significance to compare the differences in true positive rates for ten classifier algorithms and propose benchmarks for their performance measures.

MATERIALS AND METHODS

In this simulation study, we use multiple learning algorithms and test benchmarks for each of them. The computer we selected is DELL PRECISION T3610. It equips with a 64-bit Windows 7 Pro Operating System and an Intel Xeon CPU E5-1607 V2 @ 3.00 GHZ processor with 16 gigabytes memory.

In this investigation, we have used twenty three sub-attacks. We kept the number of attacks the same for each classifier algorithm. We used ten different machine learning algorithms. Then we compared and contrasted the results of the classifiers. We have used a sample of classifiers instead of the whole population of classifiers to reduce the computational complexity. Whether this sample is representative sample or not we leave it to others.

Nevertheless, we made careful observations of the variables within the selected sample of classifiers. The ten machine learning algorithms used in this research are J48 Tree (Patil & Sherekar, 2013), Naïve Bayes (Patil & Sherekar, 2013) (Wu, et al., 2008) (Ashari, Paryudi, &

Tjoa, 2013), Random Forest (Ho, 1995) (Dietterich, 2000), Support Vector Machines (Wu, et al., 2008) (Collobert & Bengio, 2004), Multilayer Perceptron (Collobert & Bengio, 2004), Radial Basis Function (Que & Belkin, 2016), Bayes Net (Heckerman, Geiger, & Chickering, 1994), Bagging (Dietterich, 2000), AdaBoostM1 (Wu, et al., 2008), and Stacking (Sikora & Al-laymoun, 2014).

RESULTS AND DISCUSSION

In this study, the total number of instances used for testing each algorithm is 494020. The ratio of number of correctly classified instances and the total number of instances used was converted into a percentage of correctly classified instances. Random Forest was found to have the highest percentage of correctly classified instances and lowest value of root mean squared error. Therefore, it is more precise than others. Furthermore, Random Forest has the highest Kappa Statistic. This result supports that this classifier has highest agreement between the actual and predicted values. The results are given in Tables 1 - 3 and in Figures 1 - 2.

We have investigated the performance of ten classifier algorithms. We used twenty three sub-attacks and determined the true positive (TP) rates, false positive (FP) rates, precision, recall, F-measure, and the receiver operating characteristic (ROC) area of each algorithm. The twenty three sub-attacks can be reduced into four major categories; namely, denial of service (DoS) attack, remote to local attack (R2L), user to root attack (U2R), surveillance (PROBE). However, instead of reduction, we decided to retain the twenty three sub-attacks and find their accuracies using the ten classifier algorithms. The results of the accuracy by class are given in Tables 4 - 13.

In this simulation, we compared and contrasted the true positives of all ten classifier algorithms. However, before we compared the true positive rates of machine algorithms, tests of normality were performed. As shown in Table 14, Kolmogorov-Smirnov and Shapiro-Wilk tests were used to test the assumption of normality. Lilliefors significance correction was used for Kolmogorov-Smirnov test. The results indicate that the model violates the assumption of normality. Therefore, parametric statistics cannot be used to analyze this data. We decided to use non-parametric statistics. The results for the normality tests are given in Table 14.

When we selected non-parametric statistics, the Kruskal-Wallis test was used to compare the differences in true positive rates of the machine learning algorithms. We input identical twenty three sub-attacks into ten different classifiers. The findings show that the differences in true positive rates for the ten classifiers are statistically significant. The result for the overall model is significant and is given in Table 15.

The pairwise comparison logically follows if the overall model is statistically significant. Only significant pairwise comparisons are given in Tables 16 & 17. The findings indicate that J48 Tree outperforms AdaBoostM1 and Stacking. Naïve Bayes outperforms Radial Basis Function, AdaboostM1 and Stacking. Random Forest outperforms Multilayer Perceptron, Radial Basis Function, AdaBoostM1 and Stacking. Multilayer Perceptron outperforms AdaboostM1 and Stacking. Support Vector Machines outperform AdaBoostM1 and Stacking. Radial Basis Function outperforms Bagging, AdaBoostM1 and Stacking. Bayes Net outperforms AdaBoostM1 and Stacking. Bagging outperforms AdaBoostM1 and Stacking.

CONCLUSION

A fundamental goal of network security is to use statistical models with the highest true positive rates. In general, network security engineers have to choose the most appropriate machine learning algorithms to prevent abnormal uses of their computer systems. However, they are faced with many competing parameters such as speed and the efficiency of the selected algorithm.

We used the KDD99 dataset as a benchmark for testing ten classifier algorithms. We found Stacking algorithm is the fastest for the time to build models. Additionally, for the correctly classified instances, Random Forest is the winner. Random Forest has the highest true positive rates. However, we infer based on our simulation results that AdaBoostM1 and the Stacking classifiers have the lowest true positives rates out of the ten classifiers. With regard to the model performance measures, our data supports that J48 Tree, Naïve Bayes, Random Forest and Support Vector Machines are the top four best performers in true positive rates.

ACKNOWLEDGEMENT

This material is based on research sponsored by the Office of the Assistant Secretary of Defense for Research and Engineering (OASD(R&E)) under agreement number FAB750-15-2-0120. The U.S. Government is authorized to reproduce and distribute reprints for Governmental purposes notwithstanding any copyright notation thereon. The views and conclusions contained herein are those of the authors and should not be interpreted as necessarily representing the official policies or endorsements, either expressed or implied, of the Office of the Assistant Secretary of Defense for Research and Engineering (OASD(R&E)) or the U.S. Government. We thank the editor and the reviewers for constructive suggestions for improvement of the paper.

REFERENCES

A. Olusola, A., S. Oladele, A., & O. Abosede, D. (2010). Analysis of KDD '99 Intrusion Detection Dataset for Selection of Relevance Features. *Proceedings of the World Congress on Engineering and Computer Science (WCECS)*, *1*, pp. 20-22. San Francisco, USA.

Ashari, A., Paryudi, I., & Tjoa, A. M. (2013). Performance Comparison Between Naive Bayes, Decision Tree and K-Nearest Neighbor in Searching Alternative Design in an Energy Simulation Tool. *International Journal of Advanced Computer Science and Applications ((IJACSA)), 4*(11), 33-39.

Callado, A., Kamienski, C., Szabó, G., Ger˝o, B. P., Kelner, J., Fernandes, S., & Sadok, D. (2009). A Survey on Internet Traffic Identification. *IEEE Communications Surveys & Tutorials, 11*(3), 37-52.

Chandiok, A., & Chaturvedi, D. K. (2015). Machine Learning Techniques for Cognitive Decision Making. *Proceedings of 2015 IEEE Workshop on Computational Intelligence: Theories, Applications and Future Directions (WCI)*, (pp. 1-6). Kanpur, India.

Chen, L., & Leneutre, J. (2009). A Game Theoretical Framework on Intrusion Detection in Heterogeneous Networks. *IEEE Transactions On Information Forensics And Security, 4*(2), 165-178.

Collobert, R., & Bengio, S. (2004). Links between Perceptrons, MLPs and SVMs. *Proceedings of the 21st International Conference on Machine Learnin.* Banff, Canada.

Crotti, M., Gringoli, F., Pelosato, P., & Salgarelli, L. (2006). A Statistical Approach to IP-level Classification of Network Traffic. *Proceedings of 2006 IEEE International Conference on Communications (ICC 2006)*, (pp. 170-176). Istanbul, Turkey.

Dao, V. N., & Vemuri, V. R. (2002). Computer Network Intrusion Detection: A Comparison of Neural Network Methods. *Differential Equations and Dynamical Systems, 10*(1&2), 201-214.

Das, A., Nguyen, D., Zambreno, J., Memik, G., & Choudhary, A. (2008). An FPGA-Based Network Intrusion Detection Architecture. *IEEE Transactions On Information Forensics And Security, 3*(1), 118-132.

Dharmapurikar, S., & John W. Lockwood. (2006). Fast and Scalable Pattern Matching for Network Intrusion Detection Systems. *IEEE Journal On Selected Areas In Communications, 24*(10), 1781-1792.

Dietterich, T. (2000). An Experimental Comparison of Three Methods for Constructing Ensembles of Decision Trees: Bagging, Boosting, and Randomization. *Machine Learning*, 139-157.

FBI. (2016). *2016 Internet Crime Report.* Retrieved from https://pdf.ic3.gov/2016_IC3Report.pdf

Gao, B., Ma, H.-Y., & Yang, Y.-H. (2002). HMMs (Hidden Markov models) based on anomaly intrusion detection method. *Proceedings of 2002 International Conference on Machine Learning and Cybernetics.* Beijing, China.

Gomez, J., & Dasgupta, D. (2001). Evolving Fuzzy Classifiers for Intrusion Detection. *Proceedings of the 2002 IEEE Workshop on Information Assurance.* West Point, New York, USA.

Gong, C., & Sarac, K. (2008). A More Practical Approach for Single-Packet IP Traceback using Packet Logging and Marking. *IEEE Transactions on Parallel and Distributed Systems, 19*(10), 1310-1324.

Goonatilake, R., Herath, A., Herath, S., Herath, S., & Herath, J. (2007). Intrusion Detection Using the Chi-Square Goodness-of-Fit Test for Information Assurance, Network, Forensics and Software Security. *Journal of Computing Sciences in Colleges - Papers of*

the Fourteenth Annual CCSC Midwestern Conference and Papers of the Sixteenth Annual CCSC Rocky Mountain Conference, 255-263.

Hadlington, L. (2017). Human Factors in Cybersecurity; Examining the Link Between Internet Addition, Impulsivity, Attitudes Towards Cybersecurity, and Risk Cybersecurity Behaviours. *Heliyon, 3*(7).

Heckerman, D., Geiger, D., & Chickering, D. M. (1994). Learning Bayesian Networks: The Combination of Knowledge and Statistical Data. *Proceedings of AAAI-94 Workshop on Knowledge Discovery in Databases*, (pp. 85-96).

Ho, T. K. (1995). Random Decision Forests. *Proceedings of the 3rd International Conference on Document Analysis and Recognition*, (pp. 278-282). Montreal, Quebec, Canada.

Hu, W., Hu, W., & Maybank, S. (2008). AdaBoost-Based Algorithm for Network Intrusion Detection. *IEEE Transactions On Systems, Man, And Cybernetics - Part B: Cybernetics, 38*(2), 577-583.

Kayacik, H. G., & Zincir-Heywood, N. (2005). Analysis of three intrusion detection system benchmark datasets using machine learning algorithms. *Proceedings of the 2005 IEEE international conference on Intelligence and Security Informatics (ISI'05)*, (pp. 362-367). Atlanta, Georgia, USA.

KDD Cup 1999 Data. (n.d.). Retrieved from http://kdd.ics.uci.edu/databases/kddcup99/kddcup99.html

Kolter, J. Z., & Maloof, M. A. (2006). Learning to Detect and Classify Malicious Executables in the Wild. *The Journal of Machine Learning Research, 7*, 2721-2744.

Mabu, S., Chen, C., Lu, N., Shimada, K., & Hirasawa, K. (2011). An Intrusion-Detection Model Based on Fuzzy Class-Association-Rule Mining Using Genetic Network Programming. *IEEE Transactions On Systems, Man, And Cybernetics - Part C: Applications And Reviews, 41*(1), 130-139.

Mannila, H. (1996). Data Mining: Machine Learning, Statistics, and Databases. *Proceedings of 8th International Conference on Scientific and Statistical Data Base Management*, (pp. 2-9). Stockholm, Sweden.

McHugh, J. (2000). Testing Intrusion detection systems: a critique of the 1998 and 1999 DARPA intrusion detection system evaluations as performed by Lincoln Laboratory. *ACM Transactions on Information and System Security (TISSEC), 3*(4), 262-294.

Murugesan, V., Shalinie, M., & Neethimani, N. (2014). A Brief Survey of IP Traceback Methodologies. *Acta Polytechnica Hungarica, 11*(9), 197-216.

Nguyen, H. A., & Choi, D. (2008). Application of Data Mining to Network Intrusion Detection: Classifier Selection Model. *Proceedings of the 11th Asia-Pacific Symposium on Network Operations and Management: Challenges for Next Generation Network Operations and Service Management (APNOMS '08)*, (pp. 399-408). Beijing, China.

Nguyen, T. T., & Armitage, G. (2008). A Survey of Techniques for Internet Traffic Classification using Machine Learning. *IEEE Communications Surveys & Tutorials, 10*(4), 56-76.

Patil, T. R., & Sherekar, S. S. (2013). Performance Analysis of Naive Bayes and J48 Classification Algorithm for Data Classification. *International Journal of Computer Science and Application, 6*(2), 256-261.

Que, Q., & Belkin, M. (2016). Back to the Future: Radial Basis Function Networks Revisited. *Proceedings of the 19th International Conference on Artificial Intelligence and Statistics (AISTATS)*, *51*, pp. 1375-1383. Cadiz, Spain.

Rabiner, L. R. (1989). A Tutorial on Hidden Markov Moels and Selected Application in Speech Recognition. *Proceedings of the IEEE*, 257-286.

Samuel, A. L. (1959). Some Studies in Machine Learning Using the Game of Checkers. *IBM Journal of Research and Development, 3*(3), 210-229.

Siddiqui, S., Khan, M. S., Ferens, K., & Kinsner, W. (2016). Detecting Advanced Persistent Threats using Fractal Dimension based Machine Learning Classification. *Proceedings of the 2016 ACM on International Workshop on Security And Privacy Analytics (IWSPA '16)*, (pp. 64-69). New Orleans, Louisiana, USA.

Sikora, R., & Al-laymoun, O. H. (2014). A Modified Stacking Ensemble Machine Learning Algorithm Using Genetic Algorithms. *Journal of International Technology and Information Management, 23*(1).

Solanki, M., & Dhamdhere, V. (2015). Intrusion Detection System Using Means of Data Mining By Using C 4.5 Algorithm. *International Journal of Application or Innovation in Engineering & Management (IJAIEM), 4*(5).

Song, D. X., & Perrig, A. (2001). Advanced and Authenticated Marking Schemes for IP Traceback. *Proceedings of IEEE INFOCOM 2001. Conference on Computer Communications. Twentieth Annual Joint Conference of the IEEE Computer and Communications Society (Cat. No.01CH37213)*, *2*, pp. 878-886. Anchorage, Alaska, USA.

Symantec. (2016, April). *Internet Security Threat Report.* Retrieved from https://www.symantec.com/content/dam/symantec/docs/reports/istr-21-2016-en.pdf

Tavallaee, M., Bagheri, E., Lu, W., & Ghorbani, A. A. (2009). A Detailed Analysis of the KDD CUP 99 Data Set. *Proceedings of the 2009 IEEE Symposium on Computational Intelligence in Security and Defense Application (CISDA 2009)*, (pp. 53-58). Ottaws, Ontario, Canada.

Tom Mitchell. (1997). *Machine Learning.* McGraw Hill.

Wang, Y. (2008). *Statistical Techniques for Network Security: Modern Statistically-Based Intrusion Detection and Protection.* IGI Global.

Weka 3: Data Mining Software in Java. (n.d.). Retrieved from http://www.cs.waikato.ac.nz/ml/weka/

Wu, X., Kumar, V., Quinlan, J. R., Ghosh, J., Yang, Q., Motoda, H., . . . Steinberg, D. (2008). Top 10 Algorithms in Data Mining. *Knowledge Information System, 14*, 1-37.

Ye, N., Li, X., Chen, Q., Emran, S., & Xu, M. (2001). Probabilistic Techniques for Intrusion Detection Based on Computer Audit Data. *IEEE Transactions on Systems, Man, and Cybernetics - Part A: Systems and Humans*, 266-274.

Zhou, M., & Lang, S.-d. (2003). Mining Frequency Content of Network Traffic for Intrusion Detection. *Proceedings of IASTED International Conference on Communication, Network and Information Security (CNIS 2003)*, (pp. 101-107). New York City, New York, USA.

Figure 1: Kappa Statistic

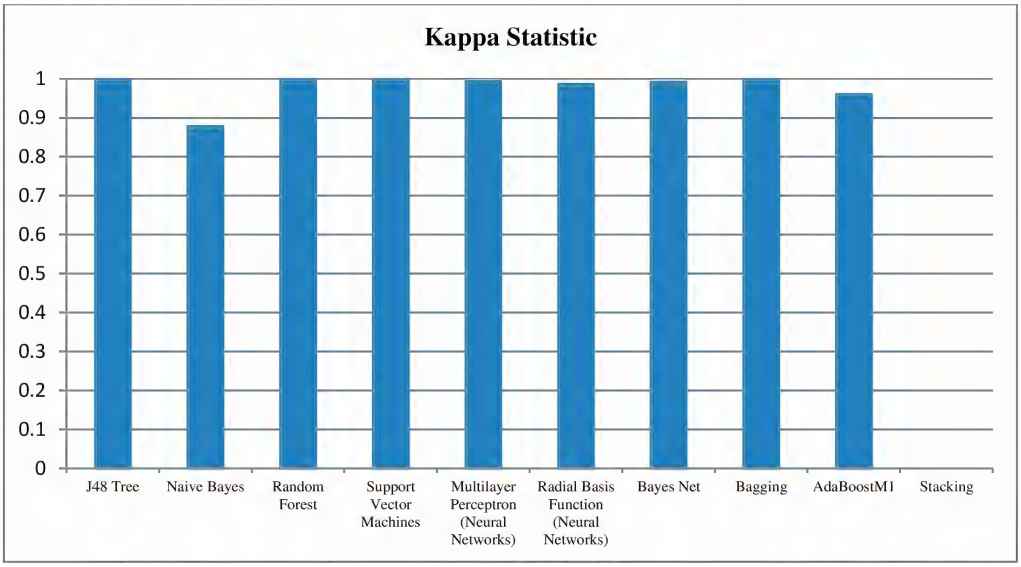

Figure 2: Root Mean Squared Error

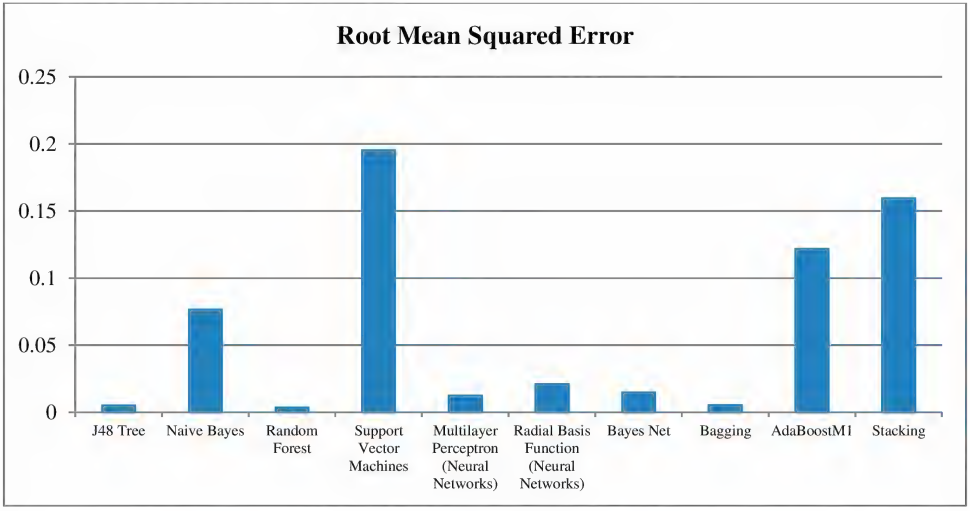

Table1: Benchmark comparison of various algorithms

Algorithm	Time to Build Model (seconds)	Correctly Classified Instances (%)	Kappa Statistic	Root Mean Squared Error
J48 Tree	69.47	99.9603 %	0.9993	0.0057
Naïve Bayes	2.89	92.7794 %	0.8806	0.0772
Random Forest	588.21	99.9794 %	0.9997	0.0041
Support Vector Machines (SVM)	254.31	99.9245 %	0.9987	0.1961
Multilayer Perceptron (Neural Networks)	46212.93	99.7911 %	0.9965	0.0132
Radial Basis Function (Neural Networks)	41623.78	99.3243%	0.9886	0.0217
Bayes Net	17.42	99.667 %	0.9944	0.0153
Bagging	206.18	99.9524 %	0.9992	0.0059
AdaBoostM1	65.12	97.8576 %	0.9635	0.1225
Stacking	2.31	56.8378 %	0	0.1603

Table 2: Benchmark comparison of various algorithms based on Time to Build Model (seconds)

Algorithm	Ranks based on Time to Build Model (seconds)
Stacking	2.31
Naïve Bayes	2.89
Bayes Net	17.42
AdaBoostM1	65.12
J48 Tree	69.47
Bagging	206.18
Support Vector Machines	254.31
Random Forest	588.21
Radial Basis Function (Neural Networks)	41623.78
Multilayer Perceptron (Neural Networks)	46212.93

Table 3: Benchmark comparison of various algorithms based on Correctly Classified Instance (%)

Algorithm	Ranks based on Correctly Classified Instances (%)
Random Forest	99.9794 %
J48 Tree	99.9603 %
Bagging	99.9524 %
Support Vector Machines	99.9245 %
Multilayer Perceptron (Neural Networks)	99.9245 %
Bayes Net	99.667 %
Radial Basis Function (Neural Networks)	99.3243 %
AdaBoostM1	97.8576 %
Naive Bayes	92.7794 %
Stacking	56.8378 %

Table 4: Accuracy by Class of Attacks (J48 Tree)

TP Rate	FP Rate	Precision	Recall	F-Measure	ROC area	Class of Attacks
0.998	0	0.998	0.998	0.998	0.999	Back
0.999	0	1	0.999	0.999	0.999	teardrop
0	0	0	0	0	0.729	load module
1	0	1	1	1	1	Neptune
0	0	0	0	0	0.622	rootkit
1	0	0.667	1	0.8	1	phf
0.989	0	0.992	0.989	0.991	0.996	Satan
0.7	0	0.656	0.7	0.677	0.895	Buffer_overflow
0	0	0	0	0	0.578	ftp_write
0.81	0	0.895	0.81	0.85	0.905	land
0	0	0	0	0	0.453	spy
0.993	0	0.994	0.993	0.993	0.999	ipsweep
0	0	0	0	0	0.857	multihop
1	0	1	1	1	1	smurf
1	0	0.996	1	0.998	1	pod
0.667	0	0.5	0.667	0.571	0.997	perl
0.979	0	0.994	0.079	0.987	0.998	warezclient
0.952	0	0.991	0.333	0.421	0.995	nmap
0.333	0	0.571	0.333	0.421	0.818	imap
0.8	0	0.889	0.8	0.842	0.923	warezmaster
0.986	0	0.993	0.986	0.989	0.997	portsweep
1	0	0.999	1	0.999	1	normal
0.943	0	0.962	0.943	0.952	0.972	Guess_passwd

Table 5: Accuracy by Class of Attacks (Naïve Bayes)

TP Rate	FP Rate	Precision	Recall	F-Measure	ROC area	Class of Attacks
0.975	0.005	0.485	0.975	0.648	0.999	Back
0.995	0.001	0.638	0.995	0.777	0.999	teardrop
0.556	0	0.022	0.556	0.041	0.999	load module
0.996	0	1	0.996	0.998	1	Neptune
0.5	0.003	0.003	0.5	0.006	0.977	rootkit
0.75	0	0.071	0.75	0.13	0.995	phf
0.954	0.002	0.58	0.954	0.722	0.996	Satan
0.133	0	0.018	0.133	0.032	0.999	Buffer_overflow
0.75	0.003	0.004	0.75	0.009	0.997	ftp_write
0.952	0	0.323	0.952	0.482	1	land
1	0	1	1	1	1	spy
0.966	0.009	0.205	0.966	0.339	0.994	ipsweep
0.429	0	0.068	0.429	0.118	1	multihop
0.999	0	1	0.999	0.999	1	smurf
0.985	0.037	0.014	0.985	0.028	0.998	pod
0.333	0	0.333	0.333	0.333	1	perl
0.478	0.006	0.143	0.478	0.22	0.988	warezclient
0.446	0.001	0.167	0.446	0.243	0.995	nmap
0.917	0	0.141	0.917	0.244	0.942	imap
0.9	0.001	0.055	0.9	0.103	0.994	warezmaster
0.907	0.001	0.65	0.907	0.757	0.998	portsweep
0.652	0.001	0.997	0.652	0.788	0.999	normal
0.943	0.001	0.07	0.943	0.13	0.989	Guess_passwd

Table 6: Accuracy by Class of Attacks (Random Forest)

TP Rate	FP Rate	Precision	Recall	F-Measure	ROC area	Class of Attacks
1	0	1	1	1	1	Back
1	0	1	1	1	1	teardrop
0.333	0	1	0.333	0.5	1	load module
1	0	1	1	1	1	Neptune
0.1	0	1	0.1	0.182	1	rootkit
0.75	0	1	0.75	0.857	1	phf
0.99	0	0.999	0.99	0.995	0.999	Satan
0.833	0	0.833	0.833	0.833	1	Buffer_overflow
0.375	0	1	0.375	0.545	0.937	ftp_write
0.857	0	0.947	0.857	0.9	1	land
0	0	0	0	0	1	spy
0.991	0	0.996	0.991	0.994	1	ipsweep
0.429	0	0.6	0.429	0.5	0.929	multihop
1	0	1	1	1	1	smurf
0.996	0	0.996	0.996	0.996	1	pod
0.667	0	1	0.667	0.8	1	perl
0.993	0	0.994	0.993	0.994	1	warezclient
0.974	0	1	0.974	0.987	1	nmap
1	0	1	1	1	1	imap
0.8	0	0.889	0.8	0.842	1	warezmaster
0.995	0	0.996	0.995	0.996	1	portsweep
1	0	0.999	1	1	1	normal
0.962	0	1	0.962	0.981	1	Guess_passwd

Table 7: Accuracy by Class of Attacks (Support Vector Machines)

TP Rate	FP Rate	Precision	Recall	F-Measure	ROC area	Class of Attacks
0.997	0	0.991	0.997	0.994	1	Back
0.998	0	1	0.998	0.999	1	teardrop
0	0	0	0	0	0.994	load module
1	0	1	1	1	1	Neptune
0	0	0	0	0	0.882	rootkit
0	0	0	0	0	1	phf
0.972	0	0.998	0.972	0.985	0.998	Satan
0.6	0	0.75	0.6	0.667	0.999	Buffer_overflow
0.5	0	0.667	0.5	0.571	0.999	ftp_write
1	0	0.955	1	0.977	1	land
0	0	0	0	0	1	spy
0.982	0	0.987	0.982	0.984	1	ipsweep
0	0	0	0	0	0.998	multihop
1	0	1	1	1	1	smurf
0.992	0	0.992	0.992	0.992	1	pod
0	0	0	0	0	1	perl
0.915	0	0.925	0.915	0.92	1	warezclient
0.965	0	0.933	0.965	0.949	0.997	nmap
0.833	0	1	0.833	0.909	1	imap
0.75	0	0.789	0.75	0.769	0.999	warezmaster
0.994	0	0.998	0.994	0.996	0.998	portsweep
0.999	0.001	0.998	0.999	0.998	0.999	normal
0.943	0	0.98	0.943	0.962	1	Guess_passwd

Table 8: Accuracy by Class of Attacks (Multilayer Perceptron)

TP Rate	FP Rate	Precision	Recall	F-Measure	ROC area	Class of Attacks
0.727	0	0.979	0.727	0.835	0.992	Back
1	0	0.998	1	0.999	1	teardrop
0	0	0	0	0	0.648	load module
1	0	1	1	1	1	Neptune
0	0	0	0	0	0.751	rootkit
0	0	0	0	0	0.931	phf
0.987	0	0.994	0.987	0.99	0.996	Satan
0.2	0	0.286	0.2	0.235	0.885	Buffer_overflow
0	0	0	0	0	0.846	ftp_write
0	0	0	0	0	0.93	land
0	0	0	0	0	0.736	spy
0.982	0	0.964	0.982	0.973	0.999	ipsweep
0	0	0	0	0	0.94	multihop
1	0	1	1	1	1	smurf
0.981	0	0.974	0.981	0.977	0.997	pod
0	0	0	0	0	0.769	perl
0.917	0	0.936	0.917	0.926	0.995	warezclient
0.792	0	0.91	0.792	0.847	0.936	nmap
0	0	0	0	0	0.918	imap
0	0	0	0	0	0.953	warezmaster
0.996	0	0.984	0.996	0.99	0.998	portsweep
0.999	0.002	0.992	0.999	0.995	0.999	normal
0.925	0	0.69	0.925	0.79	1	Guess_passwd

Table 9: Accuracy by Class of Attack (Radial Basis Function)

TP Rate	FP Rate	Precision	Recall	F-Measure	ROC area	Class of Attacks
0.907	0	0.978	0.907	0.941	0.998	Back
0.994	0	1	0.994	0.997	1	teardrop
0.333	0	0.6	0.333	0.429	0.868	load module
0.998	0	0.999	0.998	0.999	1	Neptune
0	0	0	0	0	0.66	rootkit
0.75	0	1	0.75	0.857	0.796	phf
0.897	0.001	0.824	0.897	0.859	0.999	Satan
0.567	0	0.81	0.567	0.667	0.944	Buffer_overflow
0	0	0	0	0	0.993	ftp_write
0.19	0	0.444	0.19	0.267	0.961	land
0	0	0	0	0	0.182	spy
0.52	0	0.992	0.52	0.682	0.998	ipsweep
0	0	0	0	0	0.722	multihop
0.999	0	1	0.999	0.999	1	smurf
0.841	0	0.892	0.841	0.865	1	pod
0.333	0	1	0.333	0.5	0.455	perl
0	0	0	0	0	0.994	warezclient
0.442	0	1	0.442	0.613	0.992	nmap
0.583	0	0.875	0.583	0.7	0.727	imap
0.15	0	0.5	0.15	0.231	0.931	warezmaster
0.88	0	0.963	0.88	0.92	0.997	portsweep
0.996	0.007	0.972	0.996	0.984	0.999	normal
0.83	0	0.917	0.83	0.871	0.969	Guess_passwd

Table 10: Accuracy by Class of Attacks (Bayes Net)

TP Rate	FP Rate	Precision	Recall	F-Measure	ROC area	Class of Attacks
0.997	0	1	0.997	0.998	1	Back
0.999	0	0.924	0.999	0.96	1	teardrop
0	0	0	0	0	0.999	load module
0.999	0	1	0.999	1	1	Neptune
0.4	0	0.033	0.4	0.06	0.994	rootkit
0.5	0	1	0.5	0.667	1	phf
0.913	0	0.982	0.913	0.946	1	Satan
0.767	0	0.288	0.767	0.418	1	Buffer_overflow
0.25	0	0.087	0.25	0.129	0.998	ftp_write
1	0	0.189	1	0.318	1	land
0	0	0	0	0	0.999	spy
0.929	0.001	0.729	0.929	0.817	1	ipsweep
0	0	0	0	0	0.994	multihop
1	0	1	1	1	1	smurf
0.989	0	0.779	0.989	0.871	1	pod
0	0	0	0	0	1	perl
0.996	0	0.815	0.996	0.896	1	warezclient
0.472	0	0.341	0.472	0.396	0.998	nmap
0.833	0	0.286	0.833	0.426	0.998	imap
0.75	0	0.221	0.75	0.341	0.999	warezmaster
0.977	0	0.905	0.977	0.939	1	portsweep
0.989	0	0.999	0.989	0.994	1	normal
0.962	0	0.85	0.962	0.903	1	Guess_passwd

Table 11: Accuracy by Class of Attacks (Bagging)

TP Rate	FP Rate	Precision	Recall	F-Measure	ROC area	Class of Attacks
1	0	1	1	1	1	Back
1	0	1	1	1	1	teardrop
0.444	0	0.571	0.444	0.5	0.944	load module
1	0	0.999	1	1	1	Neptune
0	0	0	0	0	0.899	rootkit
0.5	0	1	0.5	0.667	1	phf
0.981	0	0.996	0.981	0.989	0.994	Satan
0.867	0	0.722	0.867	0.788	0.967	Buffer_overflow
0	0	0	0	0	0.875	ftp_write
0.952	0	0.952	0.952	0.952	0.976	land
0	0	0	0	0	1	spy
0.974	0	0.997	0.974	0.985	0.996	ipsweep
0	0	0	0	0	0.928	multihop
1	0	1	1	1	1	smurf
1	0	0.992	1	0.996	1	pod
0.333	0	1	0.333	0.5	1	perl
0.99	0	0.979	0.99	0.984	1	warezclient
0.965	0	0.97	0.965	0.967	0.989	nmap
0.833	0	1	0.833	0.909	0.958	imap
0.85	0	0.81	0.85	0.829	0.95	warezmaster
0.951	0	0.999	0.951	0.974	0.988	portsweep
1	0	0.999	1	0.999	1	normal
0.925	0	0.942	0.925	0.933	1	Guess_passwd

Table 12: Accuracy by Class of Attacks (AdaBoostM1)

TP Rate	FP Rate	Precision	Recall	F-Measure	ROC area	Class of Attacks
0	0	0	0	0	0.692	Back
0	0	0	0	0	0.661	teardrop
0	0	0	0	0	0.643	load module
0.995	0.007	0.975	0.995	0.985	0.998	Neptune
0	0	0	0	0	0.663	rootkit
0	0	0	0	0	0.738	phf
0	0	0	0	0	0.856	Satan
0	0	0	0	0	0.665	Buffer_overflow
0	0	0	0	0	0.661	ftp_write
0	0	0	0	0	0.586	land
0	0	0	0	0	0.71	spy
0	0	0	0	0	0.588	ipsweep
0	0	0	0	0	0.662	multihop
0.999	0	1	0.999	0.999	1	smurf
0	0	0	0	0	0.584	pod
0	0	0	0	0	0.638	perl
0	0	0	0	0	0.691	warezclient
0	0	0	0	0	0.598	nmap
0	0	0	0	0	0.617	imap
0	0	0	0	0	0.599	warezmaster
0	0	0	0	0	0.608	portsweep
0.99	0.02	0.925	0.99	0.956	0.995	normal
0	0	0	0	0	0.688	Guess_passwd

Table 13: Accuracy by Class of Attacks (Stacking)

TP Rate	FP Rate	Precision	Recall	F-Measure	ROC area	Class of Attacks
0	0	0	0	0	0.5	Back
0	0	0	0	0	0.5	teardrop
0	0	0	0	0	0.45	load module
0	0	0	0	0	0.5	Neptune
0	0	0	0	0	0.5	rootkit
0	0	0	0	0	0.2	phf
0	0	0	0	0	0.5	Satan
0	0	0	0	0	0.5	Buffer_overflow
0	0	0	0	0	0.4	ftp_write
0	0	0	0	0	0.479	land
0	0	0	0	0	0.1	spy
0	0	0	0	0	0.499	ipsweep
0	0	0	0	0	0.35	multihop
1	1	0.568	1	0.725	0.5	smurf
0	0	0	0	0	0.495	pod
0	0	0	0	0	0.15	perl
0	0	0	0	0	0.5	warezclient
0	0	0	0	0	0.498	nmap
0	0	0	0	0	0.433	imap
0	0	0	0	0	0.5	warezmaster
0	0	0	0	0	0.5	portsweep
0	0	0	0	0	0.5	normal
0	0	0	0	0	0.48	Guess_passwd

Table 14: Tests of Normality

Algorithms	Kolmogorov-Smirnov Test (KS) Statistic	KS df	KS Sig.	Shapiro-Wilk Test (Sh-W) Statistic	Sh-W df	Sh-W Sig.
J48 Tree	0.287	23	0.000	0.697	23	0.000
Naïve Bayes	0.266	23	0.000	0.833	23	0.001
Random Forest	0.279	23	0.000	0.729	23	0.000
Support Vector Machines	0.281	23	0.000	0.702	23	0.000
Multilayer Perceptron	0.287	23	0.000	0.711	23	0.000
Radial Basis Function	0.173	23	0.073	0.873	23	0.007
Bayes Net	0.245	23	0.001	0.767	23	0.000
Bagging	0.310	23	0.000	0.708	23	0.000
AdaBoostM1	0.517	23	0.000	0.403	23	0.000
Stacking	0.539	23	0.000	0.215	23	0.000

Table 15: Kruskal-Wallis Test

	True Positive Rates
Chi-Square	62.965
df	9
Asymp. Signif.	0.000

Table 16: Pairwise comparison for true positive rates

Algorithms	Mann-WhitneyU	WilcoxonW	Z Statistic	Asymp. Signif. Two-tailed	Mean Rank
J48 Tree vs AdaboostM1	98.500	374.500	-3.983	0.000	J48 Tree > AdaboostM1
J48 Tree vs Stacking	75.500	351.500	-4.654	0.000	J48Tree > Stacking
Naïve Bayes vs Radial Basis Function	170.500	446.500	-2.067	0.039	Naïve Bayes > Radial Basis Function
Naïve Bayes vs AdaBoostM1	60.000	336.000	-4.690	0.000	Naïve Bayes > AdaBoostM1
Naïve Bayes vs Stacking	22.500	298.500	-5.633	0.000	Naïve Bayes > Stacking
Random Forest vs Multilayer Perceptron	169.500	445.500	-2.109	0.035	Random Forest > Multilayer Perceptron
Random Forest vs Radial Basis Function	150.500	426.500	-2.510	0.012	Random Forest > Radial Basis Function
Random Forest vs AdaBoostM1	55.000	331.000	-4.844	0.000	Random Forest > AdaBoostN1
Random Forest vs Stacking	31.000	307.000	-5.494	0.000	Random Forest > Stacking
Support Vector Machines vs AdaBoostM1	111.500	387.500	-3.713	0.000	Support Vector Machines > AdaBoostM1
Support Vector Machines vs Stacking	87.500	363.500	-4.420	0.000	Support Vector Machines > Stacking

Table 17: Pairwise comparison for true positive rates

Algorithms	Mann-Whitney U	Wilcoxon W	Z Statistic	Asymp. Sig. (2-tailed)	Mean Rank
Multilayer Perceptron vs AdaBoostM1	155.500	431.500	-2.817	0.005	Multilayer Perceptron > AdaBoostM1
Multilayer Perceptron vs Stacking	131.500	407.500	-3.589	0.000	Multilayer Perceptron > Stacking
Radial Basis Function vs Bagging	173.000	449.000	-2.020	0.043	Radial Basis Function > Bagging
Radial Basis Function vs AdaBoostM1	111.500	387.500	-3.668	0.000	Radial Basis Function > AdaBoostM1
Radial Basis Function vs Stacking	78.000	354.000	-4.587	0.000	Radial Basis Function > Stacking
Bayes Net vs AdaBoostM1	94.000	370.000	-4.044	0.000	Bayes Net > AdaBoostM1
Bayes Net vs Stacking	66.000	342.000	-4.818	0.000	Bayes Net > Stacking
Bagging vs AdaBoostM1	90.500	366.500	-4.132	0.000	Bagging > AdaBoostM1
Bagging vs Stacking	64.00	340.000	-4.876	0.000	Bagging > Stacking

Virginia Journal of Science
Volume 68, Issue 3 & 4
Fall & Winter 2017
doi: 10.25778/7PKV-FV16

Note: This manuscript has been accepted for publication and is online ahead of print. It will undergo copyediting, typesetting, and review of the resulting proof before it is published in its final form.

Predation on Artificial Turkey Nests at Radford Army Ammunition Plant in Western Virginia

Shane Brandes[1], Karen E. Powers[1, 3] and Len L. DiIoia, Jr.[2]

[1]Radford University, Radford, VA 24142
[2]Radford Army Ammunition Plant, Radford, VA 24141
[3]Corresponding author: Box 6931, Radford University, Radford VA 24142; kpowers4@radford.edu

ABSTRACT

Because ground-nesting wild turkeys (*Meleagris gallopavo*) may sustain high incidences of nest predation in western Virginia, determining their predators is essential to understanding risk and managing the birds. Our study investigated potential predators of wild turkey nests at the Radford Army Ammunition Plant, New River Unit (RFAAP; Pulaski Co., in western Virginia). Here, we established 8 artificial nests during the breeding season for wild turkey (March-April, 2017), and documented predators via game cameras. Thirty-one species of mammals and birds visited the nests over the 31-day study. Nest predation was verified 56 times across 6 species, including coyotes (*Canis latrans*), a relatively new addition to the RFAAP. Most egg loss was attributed to mesocarnivores—raccoons (*Procyon lotor*), striped skunks (*Mephitis mephitis*), and Virginia opossums (*Didelphis virginiana*)—but eastern fox squirrels (*Sciurus niger*) and American crows (*Corvus brachyrhynchos*) were predators, too. Because these nests were artificial and unguarded, further studies will elucidate predation risks to wild turkeys at the RFAAP. The RFAAP offers the unique opportunity to further study this predator-prey relationship, as hunting for wild turkey and the predators recognized in this study is not permitted on the property.

INTRODUCTION

By knowing and understanding the natural history of a game species, and the habitat in which it exists, managers can determine how best to manage a population, and which management techniques might maintain or increase the population size. In the case of the wild turkey (*Meleagris gallopavo*) in southwestern Virginia, it is possible that populations are controlled by bottom-up (food limitations, secure nest space) or top-down (predation to nests, poults, and adults) factors (Roberts and Porter 1996, Lariviere 1999), or a combination of the two pressures (Norman et al. 2001).

At the Radford Army Ammunition Plant's (RFAAP) New River Unit (Pulaski Co., western Virginia), resource managers work with the Virginia Department of Game and Inland Fisheries (VDGIF) to follow the principles of Quality Deer Management (QDM; VDGIF 2017a) to manage the 1101-ha property, in part, for white-tailed deer (*Odocoileus virginianus*). In doing so, other game species undoubtedly benefit from bottom-up QDM management efforts, e.g., the introduction of food plots benefit other browsers and granivores. Wild turkeys are common visitors to these managed food plots (Powers, personal observation). However, no investigations to date have looked at top-down controls of the population of wild turkeys on the property.

Hernandez et al. (1998) reported raccoons (*Procyon lotor*) as the principle predators of turkey nests in Texas, and secondary predators included bobcats (*Lynx rufus*), striped skunks (*Mephitis mephitis*), gray foxes (*Urocyon cinereoargenteus*), and Virginia opossums (*Didelphis virginiana*). Occasional predators of wild turkey nests included turkey vultures (*Cathartes aura*), woodrats (*Neotoma*), and other wild turkeys (Hernandez et al. 1998). The Virginia Department of Game and Inland Fisheries (2014) lists bobcats as the primary mammalian predator of wild turkeys, although raccoons have greater success as nest predators. Raptors, primarily great horned owls (*Bubo virginianus*), also feed on wild turkeys, and American crows (*Corvus brachyrynchos*) are significant nest predators (VDGIF 2014).

At the RFAAP, surveys of predatory mammals (not specific to wild turkeys) were completed in 2003 (Convery and Klopfer 2003) via camera trap surveys, track surveys, and scent stations. At that time, red (*Vulpes vulpes*) and gray foxes were the largest canids confirmed on the property. From 2012-2014, 17 months of camera trap surveys by Powers and students (Powers, unpublished data) confirmed the presence and establishment of the coyote (*Canis latrans*). These canids have been observed in photographs (via camera traps) in packs of up to five individuals, and unique identification of individual coyotes indicate that these canids are distributed across the entire 1101-ha property (Powers, personal observation).

Based on this food web alteration since the 2003 surveys (Convery and Klopfer 2003), we began an investigation of the presumed impact of coyotes (and other potential predators) on wild turkey reproductive success. As a first step to answering this question, we established artificial nests similar to those of wild turkeys in suitable habitat. Our objectives were to document all predatory species and to determine the relative "risk" by the different potential egg predators at the RFAAP. Because artificial nests are a common method for wildlife biologists to determine the relative costs of predation (e.g., Hernandez et al. 1998, Yahner and Wright 1985), we monitored these nests with wildlife game cameras to determine if coyotes were the primary predator of eggs, or if other mammalian or avian predators contributed more to nest loss.

MATERIALS AND METHODS

We established and monitored 8 artificial nest sites on the RFAAP's New River Unit for 31 nights, March 3 to April 3, 2017. We created nests by making slight depressions (about 2.5 cm deep, 20-28 cm wide, and 23-33 cm long) in the ground at the base of shrubs or in a clump of dense grasses with considerable horizontal cover and light overhead cover. Each depression was lined with ground litter (Donalty and Henke 2001). Nests were baited with 8 unwashed chicken eggs that simulated the size and shape of wild turkey eggs. Motion- and thermal-triggered

Reconyx Hyperfire (Holman, WI) and Simmons Whitetail 4MP (Overland Park, KS) cameras provided 24-h surveillance, and 2-4 cameras per nest were set to maximize detection from multiple angles. Although ideal protocol would have stipulated that nests be checked daily to immediately re-bait or move predated sites, the logistics of working at a limited-access army installation precluded such an effort. Instead, sites were checked and rebaited (if necessary) every 2-9 days.

Analysis of camera images began with a count of visits to nests. A visit was defined as any animal captured on camera, and visits by an individual were considered unique if more than 30 min had elapsed since the last detected visit (Hernandez et al. 1998). Because this project was strictly observational, and not mark-recapture, we were unable to determine if individuals were repeat predators. Next, we counted the number verified predation attempts in which images depict an individual carrying or consuming eggs. Finally, predation risk was calculated as the number of predation attempts divided by the number of visits. This provided a metric as to the threat a species might pose if it happened upon an unguarded nest. If the risk = 1, we presume that every time an individual of that species detected a nest, it preyed upon it. As the risk approached zero, we concluded that nests were predated less often, or the species posed no threat to the nest.

RESULTS

Fifteen avian and 16 mammalian species were photographed in the vicinity of the nests (Table 1, Figure 1). The most frequent visitors to the turkey nests were white-tailed deer (n = 63), raccoons (n = 61), striped skunks (n = 28), deer mice (*Peromyscus maniculatus*)/white-footed mice (*P. leucopus*; n = 28) and eastern cottontails (*Sylvilagus floridanus*; n = 25). Of these most frequent visitors to the turkey nests, only raccoons and striped skunks actively preyed upon the nests. Fifty-six nest predation events were documented from 6 species: 1 bird (American crow), and 5 mammals (coyote, raccoon, striped skunk, Virginia opossum, eastern fox squirrel [*Sciurus niger*]; Table 1). While coyotes were confirmed to be one of the 6 species that predated the turkey nests, the total number of coyote predation attempts (n= 2) was lower than those of raccoons (n = 35), striped skunks (n = 10), and Virginia opossums (n = 4). Based on the relative predation risk, coyotes posed the greatest risk to nests (0.667). Predation risk rates were lower for raccoons (0.574), Virginia opossums (0.400), American crows (0.375), striped skunks (0.357), and eastern fox squirrels (0.200; Table 1).

DISCUSSION

Wildlife managers and private landowners in Virginia often set goals for maintaining or increasing local populations of particular game species. This project provided further information about the presumed impacts of both recent (coyote) and established predators of wild turkey nests in this region, which is essential to managing this species (Larivière 1999). Multiple avian and mammalian predators could influence turkey reproductive success, if their responses to undefended artificial nests are an indicator of real predation risk (Yahner and Wright 1985, Major and Kendall 1996, Hernandez et al. 1998).

Although coyotes were detected only 3 times in the 31-night survey, they preyed upon the nests during 2 of the 3 visits. This was a greater proportion than all other predators, suggesting a greater risk factor for coyotes than others. This does not negate the influence of the smaller predatory species, which documented 49 predation events and comprised the majority of observed predation events. Raccoons are the primary nest predators of wild turkeys in Virginia (VDGIF 2014). However, results of our study with photographic evidence of 6 predatory species, suggests wild turkeys are threatened by many nest predators.

We acknowledge there were limitations to this short-term study. First, due to the artificiality, the lack of nest guarding by wild turkeys could be a concern, because the female has the some ability to defend the nest; but, not all female turkeys will actively defend their nest, especially when they are disrupted while egg laying or early in the incubation period (VGDIF 2014). Nevertheless, artificial nest studies in wildlife are seen as useful (e.g., Major and Kendal 1996). We also recognize that stationary nests do not fully reflect reality. For example, after our nests were predated, we rebuilt/re-baited them with eggs in the same location. This could have encouraged return visits by individuals that had previously predated the nest. Although females with nest failures do frequently re-nest, with some success, it is unclear whether they move nests or nest in the same locale (Miller et al. 1998, Harper and Exum 1999). Finally, our study is a 31-day snapshot in time; longer-term studies might better assess the role of wild turkeys (as eggs, poults, and adults) in predator diets.

Despite these acknowledged limitations, the findings documented that coyotes, a relative newcomer to the RFAAP, could potentially impact wild turkey nesting success at this site. Although wild turkeys are not actively hunted on this installation, the surrounding property is private lands where hunting is permitted. However, none of the predators in this study are hunted on the installation. Coyotes are hunted without bag limits in western Virginia (Morin 2015), while the remaining five species have seasonal or continuous hunting seasons (VDGIF 2017b). Therefore, determining if the RFAAP serves as a source or sink population for wild turkeys is a valid question for future management studies.

ACKNOWLEDGMENTS

The Northern Neck Wild Turkey Association provided funding for this project. The Biology Department at Radford University provided necessary equipment for the fieldwork. STATEMENT OF RESPONSIBILITY: All three authors conducted the field research. The manuscript was, authored by Brandes and Powers, with editorial support from DiIoia.

LITERATURE CITED

Convery, K.M. and S.D. Klopfer. 2003. Final report: Nest predator habitat use and an evaluation of survey techniques at the Radford Army Ammunition Plant. 2003. Blacksburg, Virginia, Conservation Management Institute. 36 pp.

Donalty, S.M. and S.E. Henke 2001. Can researchers conceal their scent from predators in artificial nest studies? Wildlife Society Bulletin 29(3):814-820.

Harper, C.A. and J.H. Exum 1999. Wild turkeys (*Meleagris gallopavo*) renest after successful hatch. Wilson Bulletin 111(3):426-427.

Hernandez, F., D. Rollins, and R. Cantu. 1998. An evaluation of Trailmaster camera systems for identifying ground-nest predators. Wildlife Society Bulletin 25(4):848-853.

Larivière, S. 1999. Reasons why predators cannot be inferred from nest remains. Condor 101:718-721.

Major, R.E. and C.E. Kendal. 1996. The contribution of artificial nests experiments to understanding avian reproductive success: A review of methods and conclusions. Ibis 138(2):298-307.

Miller, D.A., B.D. Leopold, and G.A. Hurst. 1998. Reproductive characteristics of a wild turkey population in central Mississippi. Journal of Wildlife Management 62(3):903-910.

Morin, D. 2015. Spatial ecology and demography of eastern coyotes (*Canis latrans*) in western Virginia. Ph.D. dissertation, Virginia Polytechnic Institute and State University, Blacksburg, Virginia. 186 pp.

Norman, G.W., J.C. Pack, C.I. Taylor, D.E. Steffen, and K.H. Pollock. 2001. Reproduction of eastern wild turkeys in Virginia and West Virginia. Journal of Wildlife Management 65(1):1-9.

Roberts, S.D. and W.F. Porter. 1996. Importance of demographic parameters to annual changes in wild turkey abundance. Proceedings of the National Wild Turkey Symposium 7:15-20.

Virginia Department of Game & Inland Fisheries (VDGIF). 2014. Virginia wild turkey management plan (2013-2022). Virginia Department of Game and Inland Fisheries, Richmond, Virginia. 93 pp.

Virginia Department of Game and Inland Fisheries (VDGIF). 2017a. Virginia deer management program. Retrieved from https://www.dgif.virginia.gov/wildlife/deer/deer-management-program. Date accessed 3 August 2017.

Virginia Department of Game and Inland Fisheries (VDGIF). 2017b. Hunting and trapping regulations. Retrieved from https://www.dgif.virginia.gov/hunting/regulations/. Date accessed 3 August 2017.

Yahner, R.H. and A.L. Wright. 1985. Depredation on artificial ground nests: Effects of edge and plot age. Journal of Wildlife Management 49(2):508-513.

Table 1: Species detected (No. of visits) at 8 artificial turkey nests at the Radford Army Ammunition Plant, New River Unit (Pulaski Co., Virginia) in March-April 2017. Listed are predation attempts (individual carrying or consuming eggs) and relative predation risk (predation attempts/no. visits).

Order	Family	Scientific name	Common name	Visits (No.)	Predation attempts (No.)	Predation risk
Class Mammalia						
Artiodactyla	Cervidae	*Odocoileus virginianus*	White-tailed Deer	63	0	0
Carnivora	Canidae	*Canis latrans*	Coyote	3	2	0.667
Carnivora	Canidae	*Urocyon cinereoargenteus*	Gray Fox	3	0	0
Carnivora	Didelphidae	*Didelphis virginiana*	Virginia Opossum	10	4	0.4
Carnivora	Felidae	*Felis catus*	Domestic or Feral Cat	8	0	0
Carnivora	Mephitidae	*Mephitis mephitis*	Striped Skunk	28	10	0.357
Carnivora	Mustelidae	*Mustela frenata*	Long-tailed Weasel *	2	0	0
Carnivora	Mustelidae	*Neovison vison*	American Mink *	1	0	0
Carnivora	Procyonidae	*Procyon lotor*	Raccoon	61	35	0.574
Carnivora	Ursidae	*Ursus americanus*	American Black Bear	1	0	0
Lagomorpha	Leporidae	*Sylvilagus floridanus*	Eastern Cottontail	25	0	0
Rodentia	Cricetidae	*Peromyscus leucopus/ P. maniculatus*	White-footed Mouse/ Deer Mouse	28	0	0
Rodentia	Sciuridae	*Marmota monax*	Woodchuck	1	0	0
Rodentia	Sciuridae	*Sciurus carolinensis*	Eastern Gray Squirrel	6	0	0
Rodentia	Sciuridae	*Sciurus niger*	Eastern Fox Squirrel	10	2	0.2
Rodentia	Sciuridae	*Tamias striatus*	Eastern Chipmunk	1	0	0
Class Aves						
Charadriiformes	Scolopacidae	*Scolopax scolopax*	American Woodcock **	10	0	0
Columbiformes	Columbidae	*Zenaida macroura*	Mourning Dove	1	0	0

Galliformes	Phasianidae	*Meleagris gallopavo*	Wild Turkey	11	0	0
Passeriformes	Corvidae	*Corvus brachyrhynchos*	American Crow	8	3	0.375
Passeriformes	Corvidae	*Cyanocitta cristata*	Blue Jay	2	0	0
Order	Family	Scientific Name	Common Name	Visits (No.)	Predation attempts (No.)	Predation "Risk"
Passeriformes	Cardinalidae	*Cardinalis cardinalis*	Northern Cardinal	10	0	0
Passeriformes	Emberizidae	*Pipilo erythrophthalmus*	Eastern Towhee	2	0	0
Passeriformes	Emberizidae	*Zonotrichia albicollis*	White-throated Sparrow	7	0	0
Passeriformes	Mimidae	*Mimus polyglottos*	Northern Mockingbird	7	0	0
Passeriformes	Mimidae	*Toxostoma rufum*	Brown Thrasher	7	0	0
Passeriformes	Troglodytidae	*Thryothorus ludovicianus*	Carolina Wren	1	0	0
Passeriformes	Turdidae	*Turdus migratorius*	American Robin	6	0	0
Passeriformes	Tyrannidae	*Sayornis phoebe*	Eastern Phoebe	2	0	0
Piciformes	Picidae	*Melanerpes carolinus*	Red-bellied Woodpecker	3	0	0

*Confirmed presence denotes new county record
**Confirmed presence denotes new seasonal record

Figure 1. Wildlife camera photographs of individuals actively preying upon artificial wild turkey nests at the Radford Army Ammunition Plant, New River Unit (Pulaski Co., Virginia) in March-April 2017: (A) eastern fox squirrel, (B) American crow, (C) coyote, and (D) raccoon.

(grayscale version)

Virginia Journal of Science
Volume 68, Issue 3 & 4
Fall & Winter 2017
doi: 10.25778/Q3H4-M763

Note: This manuscript has been accepted for publication and is online ahead of print. It will undergo copyediting, typesetting, and review of the resulting proof before it is published in its final form.

Effects of Vacuuming Pervious Concrete on Infiltration Rate

Demetrios E. Maurakis, College of Science, Virginia Tech, Blacksburg, VA 24061
and
Eugene G. Maurakis, Department of Biology, University of Richmond, VA 23173 and Science Museum of Virginia, 2500 W. Broad St., Richmond, VA 23220

ABSTRACT

The objectives of this research were twofold: test the infiltration rate of pervious concrete before and after vacuum cleaning, and assess infiltration variability over time. Infiltration tests were performed on a 558.2 m^2 area of pervious concrete, divided into sixteen 0.35 m^2 test areas in a parking area at the Science Museum of Virginia in Richmond, Virginia on five dates from November 4-December 30, 2013. Average infiltration rates (avg.= 22.8 and 36.3 $L/m^2/min$) immediately after vacuuming were lower than those (avg.=30.7 and 41.3 $L/m^2/min$) before vacuuming. We hypothesize that the vacuuming lifted materials towards the surface from deeper crevices of the lower profile of the pervious concrete, which clogged interstices in the upper portion of the pervious concrete, and impeded infiltration. Over time, however, average infiltration rates recovered, increasing significantly from 22.8 -44.1 $L/m^2/min$ (93% increase) from November 4 through December 30, 2013 (56 days). Ergo, over time, the infiltration capability of the pervious concrete increased as rains likely washed sediments to lower profiles and allow for increased infiltration rates, consistent with the findings of other studies. Infiltration rates on the leading edge of the pervious concrete area receiving runoff from adjacent impervious asphalt surfaces were significantly lower than those furthest away from the leading edge. In contrast to recommendations specifying that pervious concrete be regularly vacuumed monthly, we propose that annual or semiannual vacuuming of pervious concrete would allow adequate infiltration, and reduce costs significantly for pervious concrete areas located in the mid-Atlantic region.

INTRODUCTION

Urban runoff containing sediments, nitrogen, and phosphorus have contributed to eutrophication of the Chesapeake Bay (Frazer, 2005). New technologies such as pervious concrete have been demonstrated to reduce runoff volume, and nitrogen and phosphorus pollutants by 78.5 % and 70.7 %, respectively (Maurakis and Janeski, 2013). Absence of finer sands in the mix of pervious concrete increases porosity and infiltration capacity, allowing stormwater to infiltrate the pervious pavement and underlying soils, minimizing runoff from a site (Obla, 2007). Infiltration rate varies with soil type, the texture, structure, and uniformity of pervious concrete (Reynolds et al., 2002). The accumulation of the *schmutzdecke* (dirt cover), an

active biological layer responsible for pollutant removal, exists in the upper seven cm as reported by Hunt and Collins (2008) and Unger (2006). Sediment from runoff does not penetrate pervious concrete more than 2.54 cm (Mata, 2008).

Wanielista and Chopra (2007) and Bean et al. (2004) suggested that the effectiveness of pervious concrete depends upon the methods and frequency of maintenance. Bean et al. (2004) stated that a lack of maintenance of pervious concrete would eventually result in a decline in infiltration, ultimately leading to an increase in runoff. In a study of 55 sites of 1-12 year-old permeable pavements that had never been cleaned, Boogaard et al. (2014) found that infiltration decreased over time. However, Mullaney and Lucke (2013) point out that there were inconsistencies in the frequency and degree of maintenance required to clean pervious pavements.

Suozzo and Dewoolkar (2012), Chopra et al. (2010), and Boogaard et al. (2014) described the primary methods for maintaining pervious concrete: high-pressure washing, vacuuming, and a combination of both. High-pressure washing is less desirable because it forces sediments deeper into the pervious concrete, potentially clogging underlying layers (Fassman and Blackbourne, 2010). Boogaard et al. (2014) indicated that vacuuming improves infiltration of pervious pavements. However, in a study of the rejuvenation methods (i.e., vacuuming and power washing) of pervious concrete, Chopra et al. (2010) indicated that power washing was more effective in increasing infiltration by pushing clogging materials deeper into the pervious pavements.

In February 2011, the Science Museum of Virginia in Richmond, Virginia (Fig. 1) installed an area of pervious concrete covering 24 parking spots within an existing asphalt parking lot, but did not measure its average infiltration rate after installation and did not perform maintenance. The objectives of this study were to test the infiltration rate of pervious concrete before and after vacuum cleaning, and assess its infiltration variability over time.

MATERIALS AND METHODS

Infiltration tests were conducted in a 558.2 m^2 (18.3 m x 30.5 m) pervious concrete parking area at the Science Museum of Virginia (37.5614° N; -77.4657° W). The pervious concrete of this area is 15.2 cm thick and sits on top of a reservoir composed of a 22.9 cm layer of Solite™ (lightweight, high porous aggregate) supported by a 15.2 cm base layer of #57 gravel size stone (illustrated profile in Sample et al., 2014). The 558.2 m^2 area of pervious concrete was divided into four columns (A, B, C, and D) and four rows (parking spaces 2, 5, 8, and 11) (Figure 2). Column A is on the upstream edge that receives surface flow from 9,442 m^2 of impervious asphalt surface parking area. Column D is furthest from surface flow.

The four longitudinal columns and the four rows of parking spaces, resulting in 16 test locations, which were used to conduct (1) pre-vacuuming (control) and post-vacuuming infiltration tests on November 4 and December 21, 2013; and (2) long-term infiltration tests on each of five dates: November 4 and 24; and December 15, 26, and 30, 2013, where the control group was composed of the 16 un-vacuumed sites on November 4, 2013.

A single ring infiltrometer (open bottom area of 0.35 m^2) was made by cutting and removing the bottom of an 18.93 L bucket. Pliable weather stripping and plumbers putty were attached around the bottom perimeter of the infiltration bucket to form a seal between the pervious concrete and the infiltration bucket to prevent leakage.

A 2-gallon (7.6 L) dispensing bucket was used to pour 3.78 L (1 gal) of water into the infiltrometer using the falling head test procedure in Boogaard et al. (2013) and Lucke et al. (2014) at each test site. A stopwatch was used to time the infiltration rate of 3.78 L of water through the 0.35 m^2 open bottom of the infiltrometer. The stopwatch was started as soon as water hit the concrete and stopped when water inside the infiltrometer had drained. This procedure was repeated for all tests. Infiltration rates were recorded in $L/m^2/min$ as described in Obla (2007).

A new Billy Goat™ industrial duty hard surface vacuum machine manufactured by Billy Goat Industries in Kansas City, MO was used only to vacuum (2,090 CFM @ 3,600 rpm) the total surface area (9.09 m^2) of the four rows of pervious concrete for a minimum of ten times or more until no additional particles were collected. The total sand and debris material from the vacuum bag was removed, labeled, and weighed after each vacuuming of the test areas on November 2 and December 21, 2013. The ratio of g/m^2 was calculated by dividing the amount of debris by the area (9.09 m^2) vacuumed. The daily rate of sediment accumulation in $g/m^2/day$ was calculated by dividing the ratio by the total number of days between vacuuming. No winter surface treatments (i.e., sand) were applied.

Relationships between variables were analyzed using Pearson's *r*-correlation analysis at p=0.05 (SAS, 2014). Average infiltration rates among sampling locations by columns and rows and by date were analyzed with a general linear model procedure followed by Duncan's Multiple Range Test at p=0.05 (SAS, 2014).

RESULTS

There was a positive correlation between increased distance from column A to D and the infiltration rate (correlation coefficient= 0.2163; p=0.0343) (Table 1; Figs. 1 and 2). There was a significant negative correlation between infiltration rate and increased distance from row one to row four (correlation coefficient=-0.1917; p=0.0429)(Table 1; Figs. 1 and 2).

Average infiltration rate before vacuuming (30.7 $L/m^2/min$) did not differ significantly from the average infiltration rate (22.8 $L/m^2/min$) after initial vacuuming (Table 2). Before the second vacuuming on December 21, 2013, the average infiltration rate (41.3 $L/m^2/min$) did not differ significantly from post-vacuum average infiltration rate (36.3 $L/m^2/min$) (Table 2). However, infiltration rates (avg. range=36.3-41.3 $L/m^2/min$) in December, 2013, 47 days after the initiation of testing, were significantly higher than those (avg. range=22.8-30.7 $L/m^2/min$) in November, 2013 (Table 2).

Over time, infiltration rate increased steadily from 22.8 to 44.1 $L/m^2/min$ (Table 3; Fig. 4). Infiltration rates (avg. range=37.3-44.1 $L/m^2/min$) at 20, 47, and 56 days after testing began were significantly higher than the average infiltration rate (22.8 $L/m^2/min$) after post-vacuuming on the first day (Table 3). Pre-vacuuming rate (43 $L/m^2/min$) on the first day (November 4,

2013), however, did not differ significantly from the rate (44.1 L/m^2/min) on the final day (December 30, 2013).

Infiltration rates varied over columns and rows. The average infiltration rate increased from 28.1 L/m^2/min at column A to 44.2 L/m^2/min at column D (Table 4; Fig. 5). Average infiltration rate at column A (28.1 L/m^2/min) was significantly lower than those (avg. range=42.4-44.2 L/m^2/min) at columns C and D (Table 4). Average infiltration rates within rows 5 and 8 (mean range=26.2-26.3 L/m^2/min) were significantly lower than those in rows 2 and 11 (avg. range=44.5-48.4 L/m^2/min)(Table 5; Fig.6).

The amount of debris and sand vacuumed on the first day after 20 months from installation of the pervious concrete was 8,845 g (avg.=2,211.25 g/row over 260 days). On day 360 (Dec 26, 2013), a total of 1,842.72 g (avg.=460.7 g/row over 52 days) had been vacuumed from the pavement after the initial vacuuming on November 4, 2013. This resulted in an average daily accumulation per area per day rate of 0.4 g/m^2/day for the 260-day period (total 243.3 g/m^2), and an average daily accumulation per area per day rate of 0.97 g/m^2/day (50.7 g/m^2) for the 52-day period. Total rainfall during November and December, 2013 were 77.7 and 155 mm, respectively (Table 6).

DISCUSSION

Infiltration rate increased steadily from 22.8-44.1 L/m^2/min from November 4 through December 30, 2013 (56 days), a 93% increase in infiltration rate after vacuuming over the period. However, when compared to the initial infiltration rate before vacuuming at the start of the study, infiltration rate increased only 43.6% (cf. 30.7 and 44.1 L/m^2/min). Both increases in infiltration rate are consistent with the findings of Mata (2010), Bean et al. (2007), Chopra et al. (2010) and others who found that vacuuming increased infiltration rate in pervious pavements. However, immediately after vacuuming, average infiltration rates (avg.= 22.8 and 36.3 L/m^2/min) were lower than those (avg.=30.7 and 41.3 L/m^2/min) before vacuuming. This is contrary to the results of Bean et al. (2007) who reported that infiltration rates increased immediately after vacuuming. We hypothesize that materials from deeper crevices of the lower profile of the pervious concrete were drawn upwards during vacuuming, essentially clogging the pores in the upper portion of the pervious concrete, and thus impeding infiltration. Clogging allowed seepage to occur underneath the seal between the bottom of the infiltrometer and the pervious concrete), and resulted in an effect described by Chanson (2009) where water seepage follows a flow net under and away from the infiltrometer and then up to the surface, similar to the commonly observed behavior at a dam (Fig. 7). This was evident by the extensive water plane flowing downhill on the surface of the pervious concrete away from the infiltrometer. Over the 56-day period, however, infiltration rates increased, consistent with other studies that found that infiltration rate increased after vacuuming. This is probably related to the flushing of clogging materials by rains that occurred after vacuuming dates as infiltration rates continued to increase over time (Table 6).

Infiltration rates on the leading edge (column A) of the pervious concrete area receiving runoff from the adjacent impervious asphalt surface were significantly lower than those furthest away from the leading edge (columns C and D)(Table 4). These findings are consistent with Al-

Rubaei et al. (2015) and Brown and Borst (2014) who reported clogging of the leading edge of pervious pavement where infiltration is affected by more sediment input from impervious pavement. Similarly, average infiltration rates (44.5-48.4 L/m^2/min) in rows 2 and 11 were significantly greater than those (26.2-26.3 L/m^2/min) in the middle of the pervious concrete area (i.e., rows 5 and 8). This is probably related to differences in uneven distribution of pervious concrete material during construction. Row 11 was the most distant area from surface runoff streaming off the impervious asphalt and primarily entering the center areas (rows 5 and 8) of the pervious concrete parking area.

The daily rate of debris/sediment accumulation (0.97g/m^2/day) for the 52-day period was over twice that (0.4 g/m^2/day) for the 260 day-period, assuming similar conditions and rates of vehicle tire abrasion throughout the year. However, this difference may be related to the transport time of material moving from the pervious concrete to rock reservoir sub-layers during longer periods of time. This is consistent with the findings of Welker et al. (2013) and Mata (2010) who reported that sediment is transported and stored in water storage layers of rock underlying pervious concrete.

We recommend that pervious concrete should not be regularly vacuumed monthly or as needed as recommended by Kresge (2010). Even if the pervious concrete is not vacuumed, we determined that water still infiltrates as was noted by Lucke and Beecham (2011), and the more frequent vacuuming plan proposed by Kresge (2010) would be costly. For example, Terhell et al. (2015) indicated annual vacuuming costs for a 0.5 acre pervious parking lot is $400. Our recommendation is consistent with conclusions of Shackel (2010) who reported that frequent maintenance of pervious surfaces (three or more times per year) are often unnecessary. We propose that annual or semiannual vacuuming of pervious concrete is adequate for the pervious concete parking area at the museum, a facility located in the mid-Atlantic region. This approach is consistent with site specific considerations discussed by Mullaney and Lucke (2013).

One variable that could not be controlled in these experiments was the porosity of the pervious concrete. Wanielista and Chopra (2007) and Chopra et al. (2010) indicated that the mixture and pouring of pervious concrete can affect infiltration. If the mixture and pours are not consistent, then there can be a greater density of concrete with fewer pores in some areas when compared to other areas where the concrete mixture is drier, resulting in variation in porosity and subsequently, infiltration rates. We recommend that infiltration tests be conducted immediately after the pervious concrete has cured to characterize average baseline infiltration rates for different areas of the pervious concrete as part of a post-construction protocol. An examination of collected cores of concrete taken at random from pervious concrete pavements could help determine where sand and debris particles are distributed before and after vacuuming, and is recommended for future research. Additionally, as the goal of pervious concrete is to promote infiltration rather than runoff, tests should be conducted to determine the infiltration rate limitations of pervious concrete during heavy and extended duration rain events..

ACKNOWLEDGEMENTS

We thank the Science Museum of Virginia for access to the pervious concrete study site and use of its Billy Goat™ industrial vacuum; and David Sample, Biological Systems Engineering at Virginia Tech, for his thorough review and comments, which helped to improve the manuscript. Both authors equally contributed to the collection and analysis of data, and manuscript preparation.

LITERATURE CITED

Al-Rubaei, M. Viklander, and G.-T. Blecken. 2015. Long-term hydraulic performance of stormwater infiltration systems. Urban Water Journal. 12(8):660-671.

Bean, E. Z., W. F. Hunt, and D. A. Bidelspach. 2004. Study on the surface infiltration rate of permeable pavements. Interlocking Concrete Pavement Institute. Washington, DC. 24 p.

Boogaard, F., T. Lucke, and S. Beecham. 2013. Effect of age of permeable pavements on their infiltration function. Clean Soil Air Water 42(2):146-152.

Brown, R. A. and M. Borst. 2014. Evaluation of surface infiltration testing procedures in permeable pavement systems. J. Environmental Engineering. 14(3):1-12.

Chanson, H. 2009. Chapter 4: Embankment overflow protection systems and earth dam spillways (pgs. 101-132). *In*: W. P. Hayes and M. C. Barnes. 2009. Dams: Impacts, Stability and Design. Nova Science Publishers, Inc. 273 p.

Chopra, M., S. Kakuturu, C. Ballock, J. Spence, and M. Wanielista. 2010. Effect of rejuvenation methods on the infiltration rates of pervious concrete pavements. J. Hydrologic Engineering. 15(6):426-433.

Fassman, E. and S. Blackbourne. 2010. Urban runoff mitigation by a permeable pavement system over impermeable soils. J. Hydrological Engineering. 15(6):475-485.

Frazer, L. 2005. Paving Paradise: The Peril of Impervious Surfaces. Environ Health Perspect. 2005 July; 113(7): A456–A462.

Hunt, W.F. and K.A. Collins. 2008. Permeable pavement: Research update and design implications. North Carolina cooperative extension, Raleigh, NC. AG-588-14W:1-8.

Kresge, P. W. 2010. Maintenance pervades in pervious concrete. Storm Water Solutions (September/October):20-22.

Lucas, W., D. Sample, and T. Janeski. 2012. Comparing Green and Gray Infrastructure Solutions to Reducing Combined Sewer Overflows for a Catchment Within the Shockoe Creek Sewershed in Richmond. VA. Final report to National Fish & Wildlife Foundation. 52 p.

Lucke, T., F. Boogaard, and F. van de Ven. 2014. Evaluation of a new experimental test procedure to more accurately determine the surface infiltration rate of permeable pavement systems. Urban Planning and Transport Research. 2(1):22-35.

Lucke, T. and S. Beecham. 2011. Field investigation of clogging in a permeable pavement system. Building Research and Information. 39(6):603-615.

Mata, L. A. 2008. Sedimentation of pervious concrete pavement systems. Ph.D. Dissertation, North Carolina State University. Raleigh, NC. 288 p.

Maurakis, E. G. and T. V. Janeski. 2013. Final report: BMP LID demonstration, education, training, and testing stormwater facility at Science Museum of Virginia. National Fish & Wildlife Foundation Report # 2009-0055-004. 24 p.

Mullaney, J. and T. Lucke. 2013. Practical review of pervious pavement designs. Clean – Soil, Air, Water. 42(2):111-124.

Obla, K. H. 2007. Pervious concrete for sustainable development. Recent Advances in Concrete Technology:1-5.

Reynolds, W.D., D.E. Elrick, and E.G. Youngs. 2002. Ring or cylinder infiltrometers (vadose zone). P.818-820. In J.H. Dane and G.C. Topp (eds.) Methods of Soil Analysis: Part 4 physical methods. SSSA No. 5. Soil Science Society of America, Inc. Madison, WI.

Sample, D., W. Lucas, T. Janeski, R. Roseen, D. Powers, J. Freeborn, and L. Fox. 2014. Greening Richmond, USA: a sustainable urban drainage demonstration project. ICE Proc. 167(CE2):88-95.

Shackel, B. 2010. The design, construction and evaluation of permeable pavements in Australia. In 24th ARRB Conference-Building on 50 years of Road and Transport Research, Oct. 13-15, Melbourne, Australia.

SAS. 2014. Base SAS 9.4 Procedures Guide: Statistical Procedures (2nd Ed.). SAS Institute Inc., Cary, NC. 556 p.

Suozzo, M. and M. M., Dewoolkar. 2012. Long-Term Field Monitoring and Evaluation of Maintenance Practices for Pervious Concrete Pavement in Vermont. Transportation Research Record: Journal of the Transportation Research Board. 2292 (1):94-103.

Terhell, S.-L., K. Cai, D. Chiu, and J. Murphy. 2015. Cost and Benefit Analysis of Permeable Pavements in Water Sustainability. Unpublished manuscript UC Davis. 8 p.

http://watermanagement.ucdavis.edu/files/5414/3891/2393/A03_Terhell_Cai_Chiu_Murphy_ESM121_FinalReport.pdf

Unger, M. C. 2006. The Role of the Schmutzdecke in *E. coli* Removal in Slow Sand and Riverbank Filtration. University of New Hampshire. 416 p.

Welker, A., J. Jenkins, L. McCarthy, and E. Nemirovsky. 2013. Examination of the Material Found in the Pore Spaces of Two Permeable Pavements. Journal of Irrigation Drain Engineering. 139(4):278-284.

Wanielista, M. and M, Chopra. 2007. Performance assessment of Portland cement pervious pavement. Stormwater Management Academy, University of Central Florida. 164 p.

Table 1. Results of correlation analyses of day, column, row, infiltration rate (L/m^2/hr), and air temperature (C) for pervious concrete studies at the Science Museum of Virginia parking lot section from November 4- December 30, 2013. An asterisk (*) indicates significance at p=0.05.

	Day	Column	Row	Infiltration Rate	Air Temp.
Day	1.00	0.00	0.00	0.3145	-0.428
		1.00	1.00	0.0007*	<0.0001*
Column		1.00	0.00	0.3050	0.00
			1.00	0.0011*	1.00
Row			1.00	-0.1917	0.00
				0.0429*	1.00
Infiltration Rate				1.00	-0.1338
					0.1597
Air Temp.					1.00

Table 2. Results of Duncan's multiple range test for average infiltration rates (L/m^2/min) before and after vacuuming of the pervious concrete parking area at the Science Museum of Virginia from November 4-December 26, 2013. Underscored means do not differ at p=0.05.

Vacuum	Before	After	Before	After
Date	Nov.4	Nov.4	Dec. 21	Dec. 26
Day	308	308.1	355	360
Average	30.7	22.8	41.3	36.3
F=3.72				
p=0.0160				

Table 3. Results of Duncan's multiple range test for average infiltration rates (L/m^2/min) at test locations in the pervious concrete parking area at the Science Museum of Virginia from November 4-December 30 2013. Underscored means do not differ at p=0.05.

Date	Nov. 4	Nov. 4	Dec. 15	Dec. 26	Dec. 30
Day	308.1	308	328	355	364
Average	22.8	30.7	37.3	41.3	44.1
F=3.10					
p=0.02					

Table 4. Results of Duncan's multiple range test for average infiltration rates (L/m^2/min) by column in the pervious concrete parking area at the Science Museum of Virginia from November 4-December 30 2013. Underscored means do not differ at p=0.05.

Column	A	B	C	D
Avg. infiltration	28.1	30.7	42.4	44.2
F=3.60				

Table 5. Results of Duncan's multiple range test for average infiltration rates (L/m^2/min) by row in the pervious concrete parking area at the Science Museum of Virginia from November 4-December 30 2013. Underscored means do not differ at p=0.05.

Row	8	5	11	2
Average infiltration	26.2	26.3	44.5	48.4
F=8.99				
p<0.0001				

Table 6. Rainfall (mm) at Richmond International Airport from November 4-December 29, 2013.

Date	Rainfall (mm)
11/4/2013	Vacuuming
11/7/2013	1.78
11/15/2013	0.51
11/16/2013	6.86
11/17/2013	1.52
11/18/2013	1.52
11/26/2013	33.27
11/27/2013	32.26
Total Nov.	77.72
12/4/2013	1.524
12/5/2013	1.27
12/7/2013	9.144
12/8/2013	24.638
12/9/2013	9.398
12/10/2013	6.096
12/14/2013	24.892
12/17/2013	11.684
12/21/2013	Vacuuming
12/22/2013	17.018
12/23/2013	15.24
12/29/2013	34.29
Total Dec.	155.194

Figure 1. Pervious concrete parking area sampled at the Science Museum of Virginia from November 4-December 30, 2013.

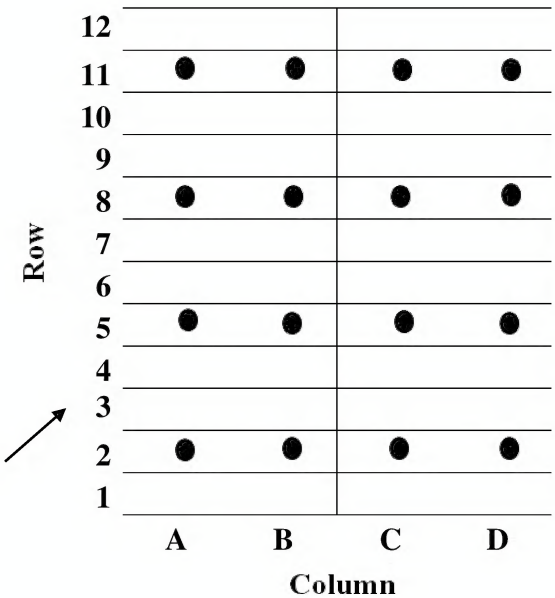

Figure 2. Illustration of infiltration testing sites (●) by column and row in the pervious concrete parking lot at the Science Museum of Virginia from November 4-December 30, 2013. Arrow indicates drainage direction. Not drawn to scale.

A.

B.

Figure 3. Un-vacuumed (A) and vacuumed (B) areas of pervious concrete in the parking lot at the Science Museum of Virginia in Richmond, VA on November 4, 2013.

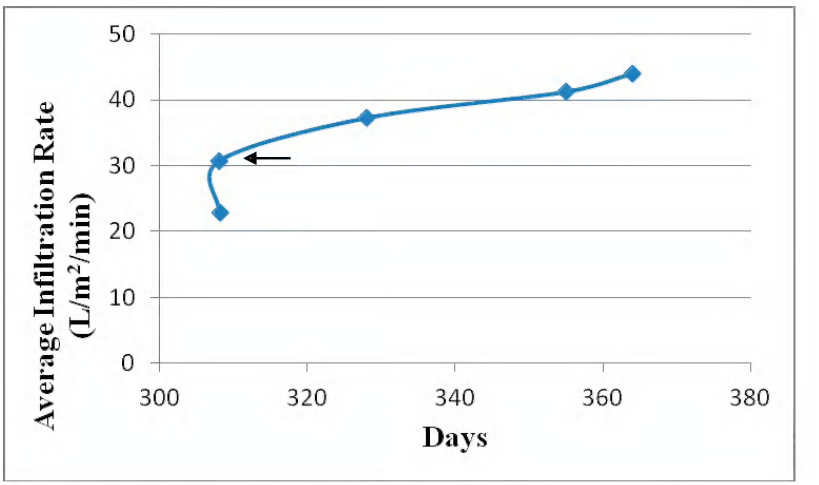

Figure 4. Average infiltration rate (L/m^2/min) by day at testing sites in the pervious concrete parking lot at the Science Museum of Virginia from November 4-December 30, 2013. Arrow indicates initial un-vacuumed infiltration rate.

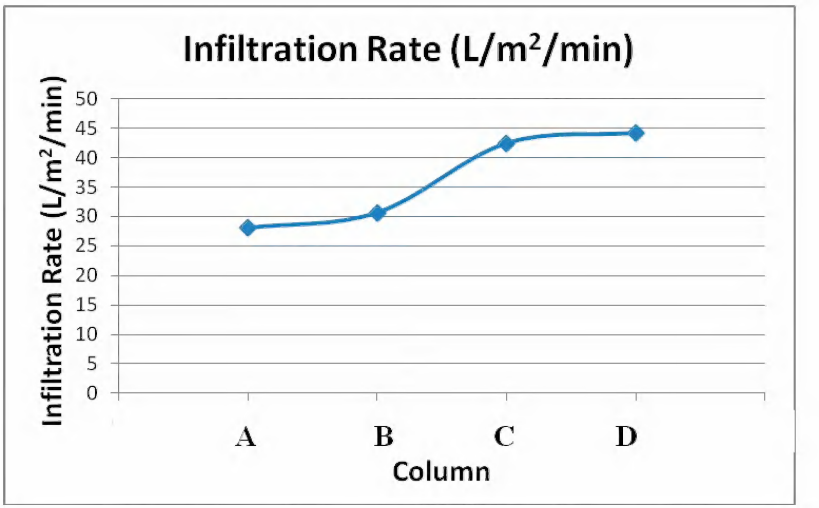

Figure 5. Average infiltration rate (L/m^2/min) by column in the pervious concrete parking lot at the Science Museum of Virginia from November 4-December 30, 2013.

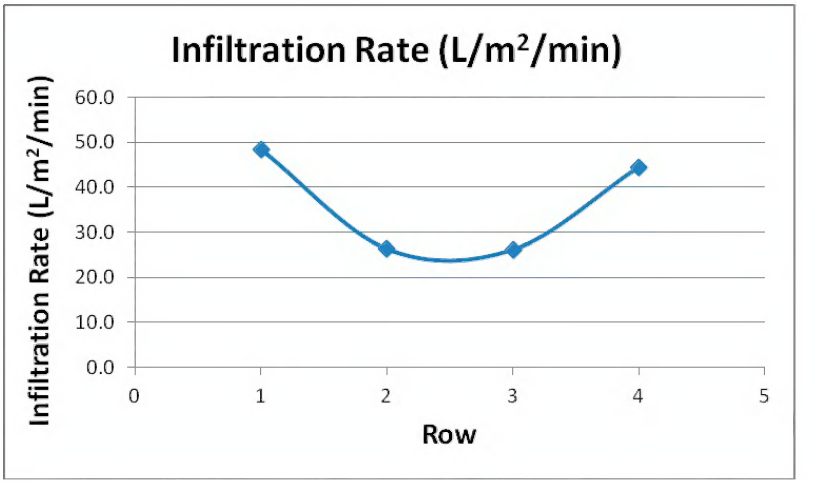

Figure 6. Average infiltration rate (L/m^2/min) by row in the pervious concrete parking lot at the Science Museum of Virginia from November 4-December 30, 2013.

Figure 7. Extensive water plane flowing downhill on the surface of the pervious concrete away from the infiltrometer immediately after vacuum cleaning of pervious concrete at the Science Museum of Virginia on November 4, 2013.